ESECMaSE

Enhanced Safety and Efficient Construction of Masonry Structures in Europe

Project No. Coll – Ct - 2003 - 500291

ESECMaSE

Enhanced Safety and Efficient Construction of Masonry Structures in Europe

Horizontal Research Activities Involving SMEs

Collective Research

Work Package N°: 7

D 7.1b Test results on the behaviour of masonry under static cyclic in plane lateral loads

Prof. Dr.-Ing. habil. Dr.-Ing. E. h. K. Zilch, Dipl.-Ing. W. Finckh, Dipl.-Ing. S. Grabowski, Dr.-Ing. D. Schermer, Dipl.-Ing. W. Scheufler,

Due date of deliverable: 01.06.2008
Actual submission date:01.09.2008

Start date of project: 10.June 2004 — Duration: 36 month

Technical University of Munich
Department of civil engineering and geodesy
Chair of Structural Concrete
80290 Munich

Draft N°: …1

Project co-funded by the European Commision within the Sixth Framework Programme (2002-2006)		
Dissemination Level		
PU	Public	X
PP	Restricted to other programme participants (including the Commission Services)	
RE	Restricted to a group specified by the consortium (including the Commission Services)	
CO	Confidential, only for members of the consortium (including the Commission Services)	

TECHNISCHE
UNIVERSITÄT
MÜNCHEN

Institut für Baustoffe und Konstruktion

MPA BAU

Lehrstuhl für Massivbau
Univ.-Prof.
Dr.-Ing. K. Zilch

Arbeitsgruppe 4
Mauerwerk

ESECMASE

No. sw-2408201
Date....2008-08-21

Deliverable D7.1 b: **Test results on the behaviour of masonry under static cyclic in plane lateral loads**

Project: Enhanced Safety and Efficient Construction of Masonry Structures in Europe

Client: European Commission
RESEARCH DIRECTORATE-GENERAL

Person in charge: Dipl.-Ing. W. Scheufler

The investigation report includes: 13 Pages
48 Annex

MAILING ADDRESS:	D-80290 MUENCHEN	PHONE +49 / 89 / 289 - 23038/39	FAX +49 / 89 / 289 - 23046
ADDRESS:	BUILDING N6	THERESIENSTR. 90	D-80333 MUENCHEN
BANK DATA:	BAYER. LANDESBANK MUENCHEN	ACCOUNT NO: 24 866	BANK CODE: 700 500 00
CONTACT PERSON:	DIPL.-ING. W. SCHEUFLER	E-MAIL:esecmase@mb.bv.tum.de	PHONE +49 / 89 / 289-23025

Contents

1. Introduction

Deliverable 7.1 of ESECMaSe deals with the static cyclic tests on masonry walls. Since the static cyclic wall tests of the ESECMaSE project were carried out at three different laboratories, the deliverable is divided into three parts:

⇒ D 7.1 a – University of Kassel (UNIK)
⇒ D 7.1 b – Technical University of Munich (TUM)
⇒ D 7.1 c – University of Pavia (UPavia)

This report describes the static cyclic wall tests with a test set-up developed in WP 6 on different kinds of masonry (clay, calcium silicate) with different specimen dimensions, carried out at Technical University of Munich.

2. Specimen and material properties

Totally eight tests on walls were performed within this part of this work package 7.1, deliverable 7.1b. The thickness of the walls was 175 mm for all specimens and also the height of 2.5m was constant for all tests. The details of the material properties of the different kind of units and mortar can be found in deliverable 5.5.

Table 1: Overview of the tested wall specimen under static cyclic loading

Name	**l[m]**	**σ_V [MPa]**	**Unit size [mm³]**	**Reinforcement**	**Bed joints (thin layer)**	**Head joints**	**Minimum overlapping length**
CS01	1.25	1,0	248x175x248 conventional units	No	Quick mix KSK grob	unfilled	$l_{unit}/2$ = 12,5cm
CS02	1.25	1,0	248x175x248 optimised units	No	Quick mix KSK grob	unfilled	$l_{unit}/2$ = 12,5cm
CS03	2.5	1,0	998x175x625	No	Quick mix KSK grob	filled	$l_{unit}/2$ = 50cm
CS04	1.25	1,0	998x175x625	Internal	WEP	filled	$l_{unit}/2$ = 50cm
CS05	2.5	1,0	998x175x625	Internal	WEP	filled	$l_{unit}/2$ = 50cm
CS06 (*)	2.5	1,0	998x175x625	Internal	WEP	filled	25cm (*)
CS07	2.5	2,0	998x175x625	Internal	WEP	filled	$l_{unit}/2$ = 50cm
Clay01	1.5	0,44	375x175x248 (HLZ-Plan-12/0,9-17,5) Opti 2	No	DM	unfilled	$l_{unit}/2$ = 18cm
(*) here the minimum overlapping length was reduced from $l_{unit}/2$ to 25cm							

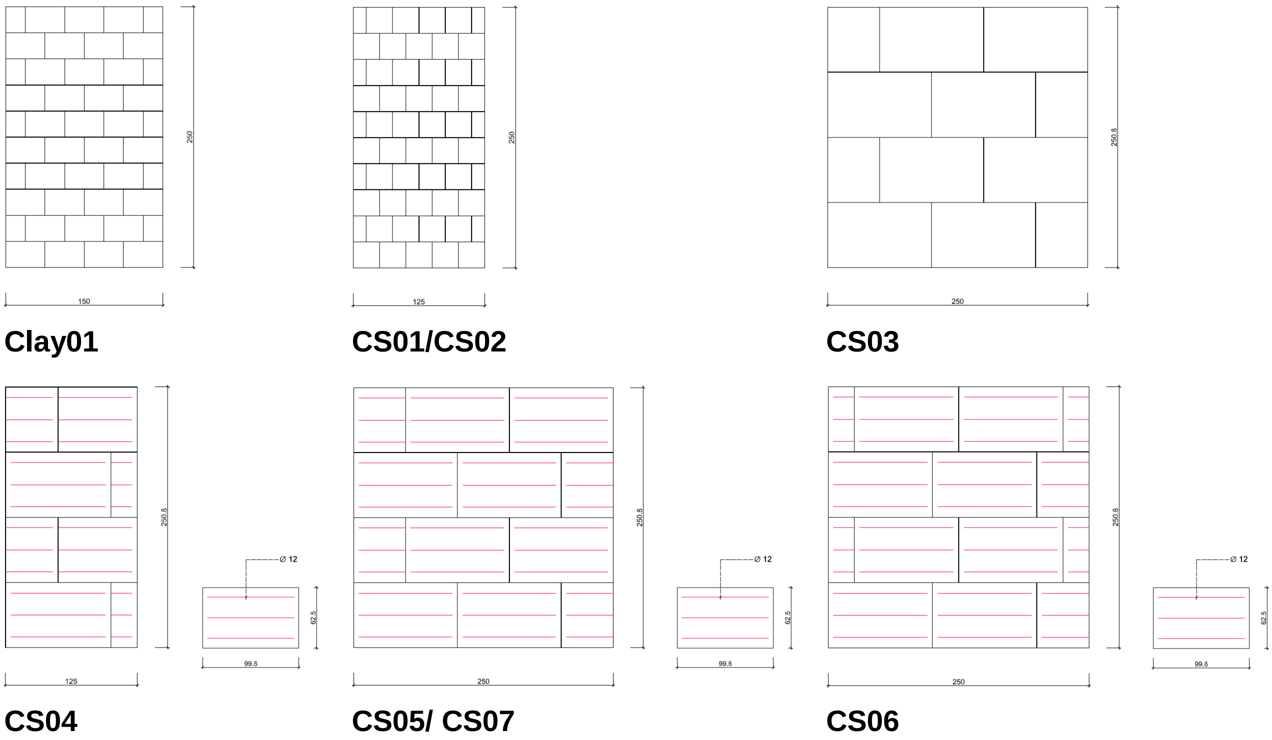

Figure 1: Overview of the wall specimen

2.1. Materials used

2.1.1. Walls made of Clay units

Specimen Clay01 was built with a vertically perforated clay brick, type: Bellenberg HLZ – Plan – 12 – 0.9 9DF, optimized 2. The width of the brick was 175mm, the height 249mm and the length 363mm. The head joints were left unfilled according to the groove and tongue of the units. As mortar for the bed joints, a thin layer mortar type “Bellenberger Planziegel Dünnbettmörtel (DIBT Zul.-Nr. Z.17.1-261)” was used

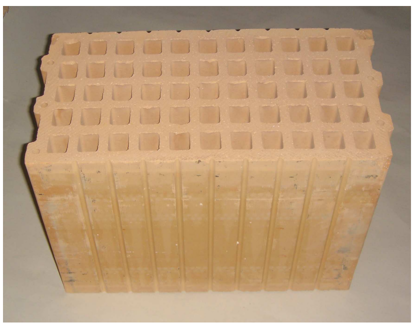

Figure 2: Bellenberg HLZ – Plan – 12 – 0.9 9DF, optimized 2

2.1.2. Walls made of Calcium silicate units

Three different types of calcium silicate units were used. Specimen CS01 and CS02 were built with units type KSP 20-1.8-6DF (248x175x248 mm) (conventional and optimized), and a thin layer mortar (class M10, according to DIN EN998-2) for the bed joints. The head joints were left unfilled.

For the other specimen, CS03 to CS07, large-sized units, type KS XL-PE (width: 175mm, height: 623mm, length: 998 mm) were used. The units of CS 03 and the remaining calcium silicate Walls differ from each other by the existence of an internal reinforcement (three reinforcing bars, diameter 12 mm, per unit) inside the units and the usage of two different kinds of mortar (CS03: thin layer mortar class M10, DIN EN998-2 ; CS04-CS07: optimized thin layer mortar “KS-Werkplanmörtel”, In the following referred to as “WEP”, with a higher adhesive tensile strength). The head joints of all Specimens were filled with the same mortar which was used for the bed joints.

Figure 3: KSP 20-1.8-6DF (175), conventional

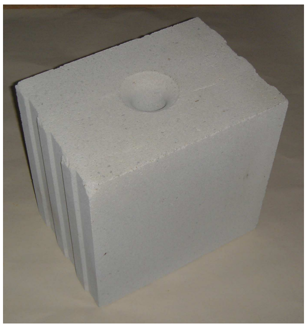

Figure 4: KSP 20-1.8-6DF (175), optimized

Figure 5: KS XL-P (175) with internal reinforcement

3. Experimental results

3.1. Test method

The tests were performed on full scale masonry walls with nearly a constant axial compression force N and a cyclic application of a displacement at the top of the wall. As the vertical axial force was applied by two independently force-controlled vertical actuators, also an in-plane bending moment could be applied. To avoid rotations of the top of the wall caused by the horizontal loadings, a counteracting moment was applied at the top of the wall. The aim was, to get the in-plane bending moment at mid height of the wall to zero.

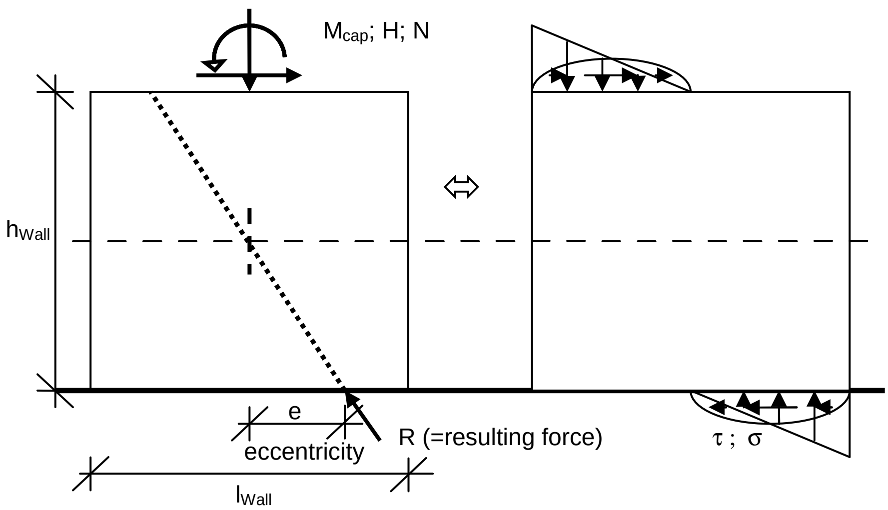

Figure 6: Idealized load and stress state at a single wall according to the defined boundary conditions [Deliverable 6.3]

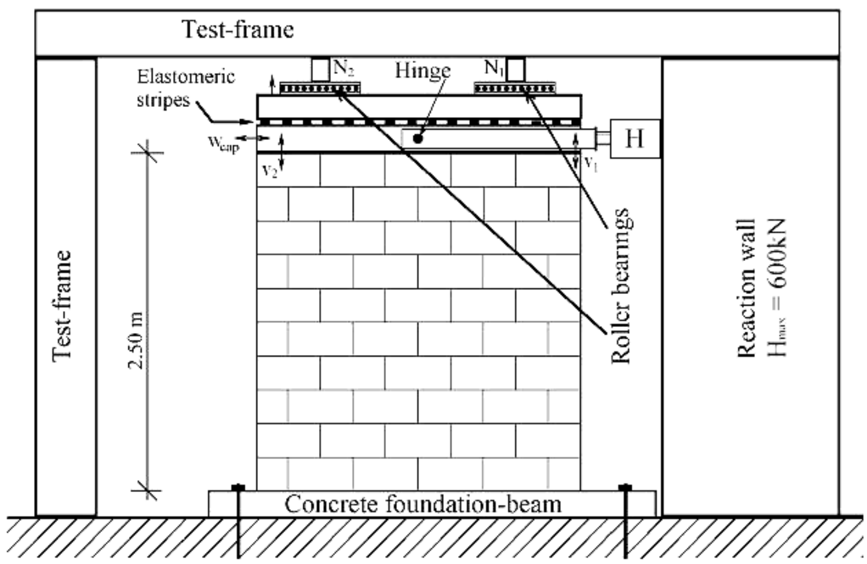

Figure 7: Test set-up used for the static-cyclic tests at the TU Munich [Deliverable 6]

3.2. Maximum horizontal force and deformation capacity

The results of the tests concerning the maximum horizontal load H_{max} and the maximum displacements d_{max} are given below.

Table 2: Normal forces and maximum horizontal loads

Name	N	H_{max}	d_{max}	H/N	Geometry l/h (*)
CS01	219 kN	84 / -85 kN	13 / -13 mm	0.38	0.5
CS02	219 kN	86 / -82 kN	7 / -6 mm	0.38	0.5
CS03	438 kN	243 / -228 kN	10 / -10 mm	0.53	1
CS04	219 kN	92 / -90 kN	8 / -8 mm	0.42	0.5
CS05	438 kN	316 / -341 kN	6 / -6 mm	0.75	1
CS06	438 kN	292 / -316 kN	6 / -6 mm	0.69	1
CS07	875 kN	462 / - 445 kN	7 / -7 mm	0.52	1
Clay01	97 kN	50 / -50 kN	20 / -20 mm	0.52	0.5
(*) assuming rocking limitation and double fixation					

The deformation capacity of the walls is determined from the load-displacement curves obtained from the tests according to deliverable 7.1a.

The relevant parameters were the point of the first crack (H_C and u), the maximum load H_F and the maximum deformations d_{u1} and d_{u2} on both sides were taken from the data. The calculation of the ductilities is carried out assuming

$$\mu = \frac{d_u}{d_e}\text{ , where } d_e = \frac{d_{cr} \cdot H_u}{H_{cr}}$$

Table 3: Overview about the results of the static cyclic tests

Name	d_{u1} [mm]	d_{u2} [mm]	d_{cr1} [mm]	d_{cr2} [mm]	H_{cr1} [kN]	H_{cr2} [kN]	H_{u1} [kN]	H_{u2} [kN]	d_{e1} [mm]	d_{e2} [mm]	μ_1 [-]	μ_2 [-]
CS01	13,1	-13,2	1,2	-1,2	49	-50	72	-70	1,8	-1,7	7,4	7,9
CS02	5,7	-5,9	1,1	-1,0	63	-47	79	-72	1,4	-1,5	4,1	3,9
CS03	8,9	-7,2	1,3	-1,0	179	-136	216	-187	1,6	-1,4	5,7	5,2
CS04	7,0	-6,6	1,1	-0,9	63	-52	81	-81	1,4	-1,4	4,9	4,7
CS05	5,3	-5,2	1,0	-0,8	239	-267	278	-311	1,2	-0,9	4,5	5,9
CS06	5,4	-5,0	0,8	-0,8	217	-233	272	-294	1,0	-1,0	5,3	4,9
CS07	6,6	-6,5	1,4	-1,3	333	-337	421	-397	1,8	-1,6	3,7	4,2
Clay01	16,6	-17,9	1,0	-1,2	38	-37	48	-48	1,3	-1,6	13,1	11,4

Regarding the calculated ductilities of clay01 it has to be mentioned, that the level of axial compression was relatively low.

3.3. Comparison of different vertical compression level

The walls CS05 and CS07 were build with the same material and the same geometry. During the tests the vertical compression level was doubled within the test on wall CS07 compared to CS05.

The behaviour of the specimen CS05 and its crack pattern is dominated by cracks in the joints (head and bed joints) where the behaviour of the specimen CS07 and its crack pattern is dominated by diagonal cracks running through the units. The dissipated energy is significantly higher in the tests of CS05 compared to the hysteresis of CS07.

The maximum horizontal load bearing capacity is not proportionally increased with the rising axial force.

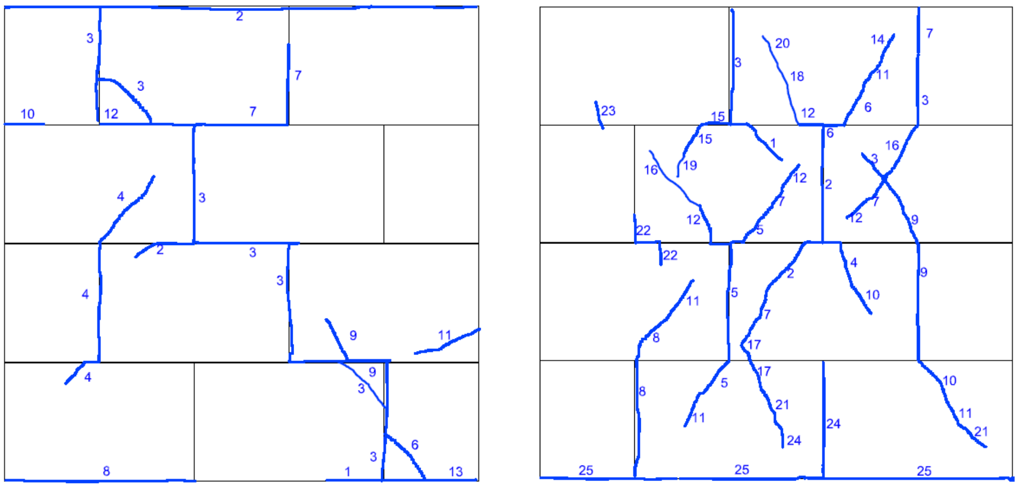

Figure 8: Crack pattern of the specimen CS05 and CS07

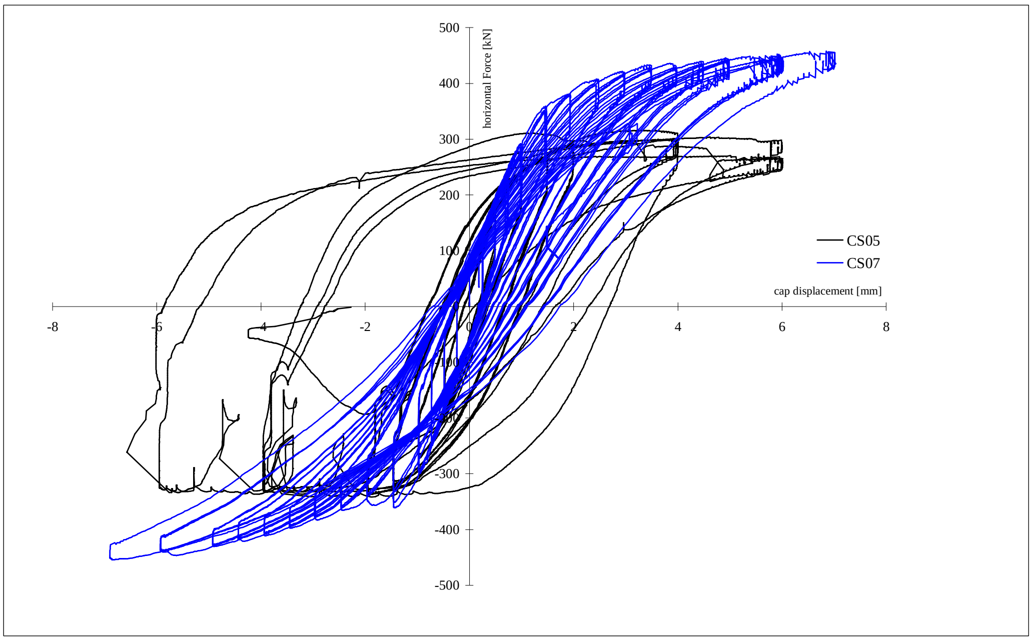

Figure 9: Hysteresis of the tests on the specimen CS05 and CS07

3.4. Comparison of optimisation process

The walls CS01 and CS02 were build with conventional resp. optimised cs-units. All other parameters were not varied during the tests.

Regarding the crack pattern and load displacement curve it is obvious, that the reduced compression strength of the optimized units leads to unfavourable behaviour. The displacement capacity of CS02 is reduced significantly caused by the cracks in the units. The load bearing capacity is not influenced significantly.

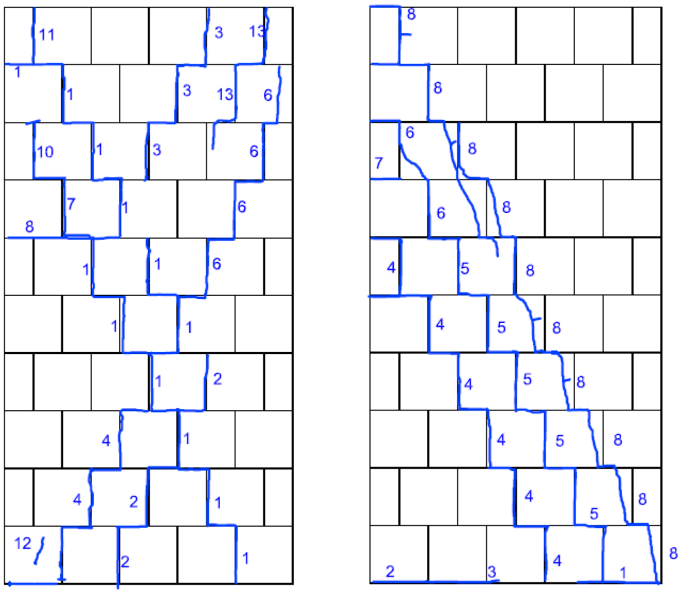

Figure 10: Crack pattern of the specimen CS01 and CS02

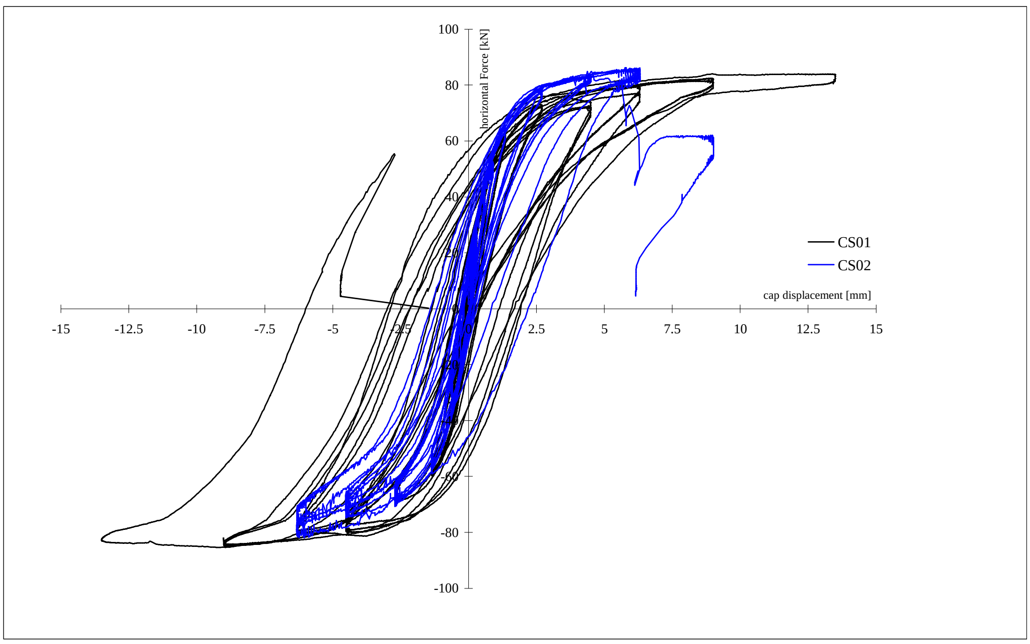

Figure 11: Hysteresis of the tests on the specimen CS01 and CS02

3.5. Comparison of the effect of internal reinforcement

The difference between the test on the specimen CS03 and CS05 is the internal reinforcement in the CS-units in CS05 and the usage of a mortar with higher adhesion. The load bearing capacity is increased significantly by the internal reinforcement. The reinforcement cannot avoid cracks but after the opening of the cracks additional dowel effects can be activated. The energy dissipation described by the fullness of the hysteresis is increased noticeable by the internal reinforcement. Specimen CS05 shows also a considerable higher stiffness at the beginning of the experiment. This is probably a consequence of the usage of the mortar with higher adhesion.

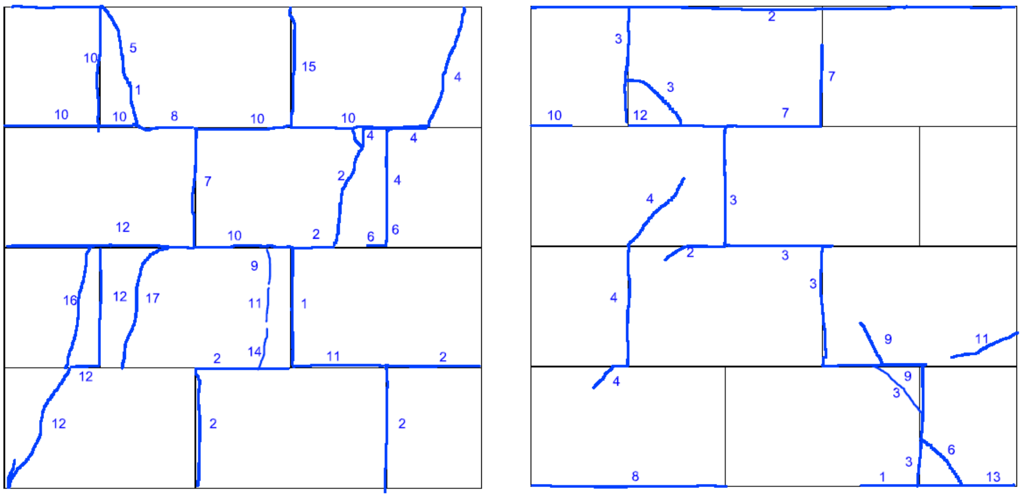

Figure 12: Crack pattern of the specimen CS03 and CS05

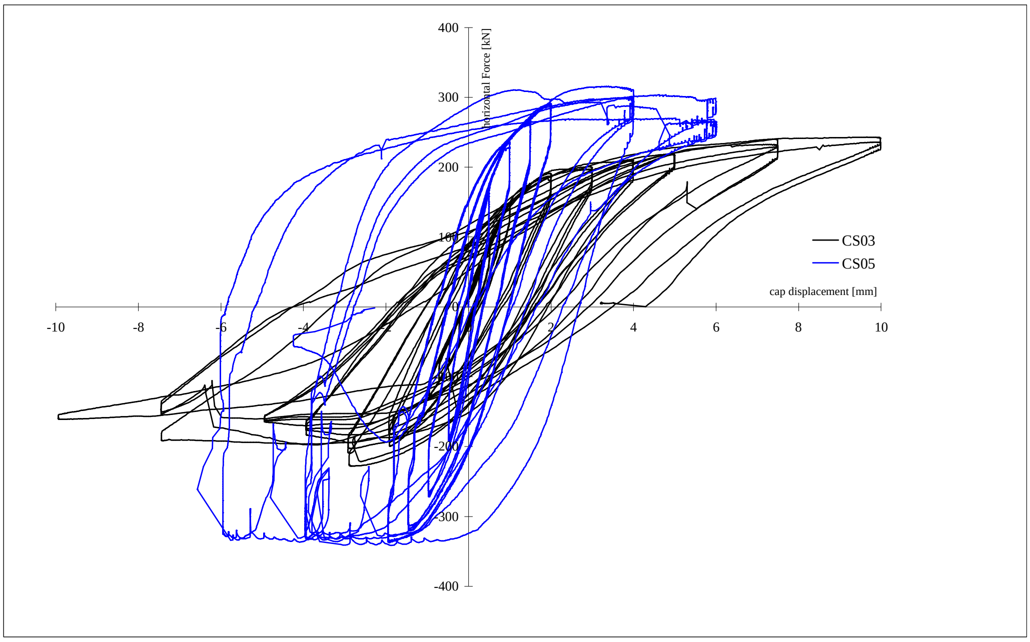

Figure 13: Hysteresis of the tests on the specimen CS03 and CS05

3.6. Comparison of the effect of overlapping length

The difference between the specimen CS05 and CS06 is the overlapping length of the units. For specimen CS06 it was reduced from 50cm (=half of length of the units) to 25cm. The load bearing capacity is decreased through the reduction of the overlapping length, particularly at a higher level of horizontal displacement. The crack pattern of specimen CS06 is dominated by diagonal cracks inside the units, contrary to the crack pattern of specimen CS05, which shows mainly cracks of the bed and head joints. The dissipated energy is significantly lower in the test of CS06 compared to the hysteresis of CS05.

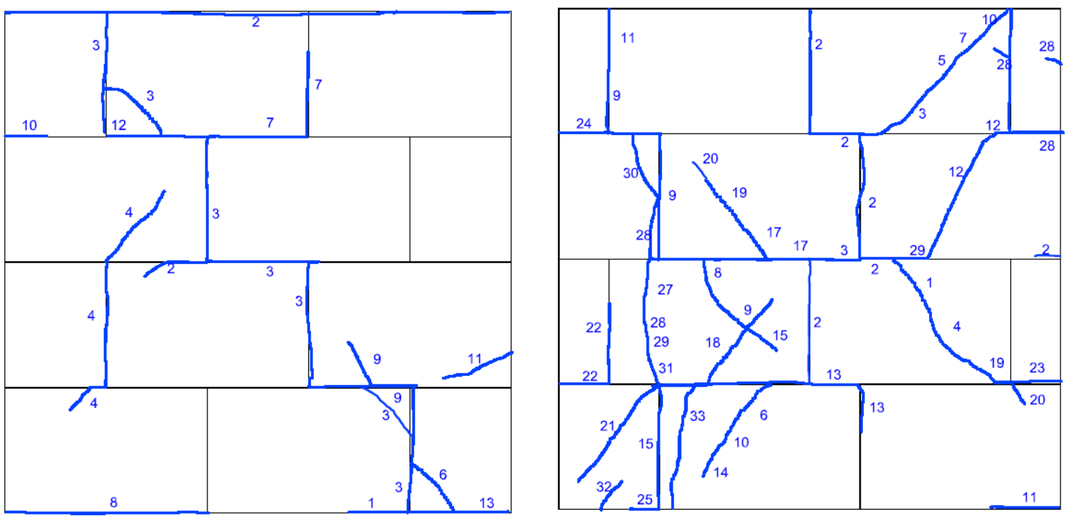

Figure 14: Crack pattern of the specimen CS05 and CS06

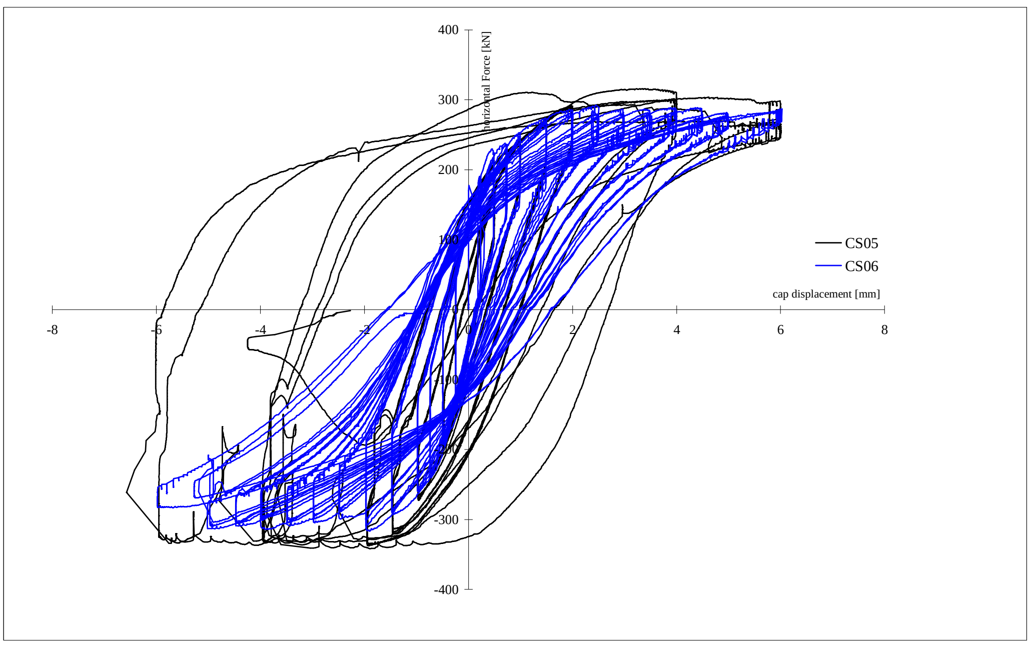

Figure 15: Hysteresis of the tests on the specimen CS05 and CS06

3.7. Comparison of the effect of the length of the Wall

Specimen CS04, CS05 and CS06 were tested under the same compression stress but CS04 was half of the length of specimen CS05 resp. CS06. The load bearing capacity of CS04 was ca. 90 kN whereas the maximum load of CS05 and CS06 was about 315 kN. This is an enhancement of approx. 350% for the maximum load. The behaviour of CS04 is dominated by rocking of the whole wall (crack number 1 occurred in the first and last mortar layer of the wall) therefore the hysteresis shows only a little fullness. Specimen CS05 and CS06 however, showed a completely different behaviour. The first cracks suggest a failure of the bed and head joints followed by cracking of the units. The comparison of these specimens therefore is not reasonably, because of the dominant effect of the geometric restriction of specimen CS04.

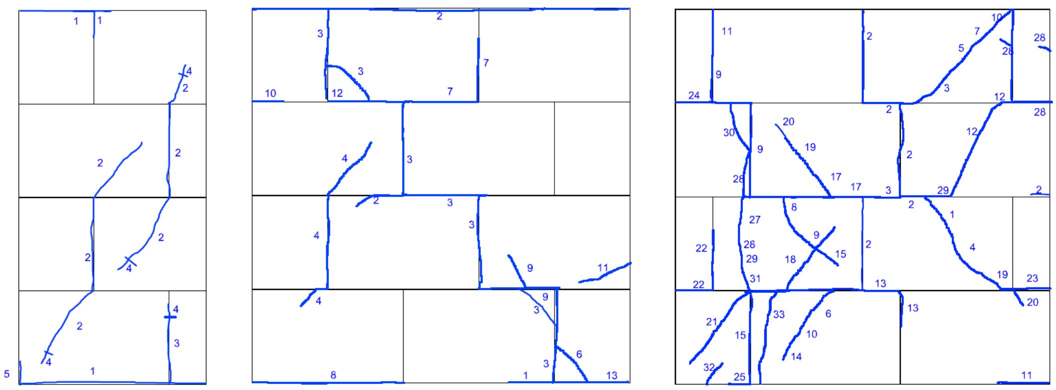

Figure 16: Crack pattern of the specimen CS04, CS05 and CS06

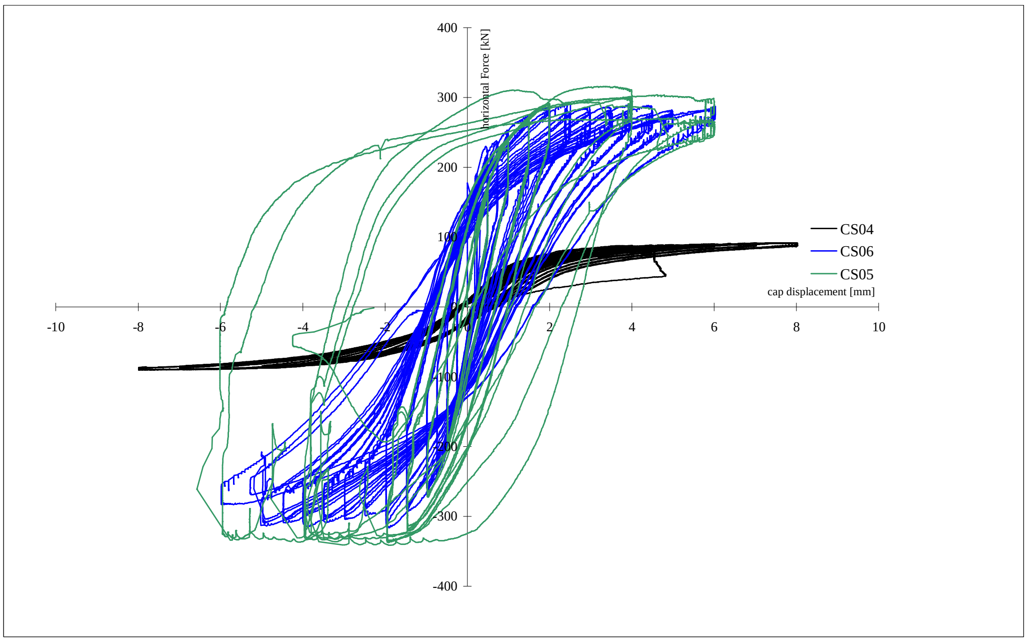

Figure 17: Hysteresis of the tests on the specimen CS04, CS05 and CS06

4. Summary

At the Technical University of Munich eight tests on different full scale masonry walls under static-cyclic loading were performed, to investigate the behaviour under seismic loading. Seven wall specimens were built of calcium silicate units with different dimensions and material properties, one specimen was constructed with clay bricks. Chapter 2 gives a detailed overview of the materials and the geometric dimensions of the specimen.

In chapter 3 the test setup is described and the results, especially the maximum horizontal load bearing capacity, the horizontal deformation capacity and the ductility of the different walls, are displayed. In addition to it, the results of walls with different properties are compared to each other. Among others, the comparison of the influence of the vertical compression level shows, that an increasing normal force leads to an increasing maximum horizontal bearing capacity, but the enhancement is not proportionally.

The comparison of tests with specimens, constructed with calcium silicate elements with an internal reinforcement, to the unreinforced ones, shows the significantly increased load bearing capacity of the reinforced elements and an enormous enhancement of the fullness of the hysteresis.

The reduction of the overlapping length of the calcium silicate elements, compared to an overlapping length of half an unit, leads only to a small reduction of the maximum horizontal force, but at the same time, the specimens showed completely different crack pattern.

The comparison of specimen CS04 with CS05 resp. CS06 should display the influence of the length of the tested walls. Unfortunately, the behaviour of the specimen was totally different. Therefore, a reasonable conclusion about this influence was not possible. To get authoritative results, some additional tests with miscellaneous geometries have to be carried out.

5. References

[1] Fehling, E.; Stürz, J.; Schermer, D.: Theoretical Investigation on Shear Test Methods, Consttruction of test setup for shear tests for validation of proposed method; Technical report of the collective Research project ESECMaSE, 2006

[2] Fehling, E.; Stürz, J.; Schermer, D.: Theoretical Investigation on Shear Test Methods, Series of shear test for validation; Technical report of the collective Research project ESECMaSE, 2006

[3] Grabowski, S.: Material properties for the tests in WP7 and 8 and the verification of the design model of WP4. Technical report of the collective Research project ESECMaSE, 2005

[4] Grabowski, S.: Tests on the relevant material properties on improved clay units; Technical report of the collective Research project ESECMaSE, 2006

[5] Schermer, D.: Verhalten von unbewehrtem Mauerwerk unter Erdbebenbeanspruchung; Dissertation; TU München, Institut für Baustoffe und Konstruktion, Lehrstuhl für Massivbau; 2004

[6] Schermer, D.: Theoretical Investigation on Stress States of Masonry Structures Subjected to Static and Dynamic Shear Loads (Lateral Loads); Analysis of Apartment House; Technical report of the collective Research project ESECMaSE, 2005

6. ANNEX

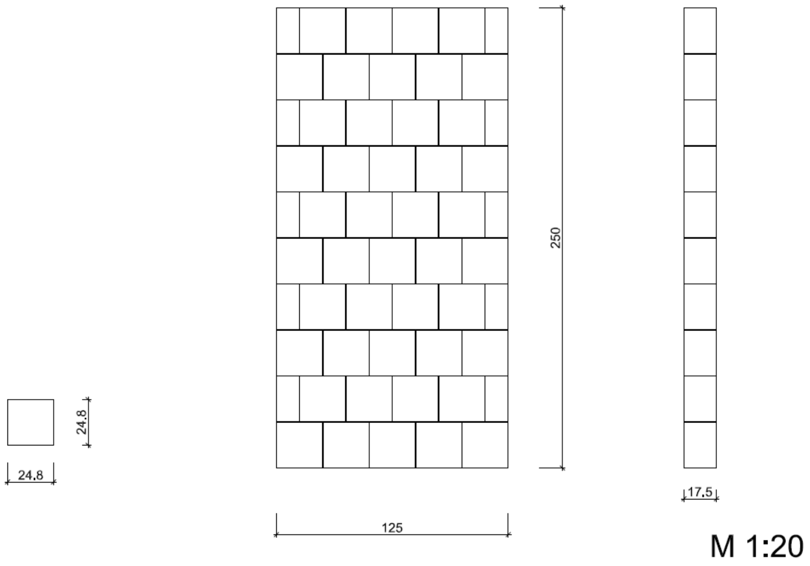

Figure 18: Dimension of the test specimen CS01

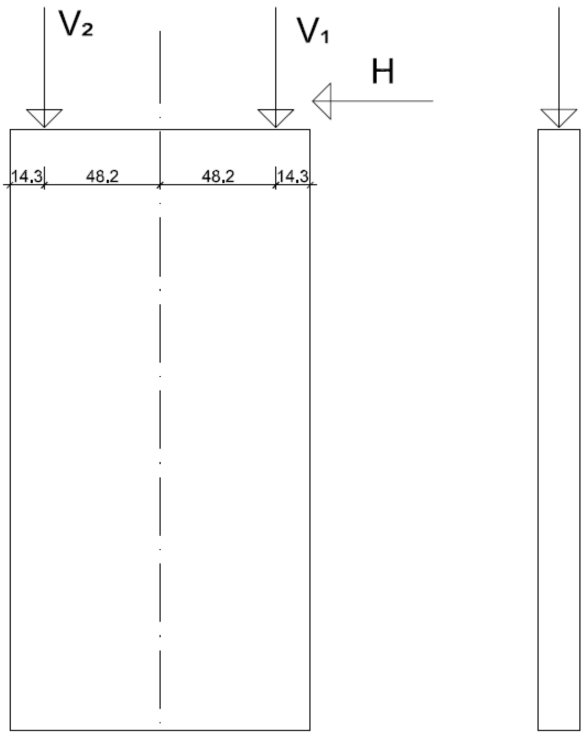

Figure 19: Position of the hydraulic actuators at test specimen CS01

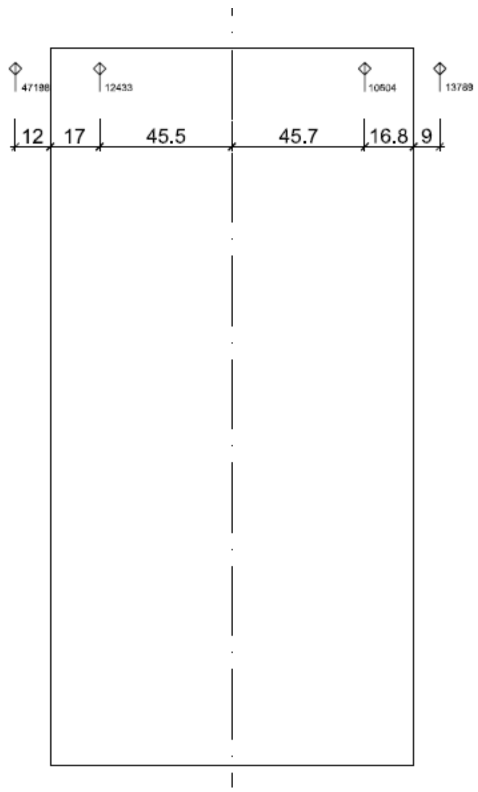

Figure 20: Position of the LVDTs at test specimen CS01

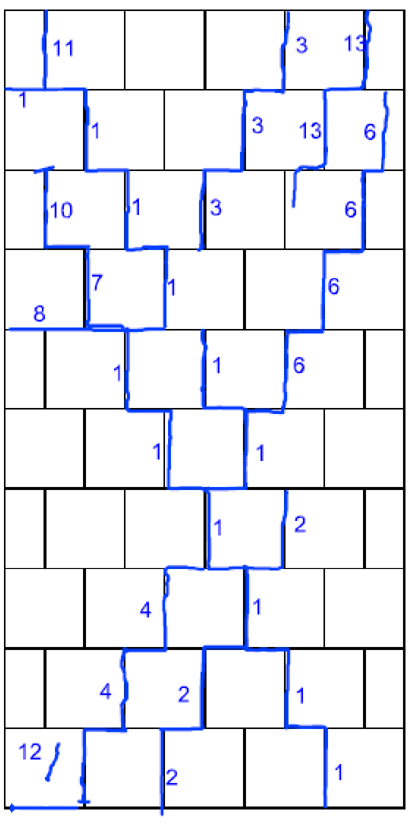

Figure 21: Crack pattern of the test specimen CS01

First crack:

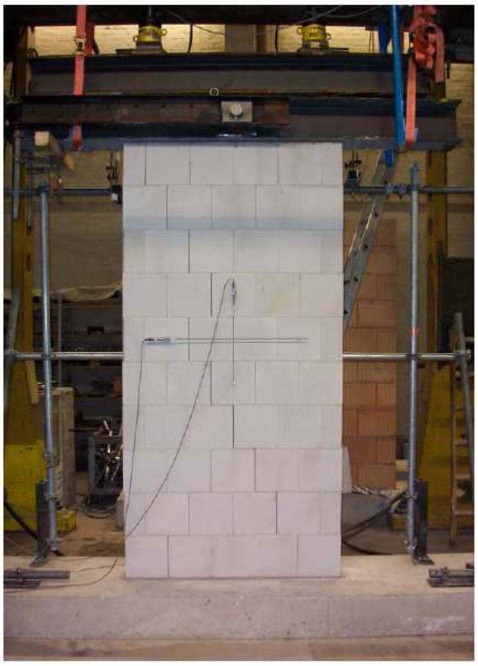

Final cracks:

Figure 22: Crack pattern of the test specimen CS01

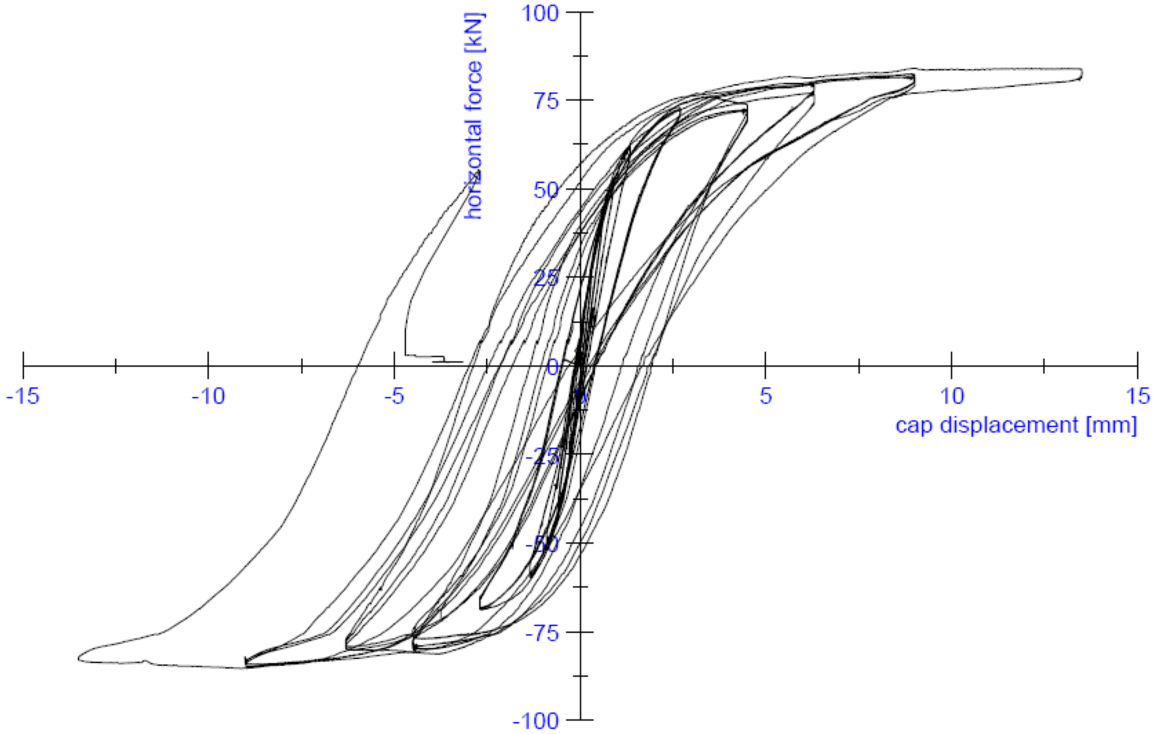

Figure 23: Load-displacement curve (hysteresis) of the test on specimen CS01

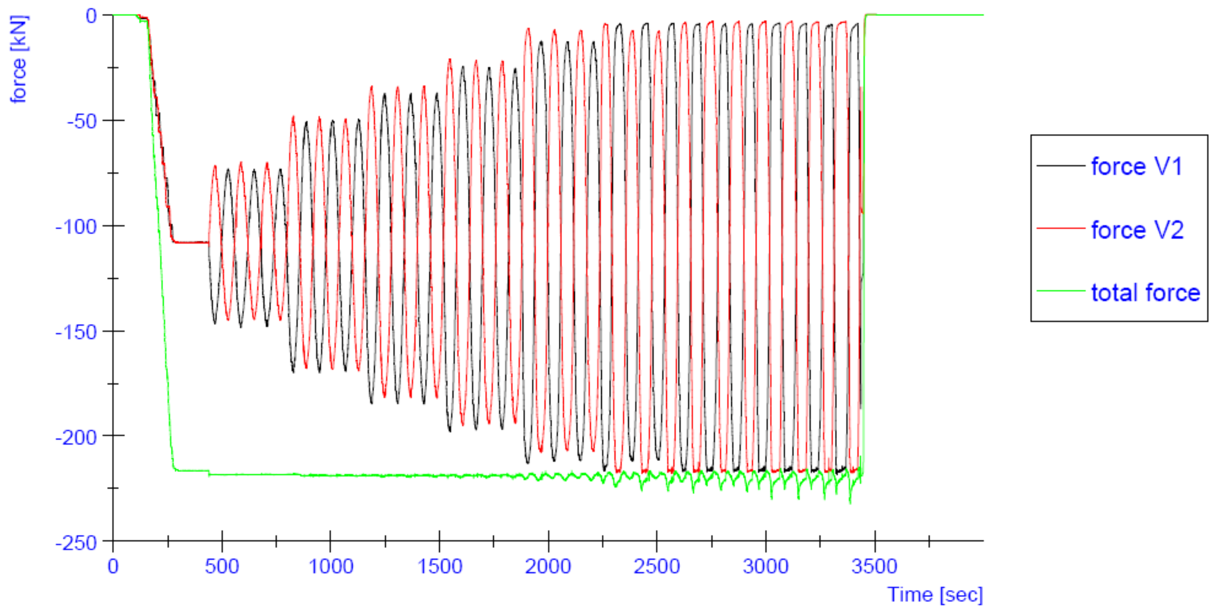

Figure 24: Progress of the vertical forces V1 and V2 during the test on specimen CS01

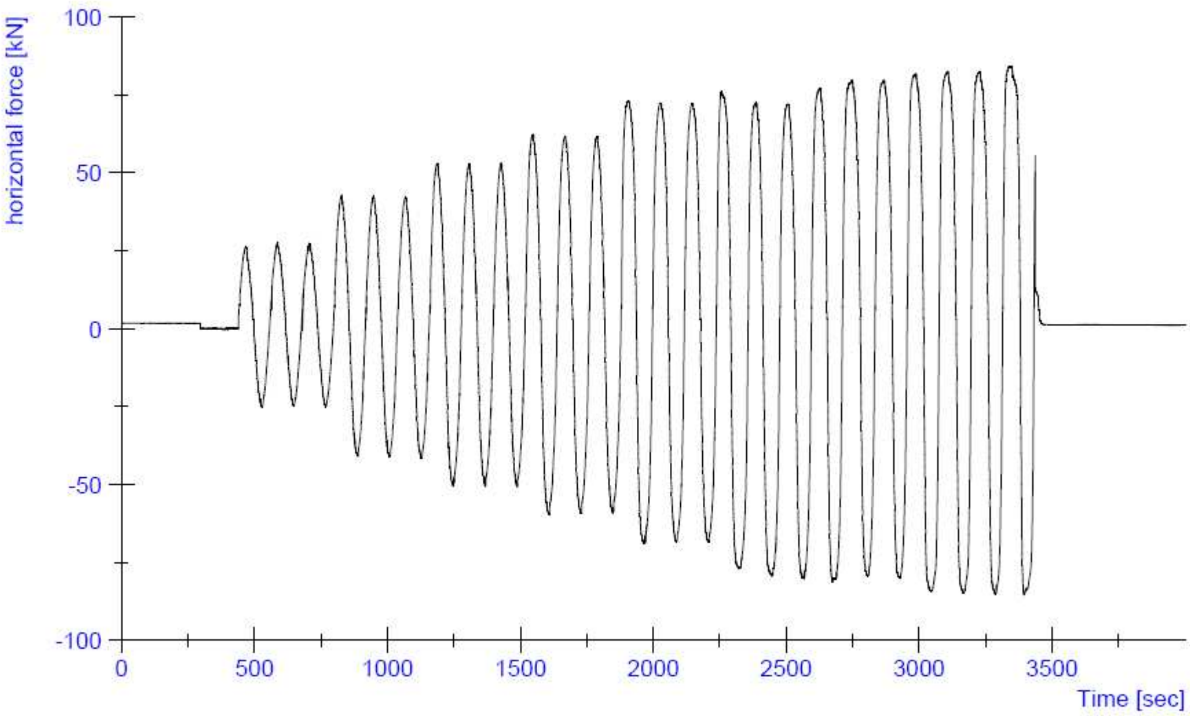

Figure 25: Progress of the horizontal force H during the test on specimen CS01

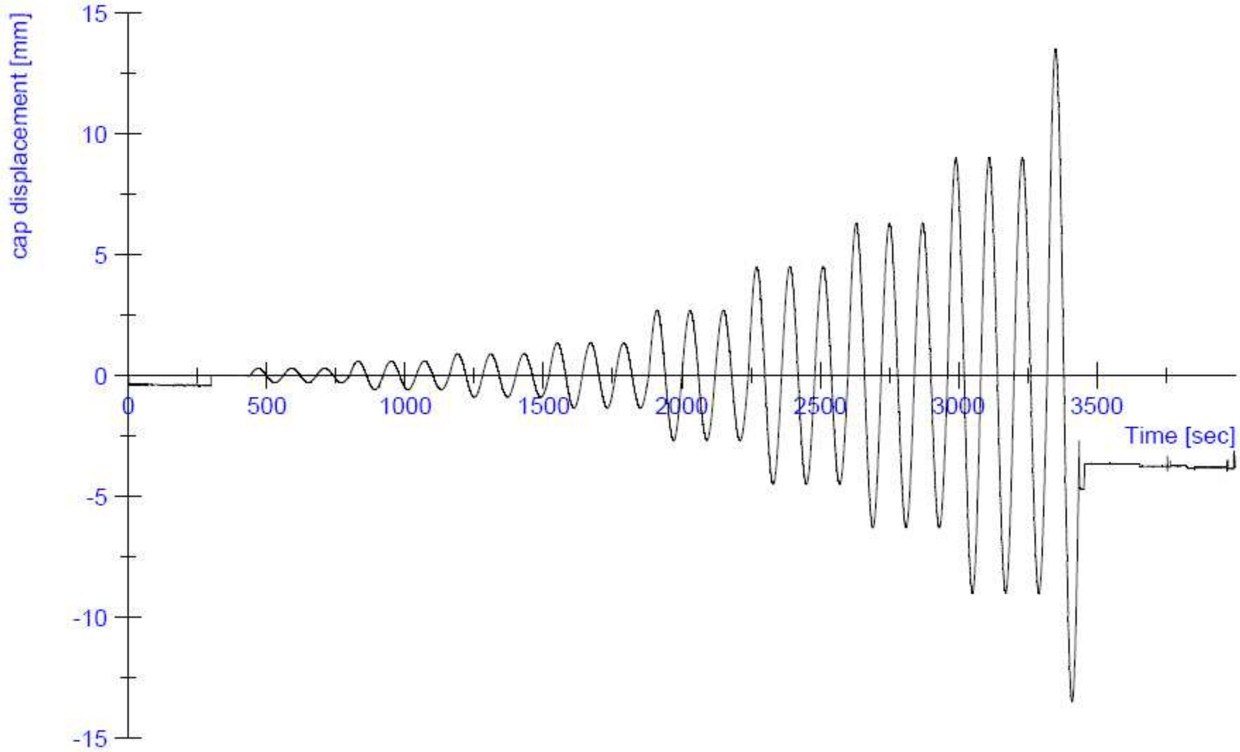

Figure 26: Progress of the horizontal displacement during the test on specimen CS01

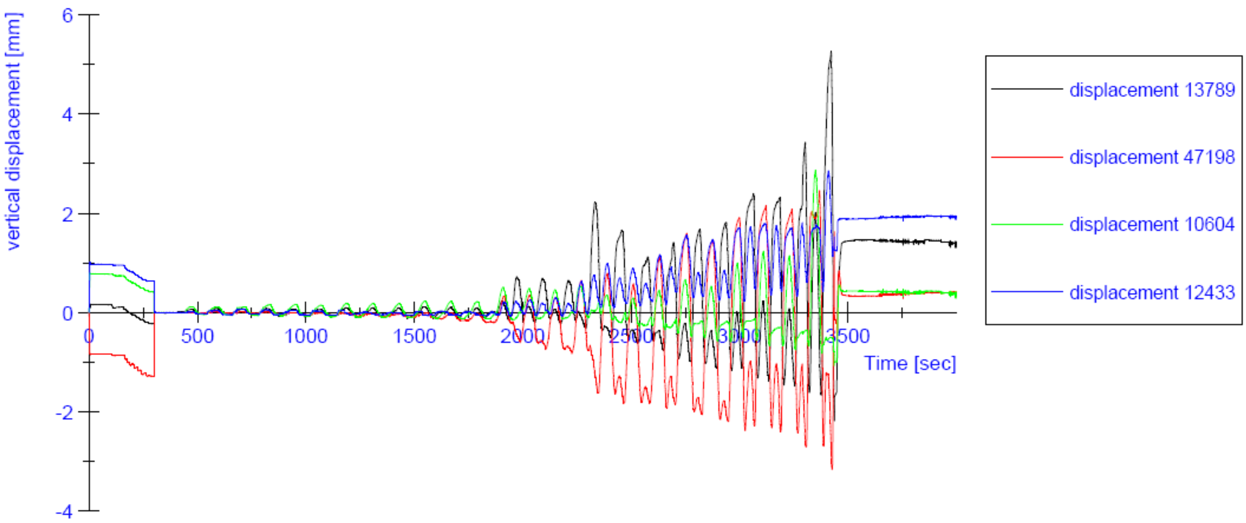

Figure 27: Progress of the vertical displacements during the test on specimen CS01

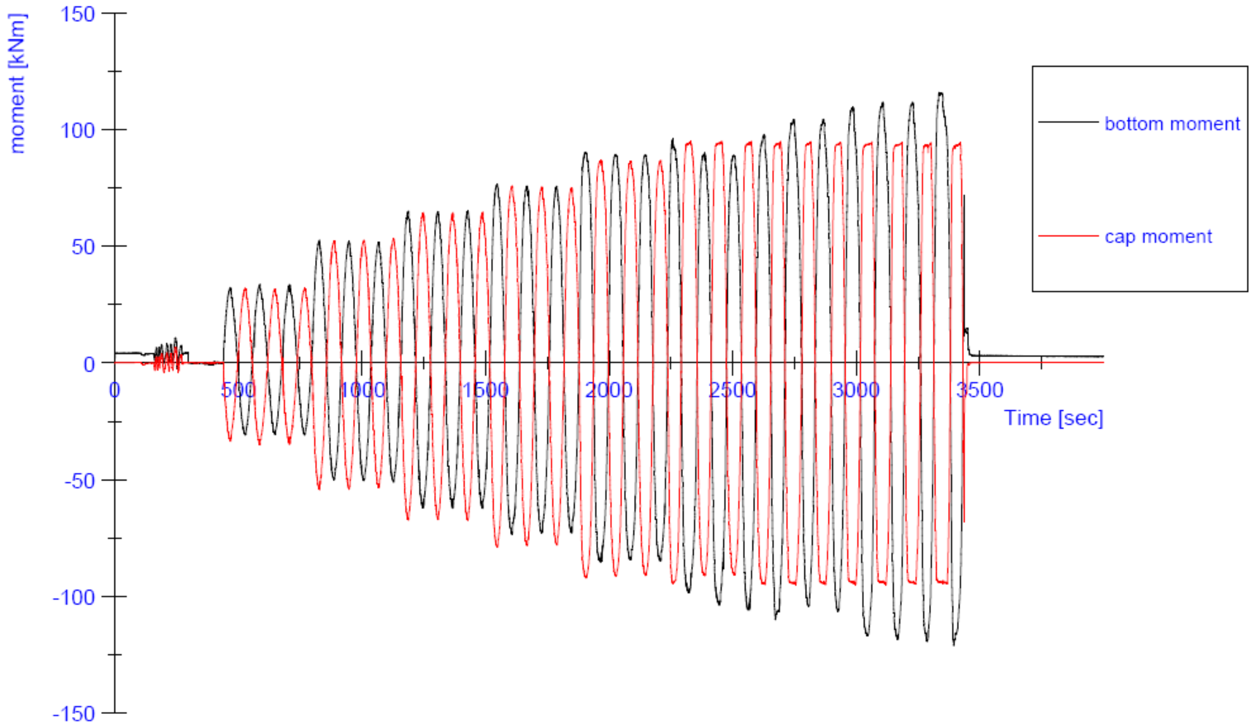

Figure 28: Progress of the in-plane bending moments at the top and at the bottom of the wall during the test on specimen CS01

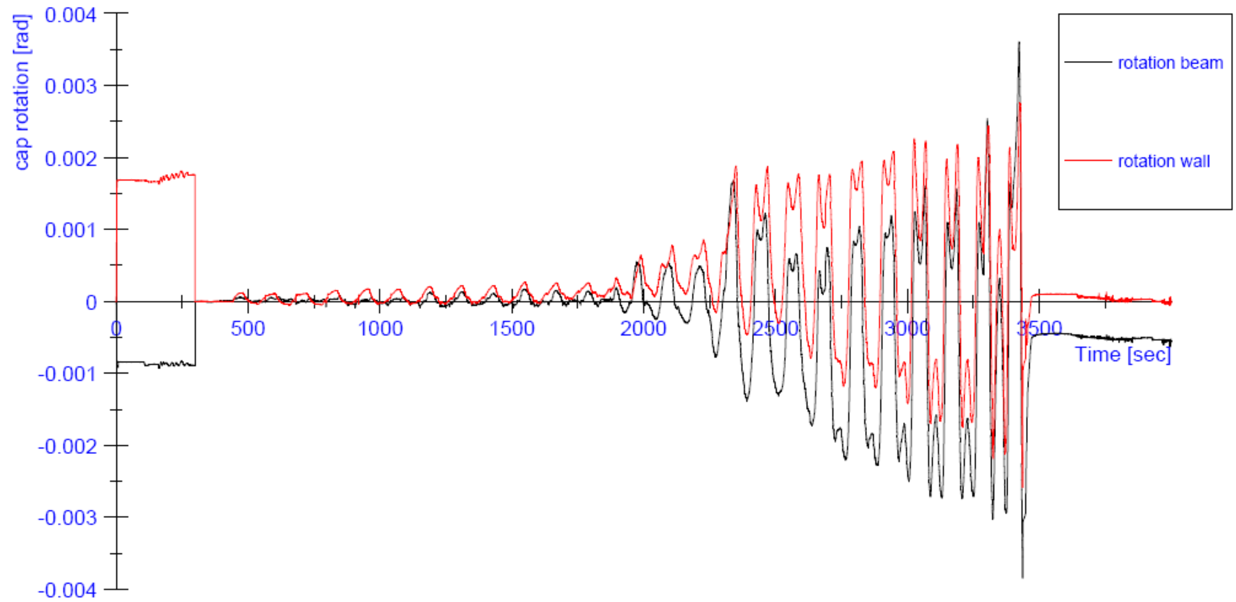

Figure 29: Progress of the in-plane rotation at the top of the wall during the test on specimen CS01

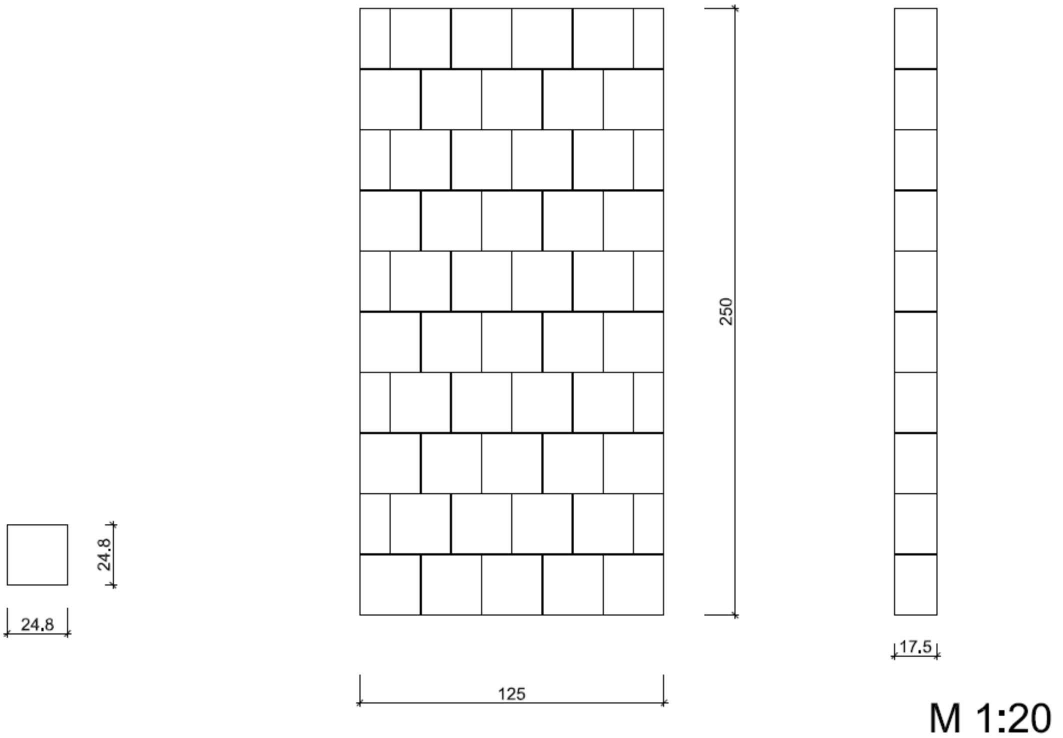

Figure 30: Dimension of the test specimen CS02

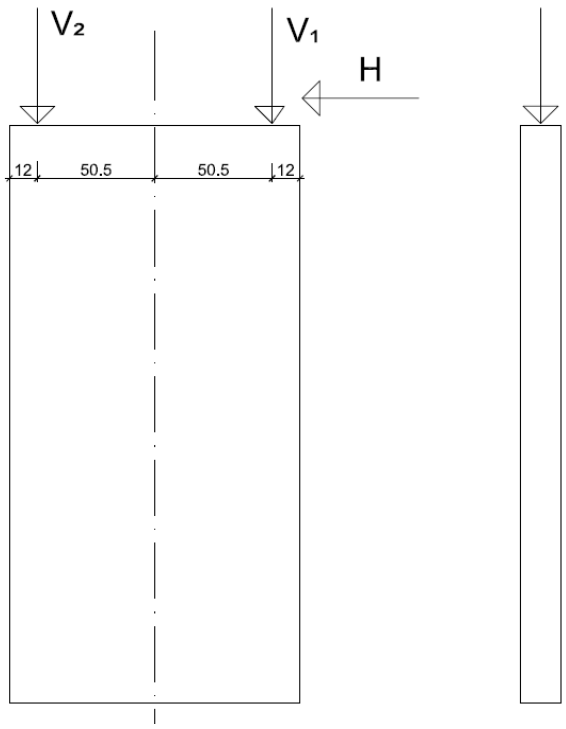

Figure 31: Position of the hydraulic actuators at test specimen CS02

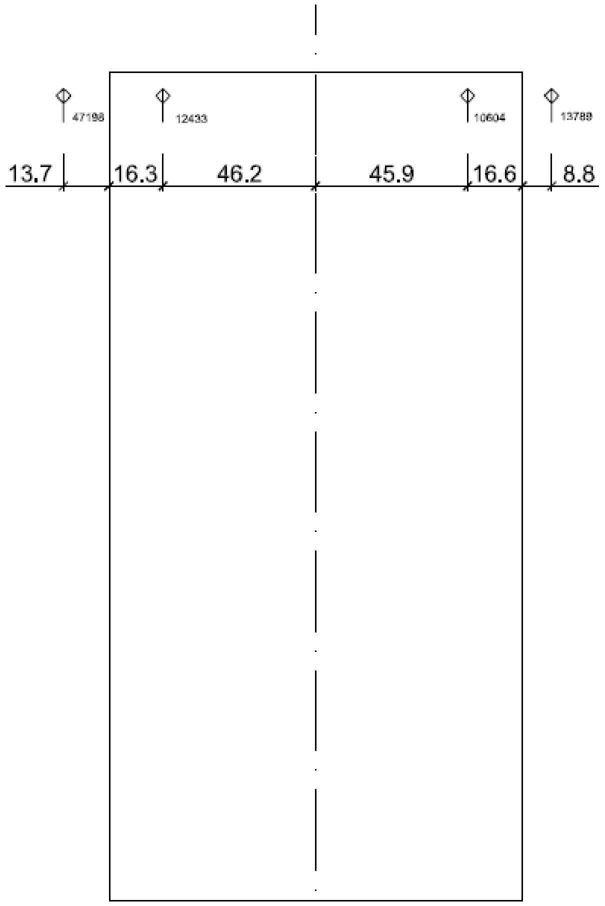

Figure 32: Position of the LVDTs at test specimen CS02

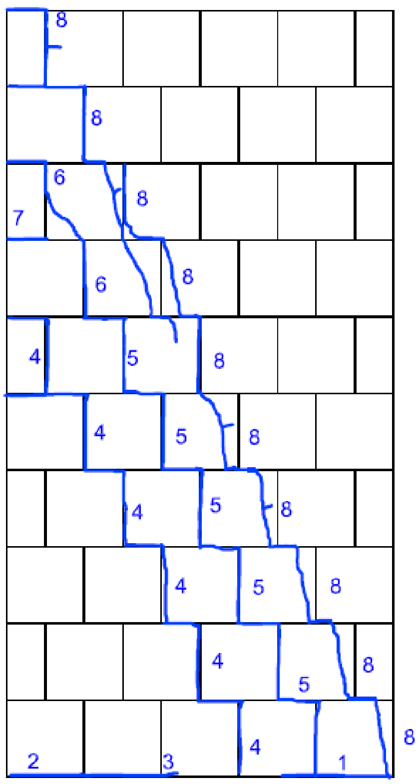

Figure 33: Crack pattern of the test specimen CS02

First crack: Final cracks:

Figure 34: Crack pattern of the test specimen CS02

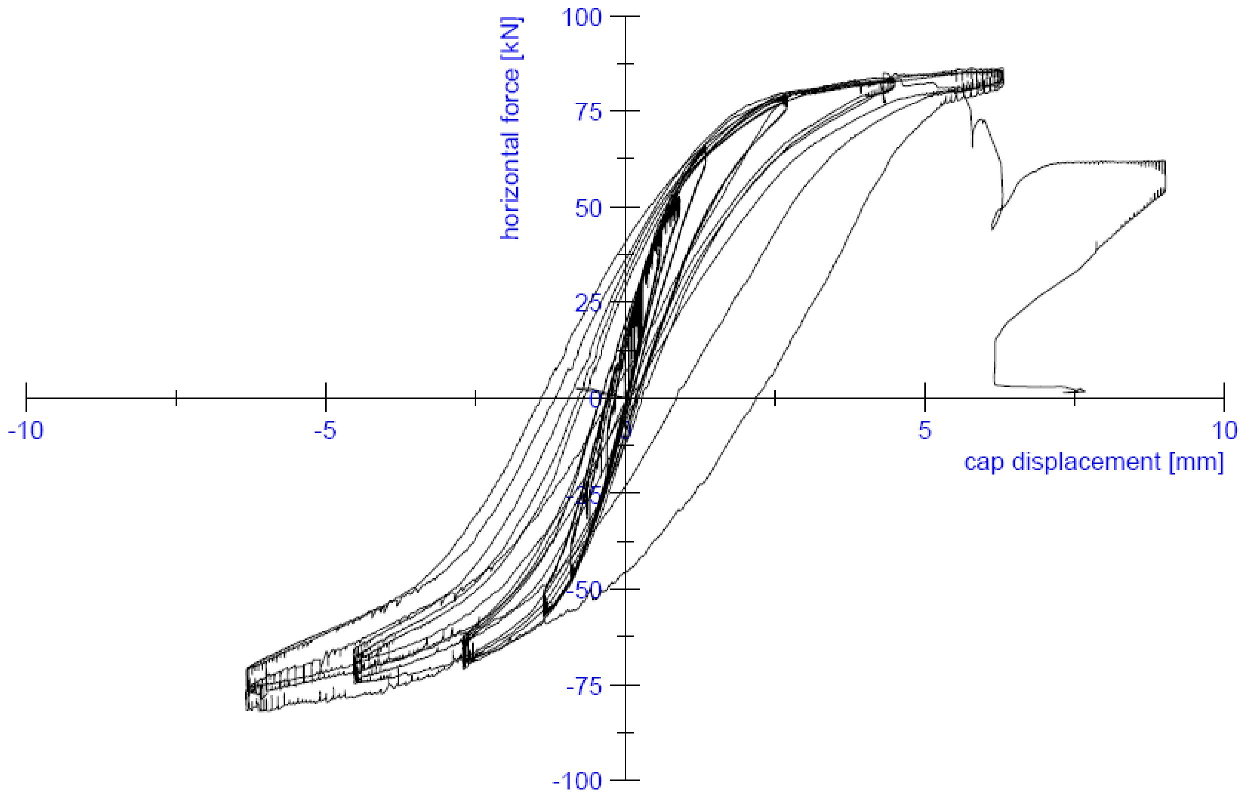

Figure 35: Load-displacement curve (hysteresis) of the test on specimen CS02

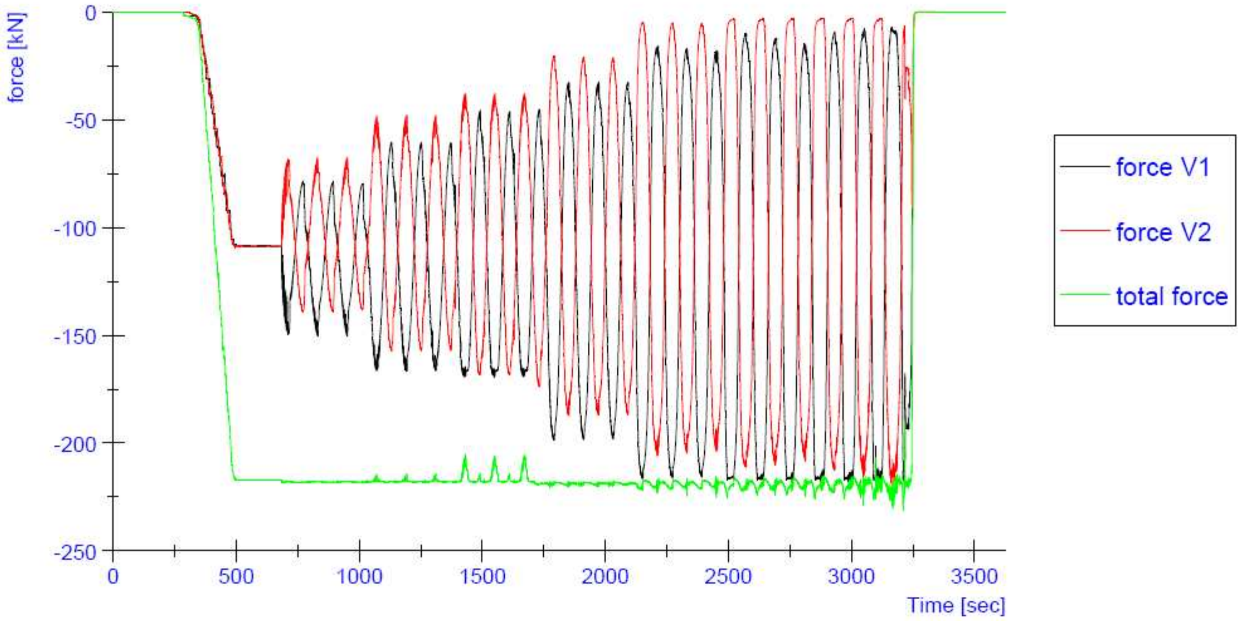

Figure 36: Progress of the vertical forces V1 and V2 during the test on specimen CS02

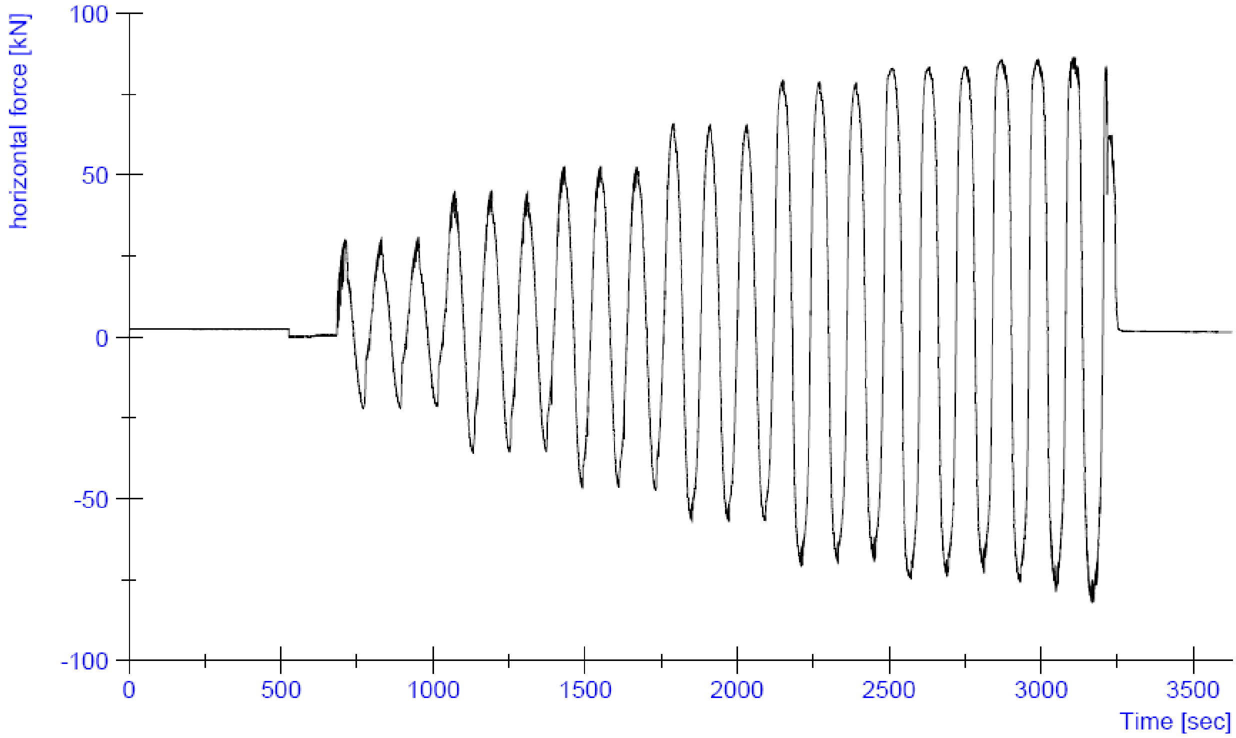

Figure 37: Progress of the horizontal force H during the test on specimen CS02

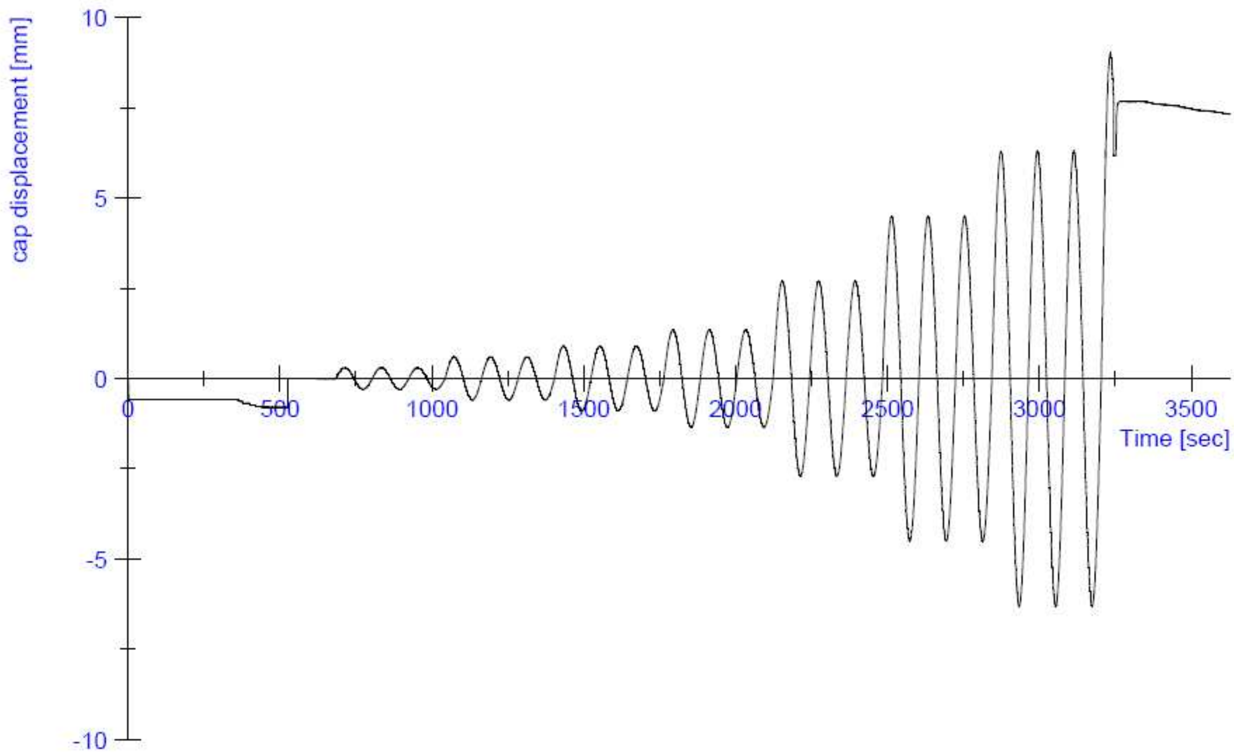

Figure 38: Progress of the horizontal displacement during the test on specimen CS02

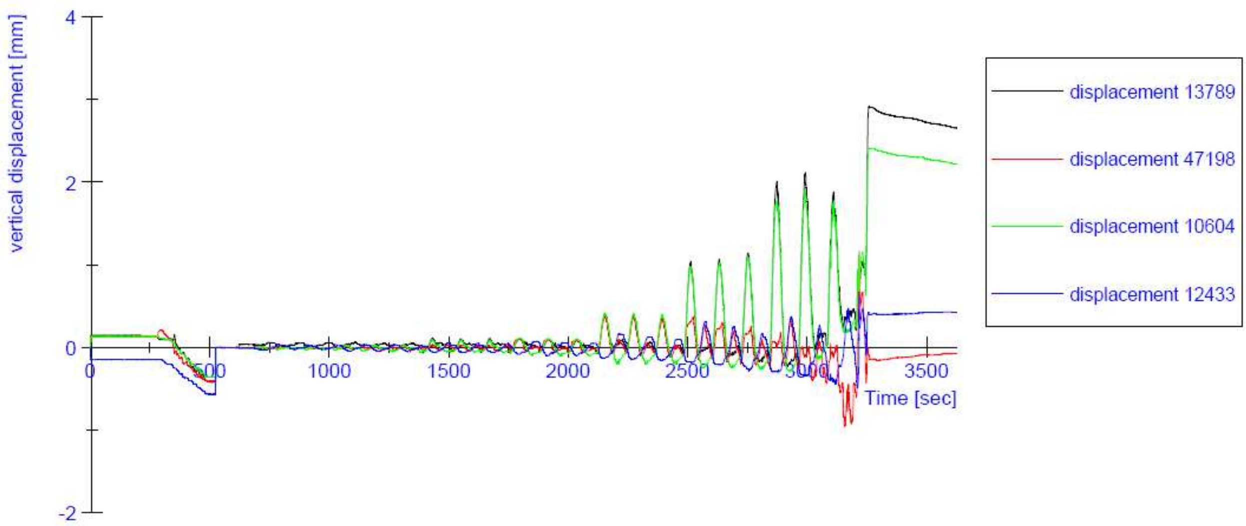

Figure 39: Progress of the vertical displacements during the test on specimen CS02

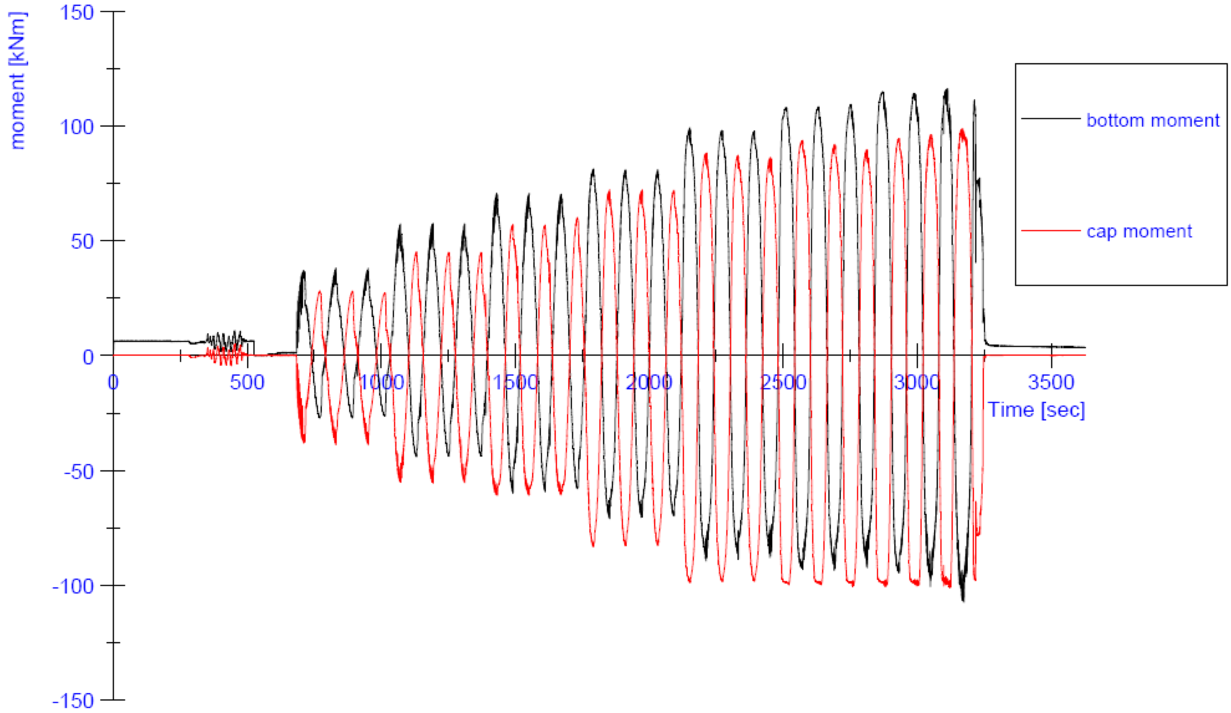

Figure 40: Progress of the in-plane bending moments at the top and at the bottom of the wall during the test on specimen CS02

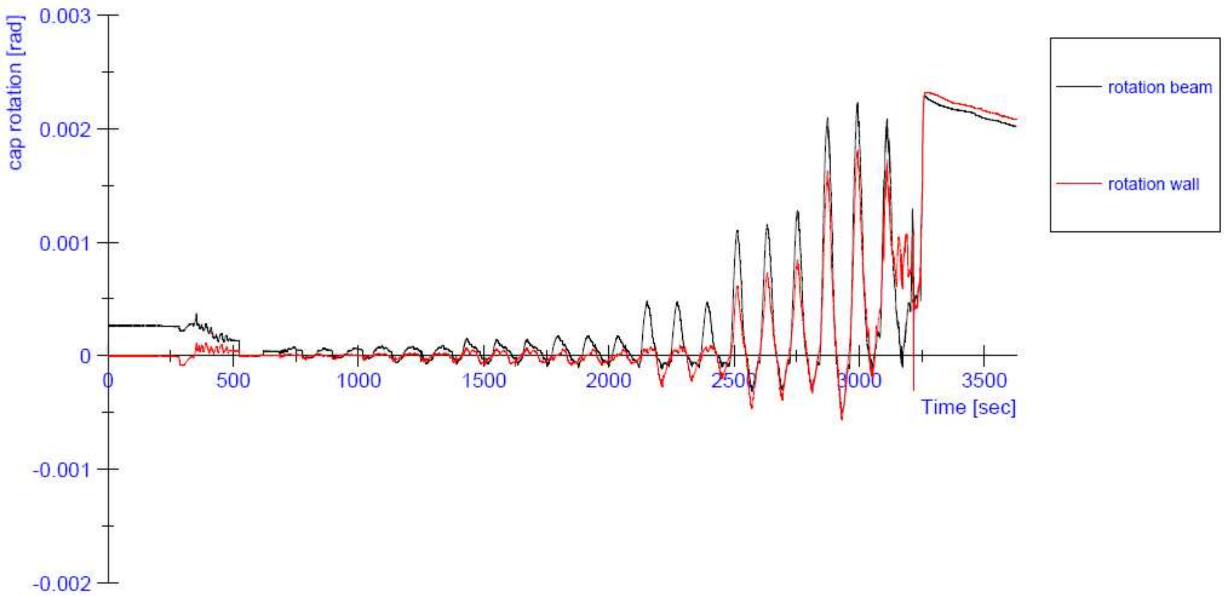

Figure 41: Progress of the in-plane rotation at the top of the wall during the test on specimen CS02

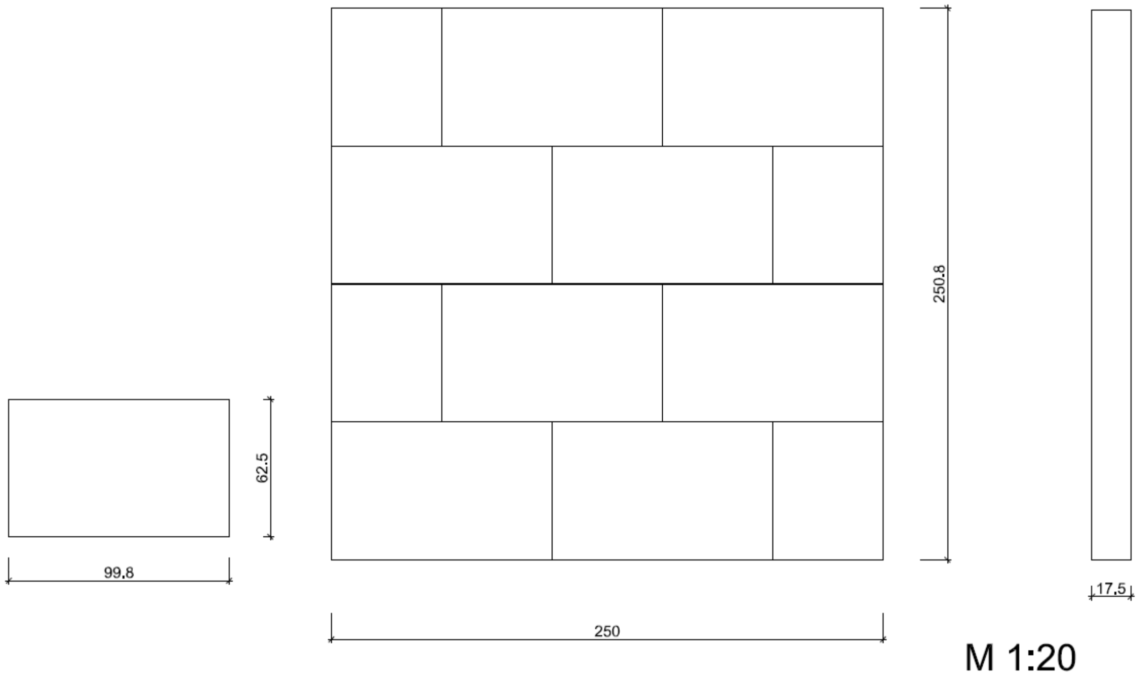

Figure 42: Dimension of the test specimen CS03

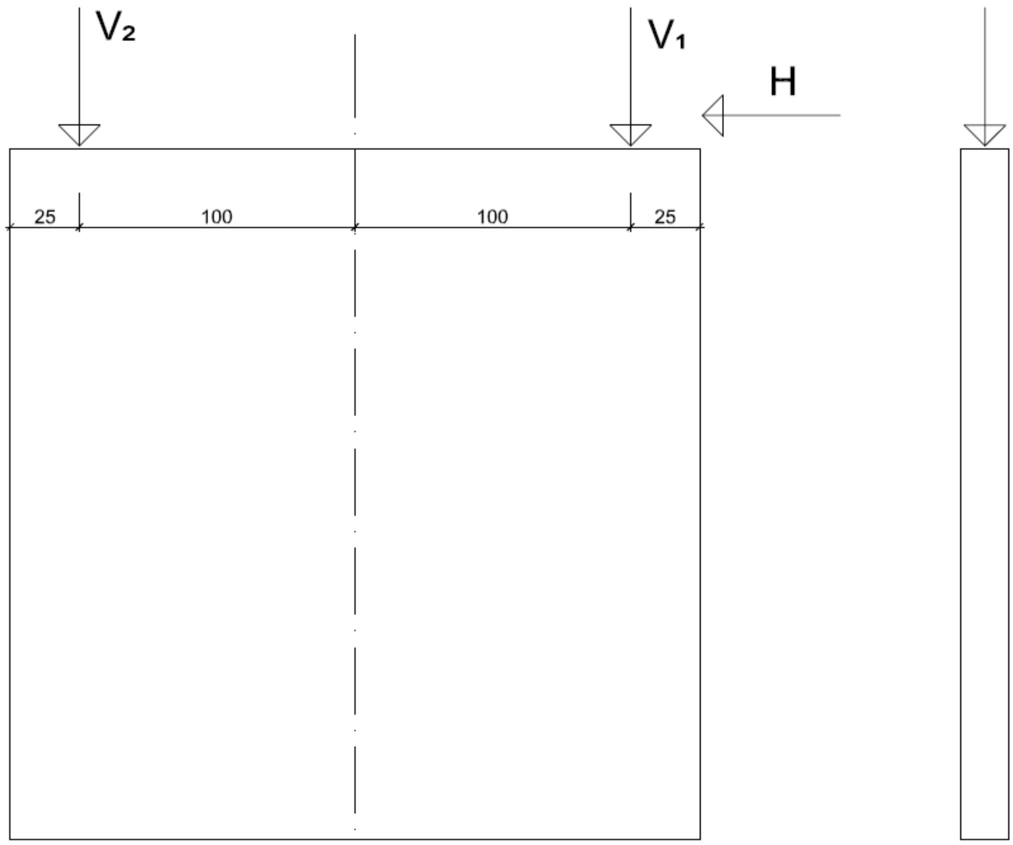

Figure 43: Position of the hydraulic actuators at test specimen CS03

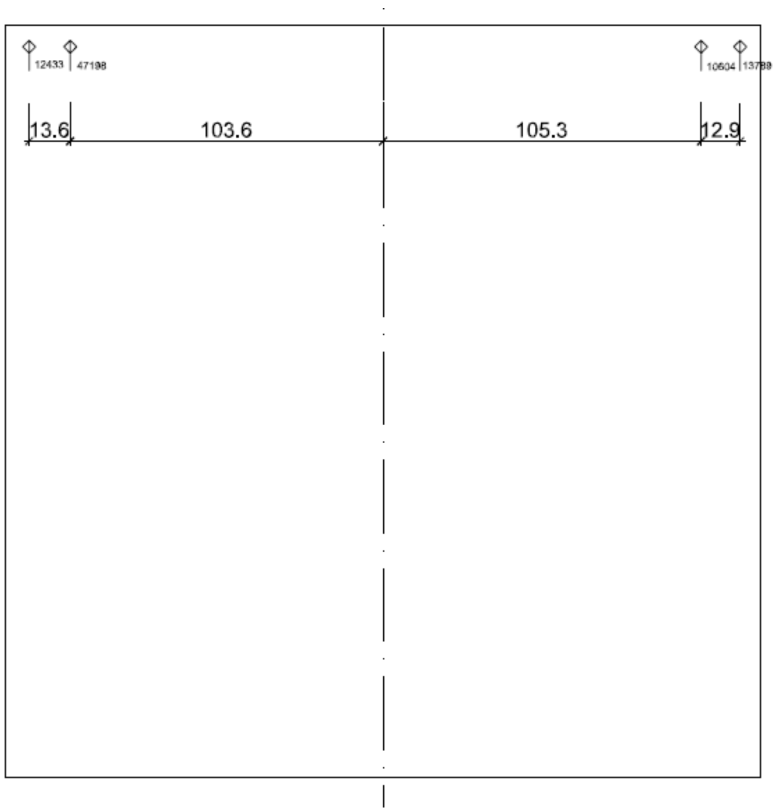

Figure 44: Position of the LVDTs at test specimen CS03

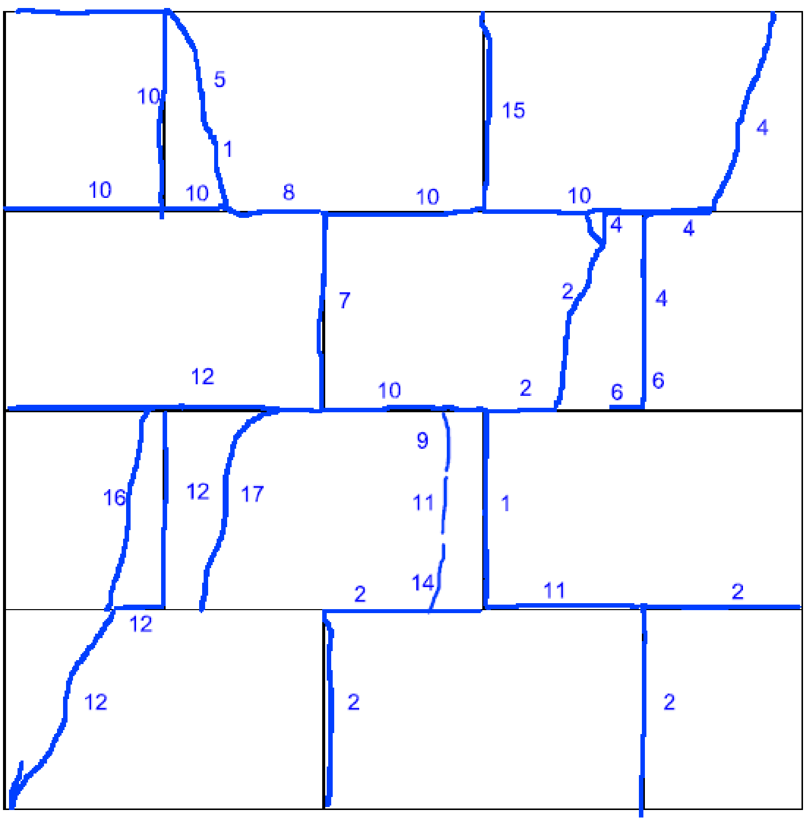

Figure 45: Crack pattern of the test specimen CS03

First crack:

Final cracks:

Figure 46: Crack pattern of the test specimen CS03

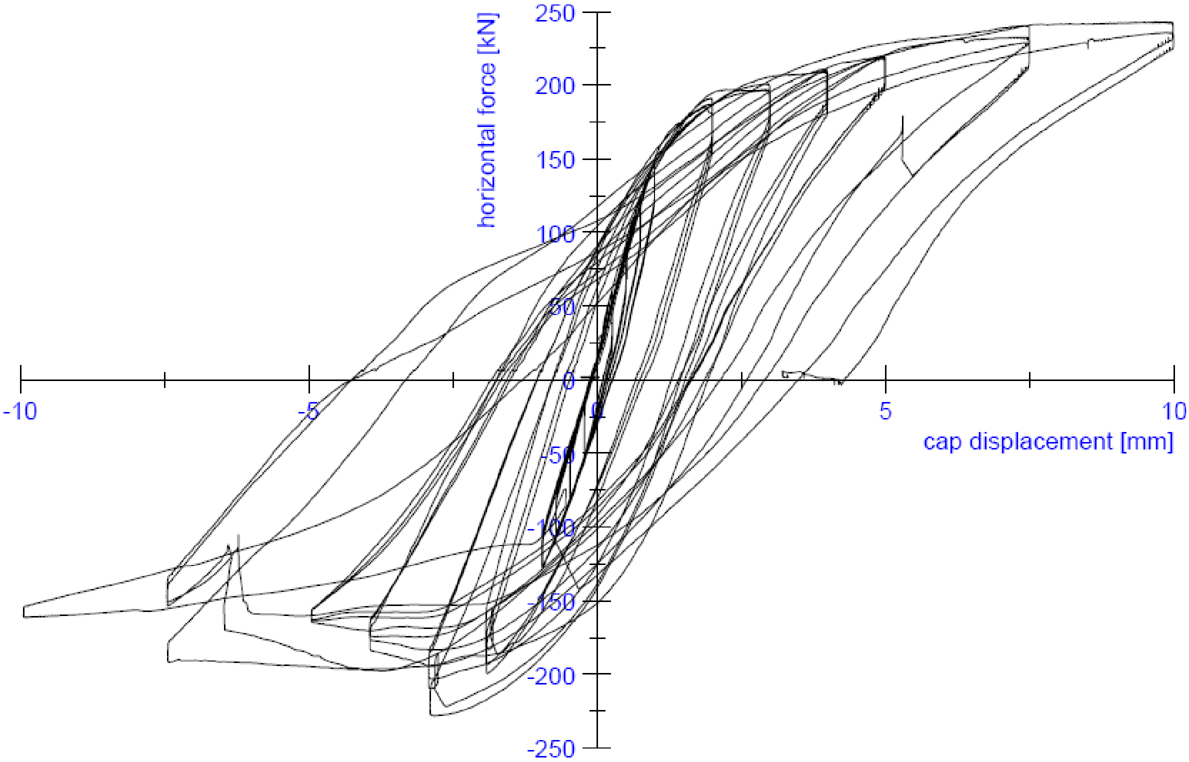

Figure 47: Load-displacement curve (hysteresis) of the test on specimen CS03

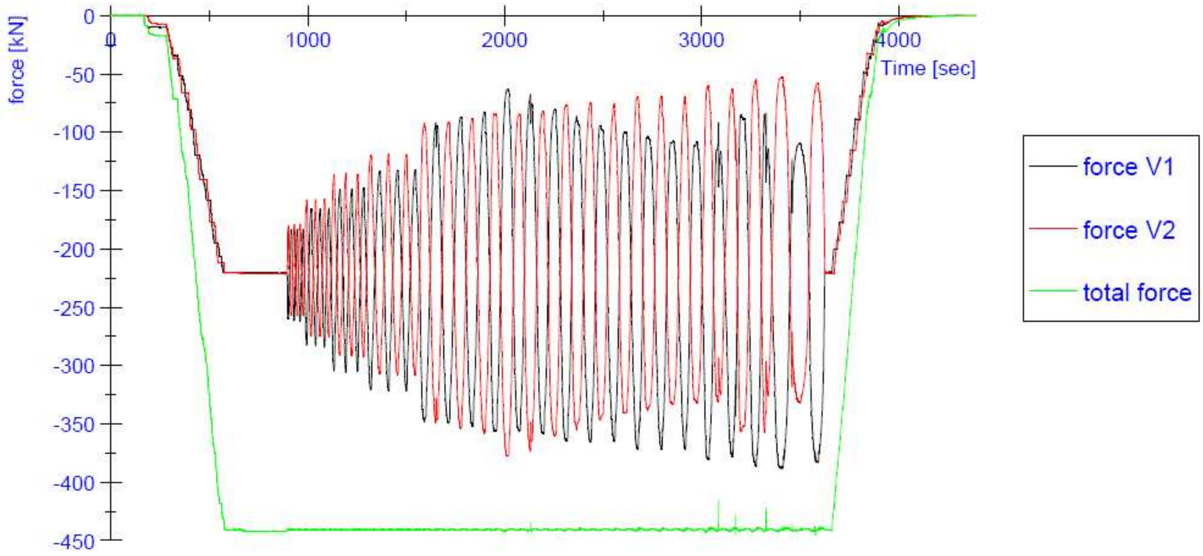

Figure 48: Progress of the vertical forces V1 and V2 during the test on specimen CS03

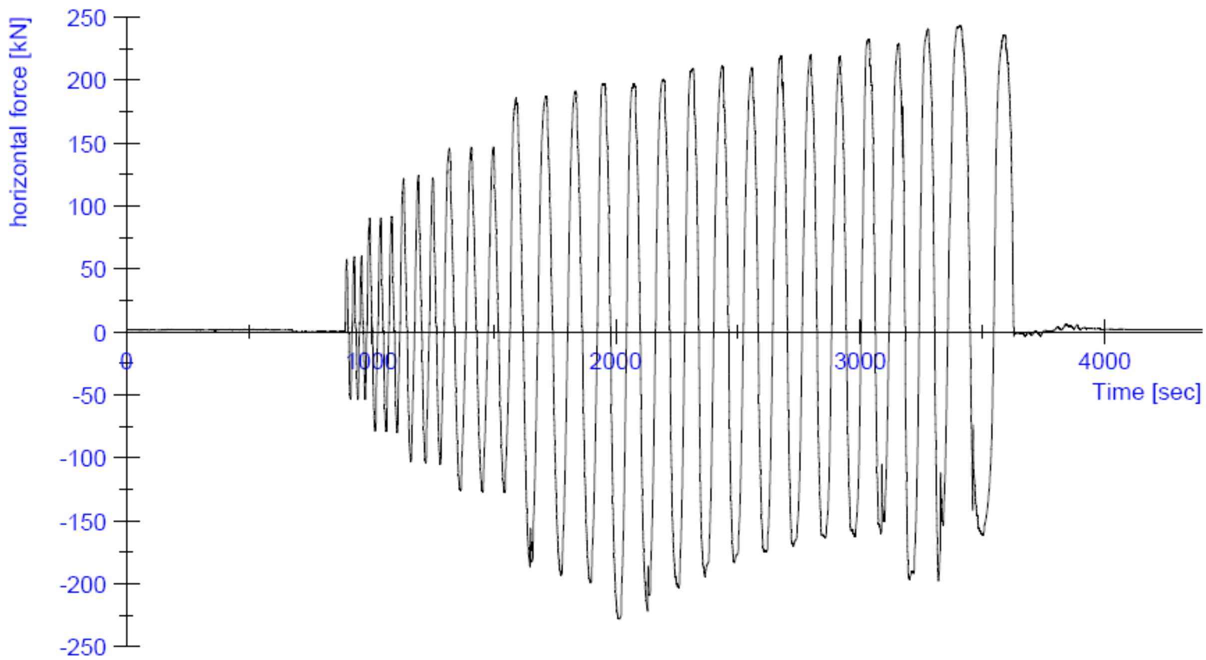

Figure 49: Progress of the horizontal force H during the test on specimen CS03

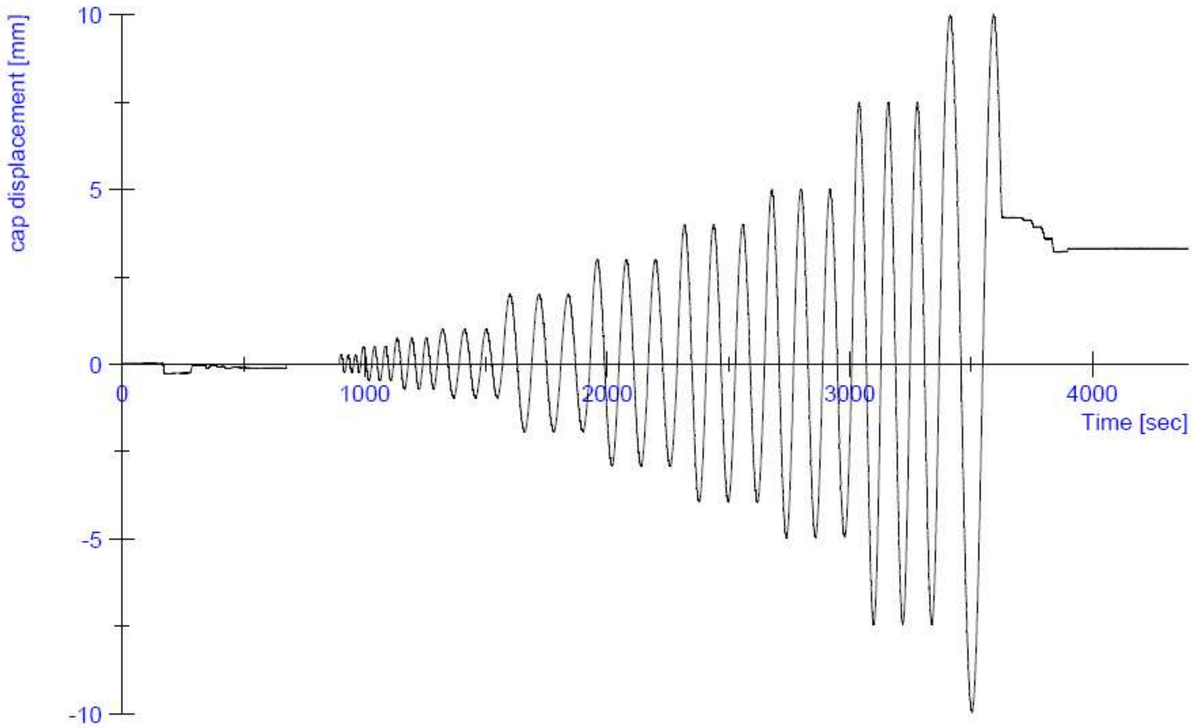

Figure 50: Progress of the horizontal displacement during the test on specimen CS03

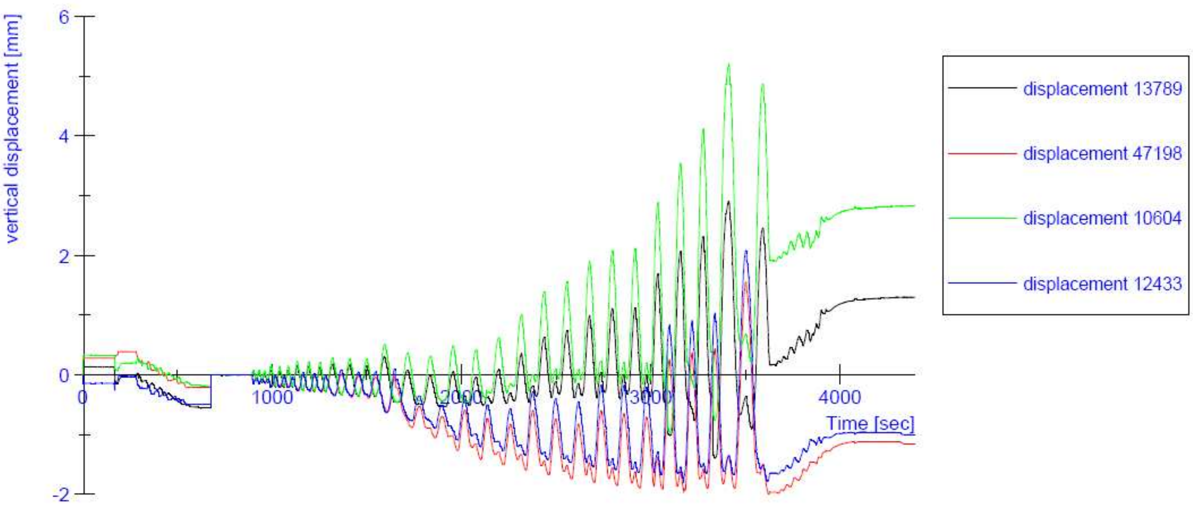

Figure 51: Progress of the vertical displacements during the test on specimen CS03

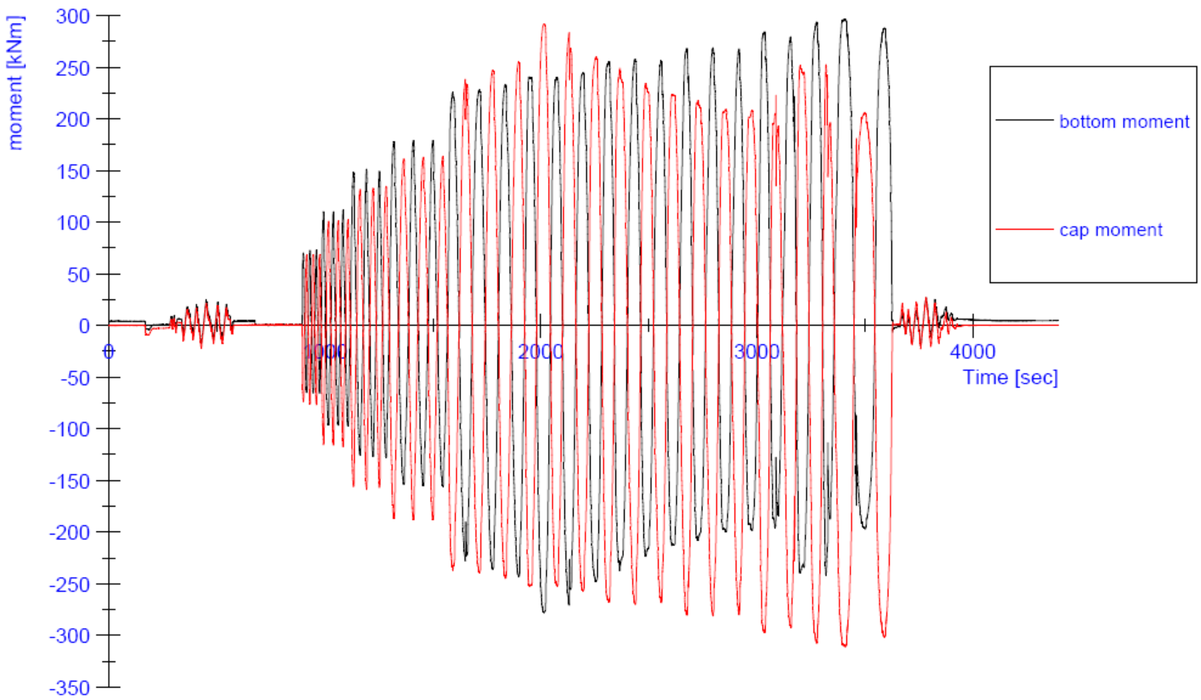

Figure 52: Progress of the in-plane bending moments at the top and at the bottom of the wall during the test on specimen CS03

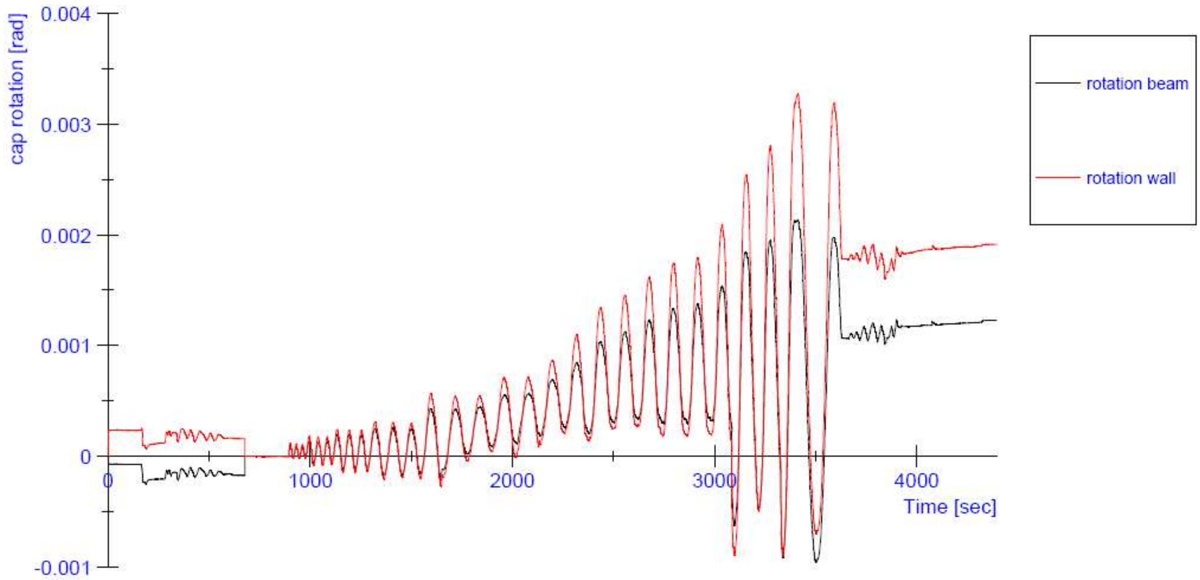

Figure 53: Progress of the in-plane rotation at the top of the wall during the test on specimen CS03

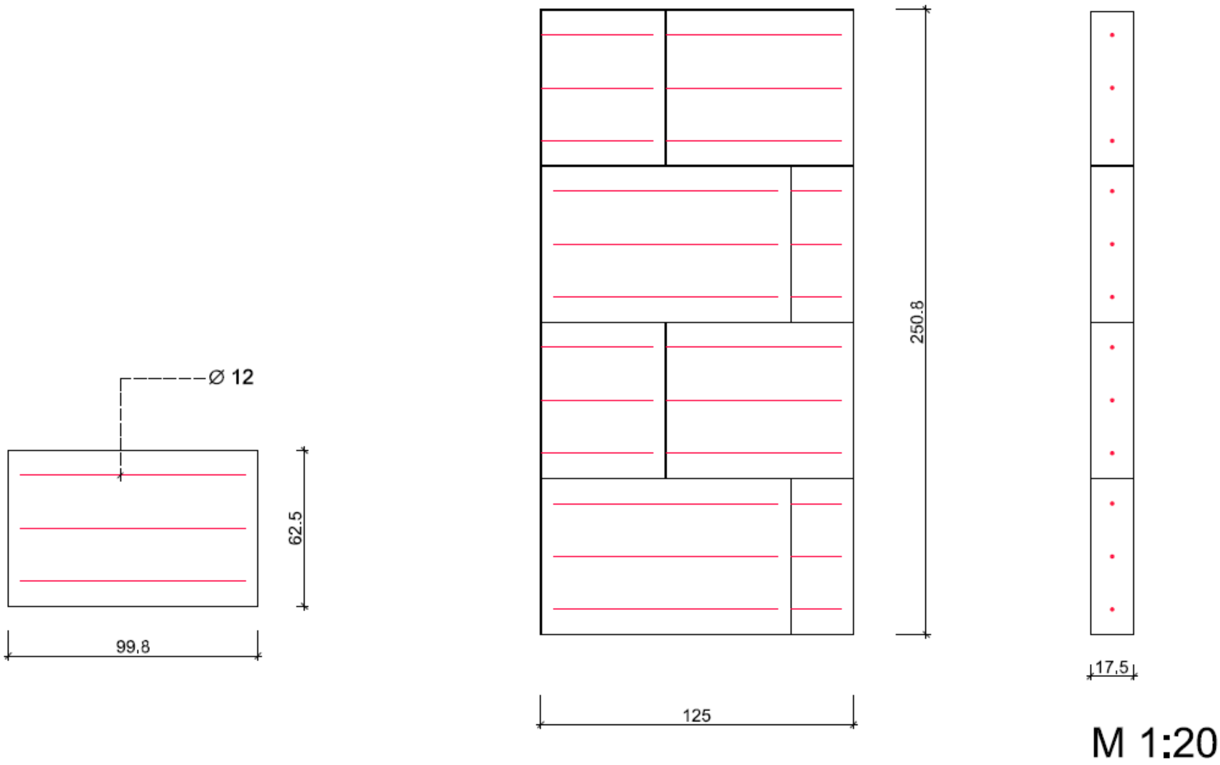

Figure 54: Dimension of the test specimen CS04 with the internal reinforcement

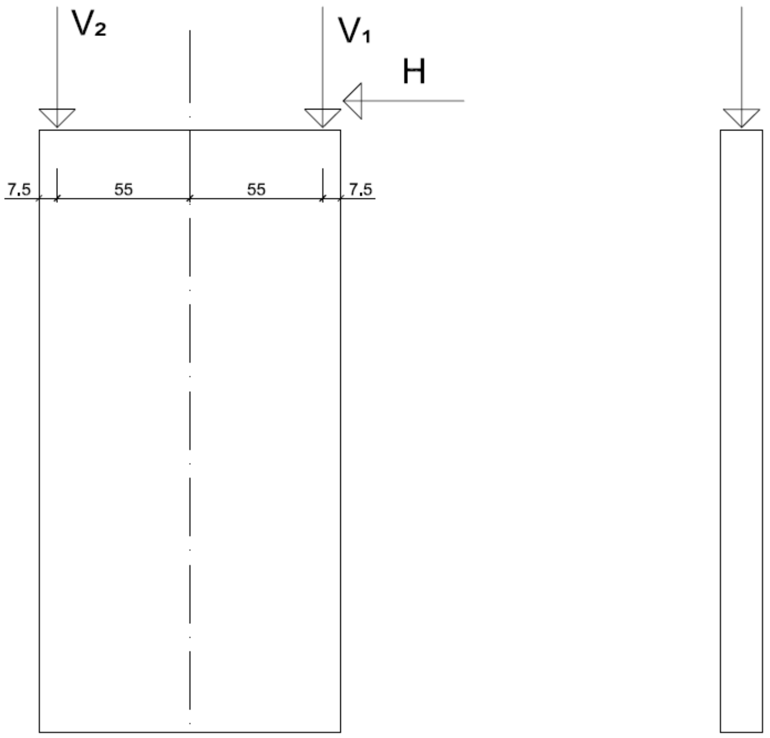

Figure 55: Position of the hydraulic actuators at test specimen CS04

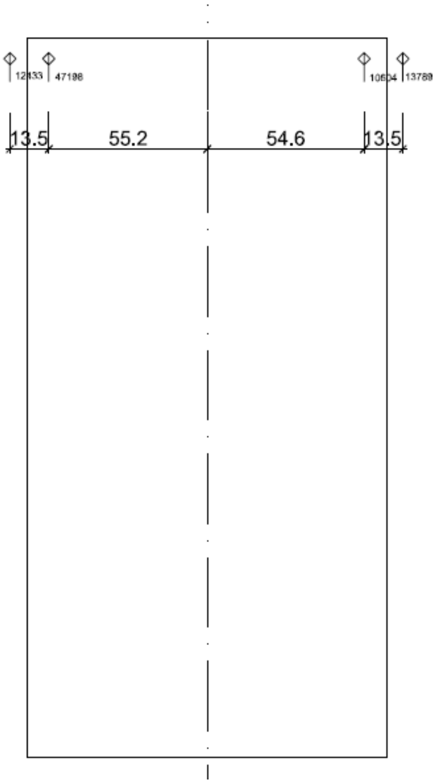

Figure 56: Position of the LVDTs at test specimen CS04

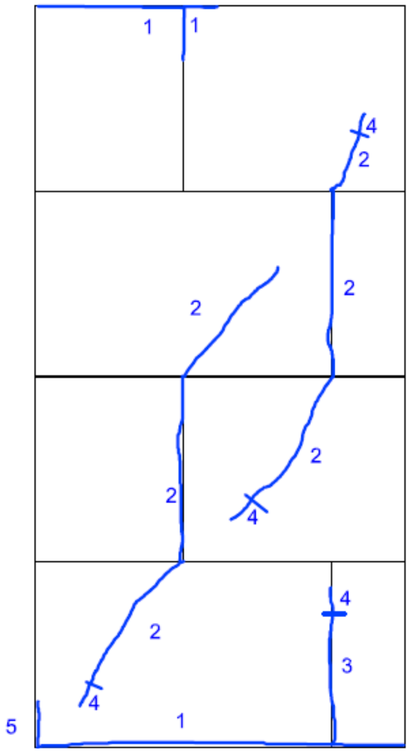

Figure 57: Crack pattern of the test specimen CS04

Final cracks:

Figure 58: Crack pattern of the test specimen CS04

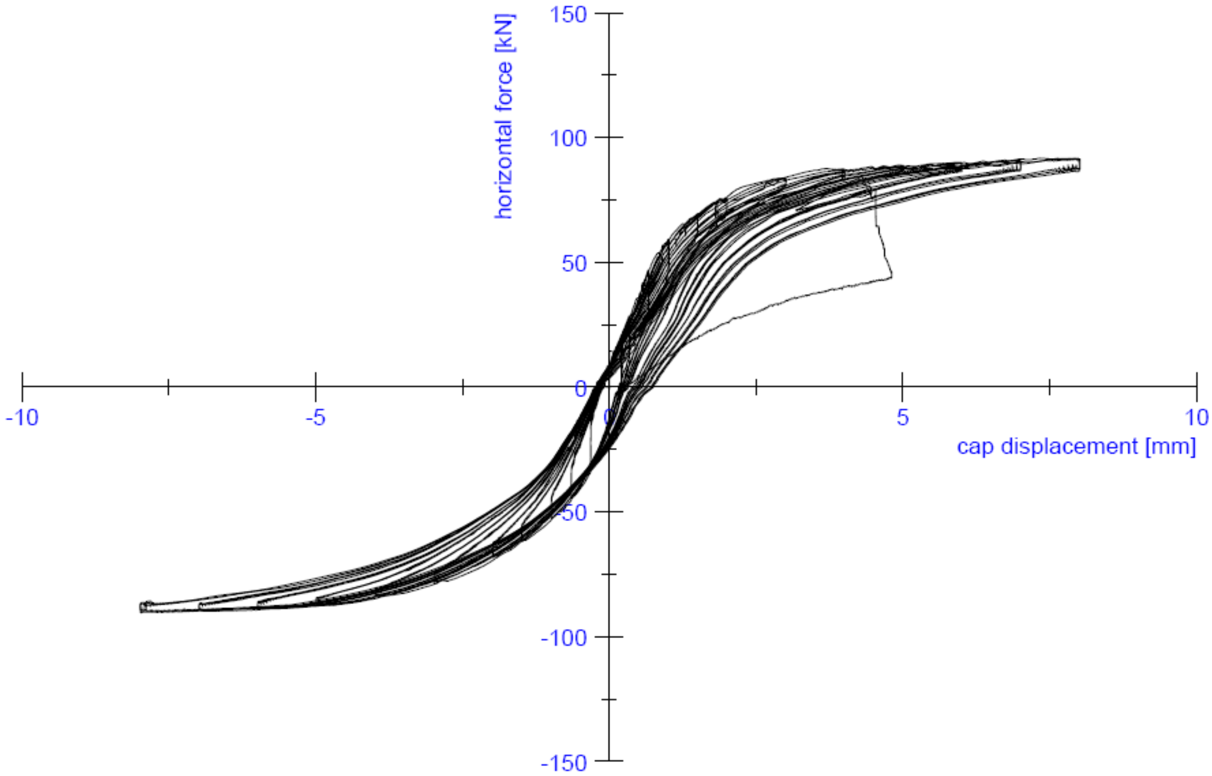

Figure 59: Load-displacement curve (hysteresis) of the test on specimen CS04

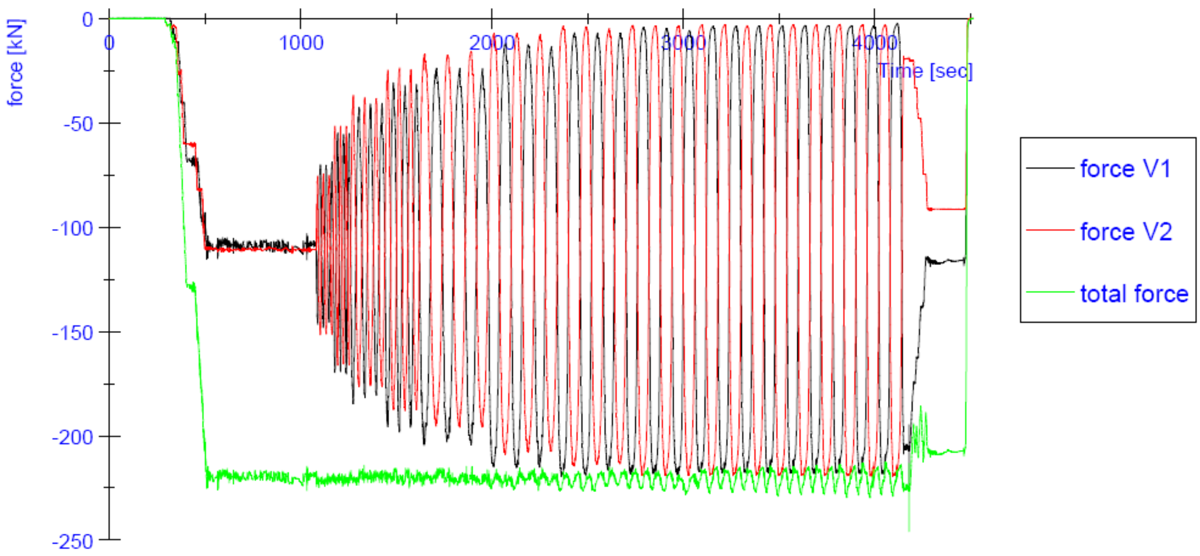

Figure 60: Progress of the vertical forces V1 and V2 during the test on specimen CS04

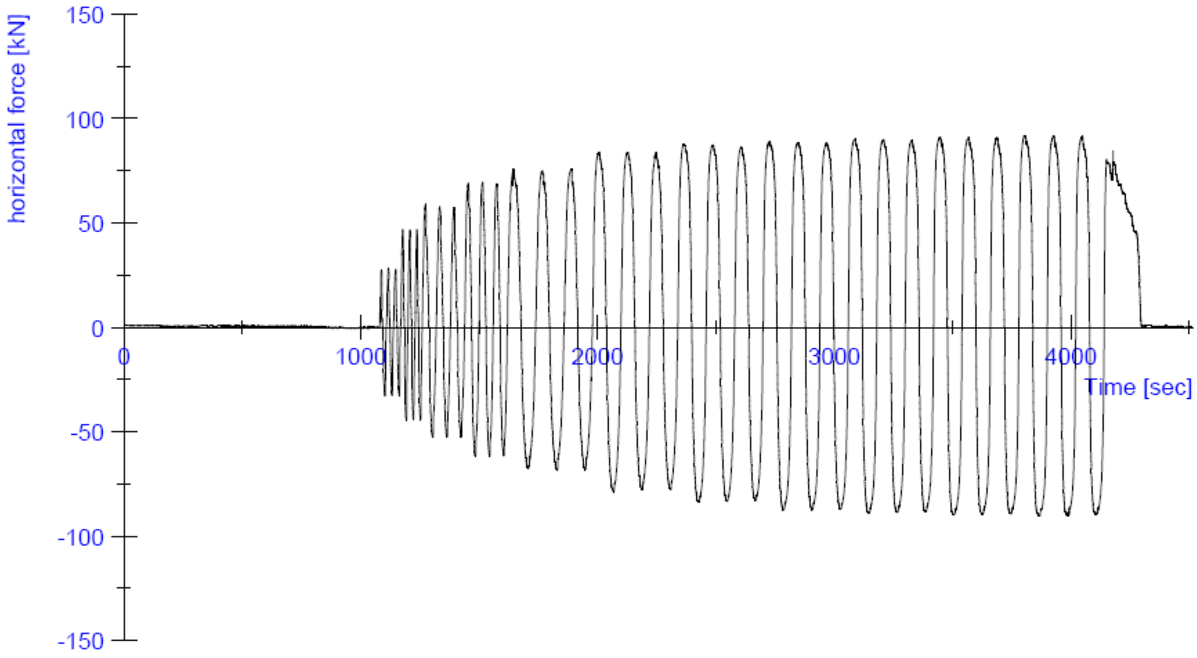

Figure 61: Progress of the horizontal force H during the test on specimen CS04

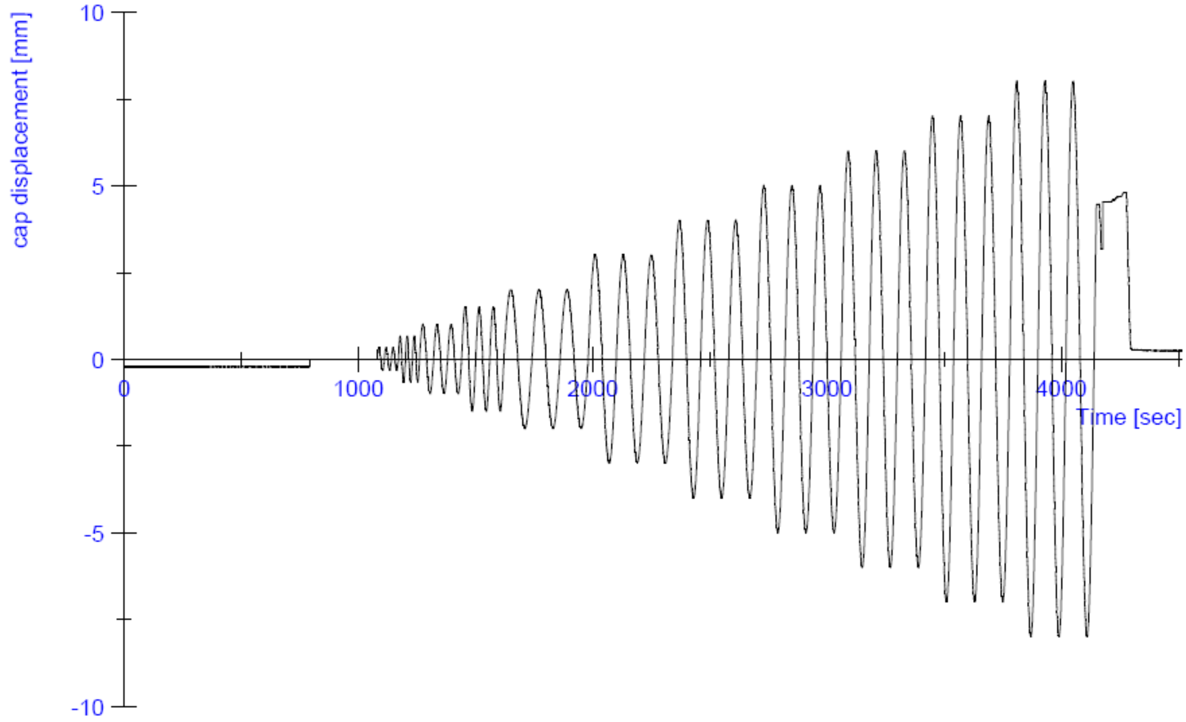

Figure 62: Progress of the horizontal displacement during the test on specimen CS04

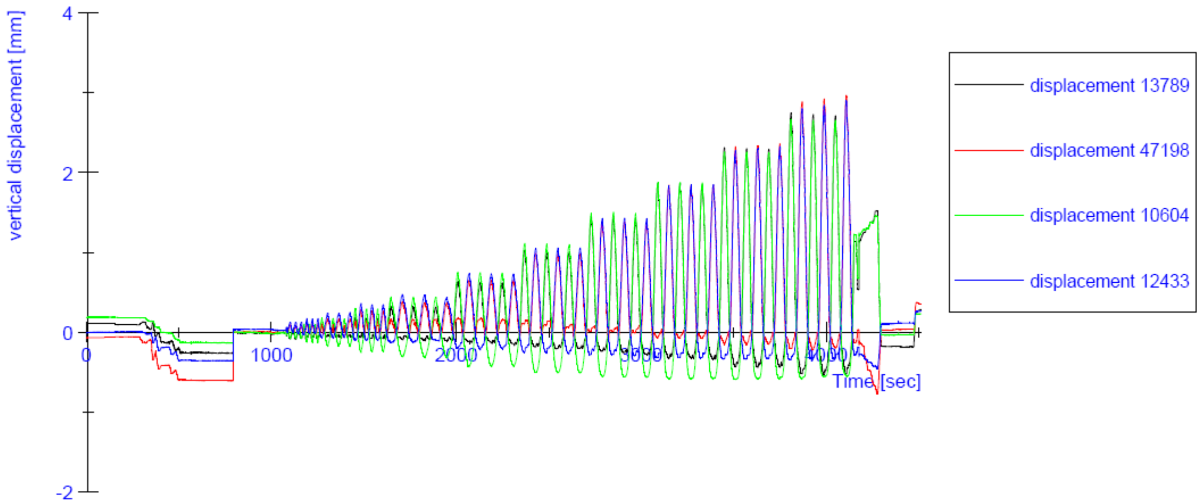

Figure 63: Progress of the vertical displacements during the test on specimen CS04

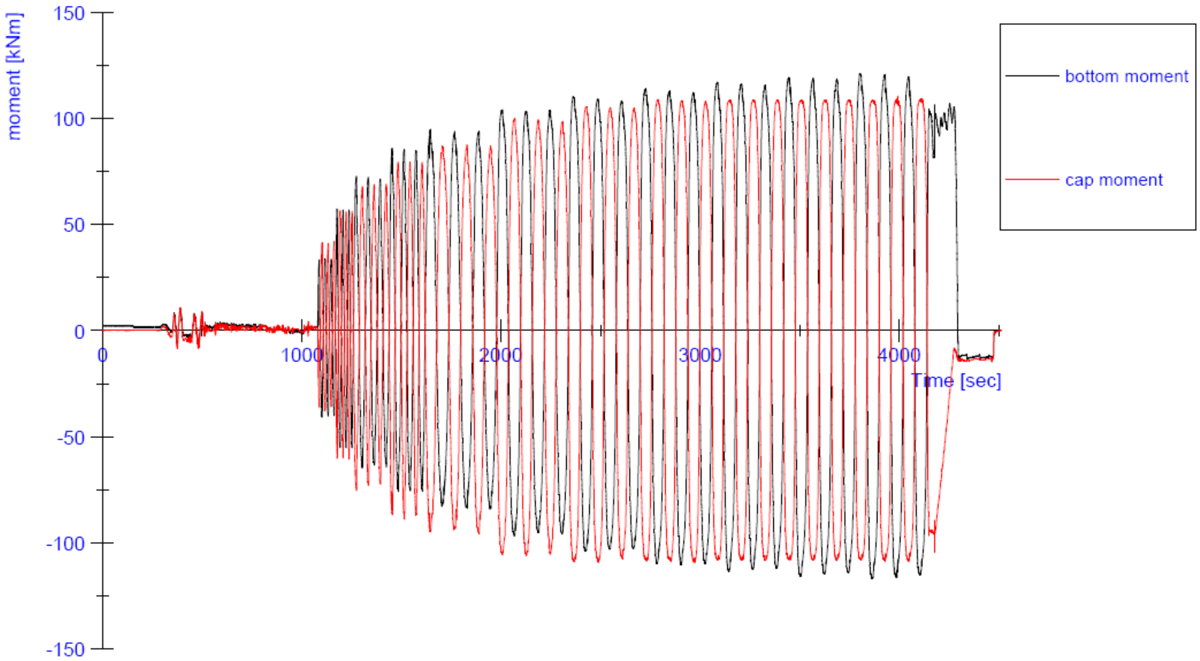

Figure 64: Progress of the in-plane bending moments at the top and at the bottom of the wall during the test on specimen CS04

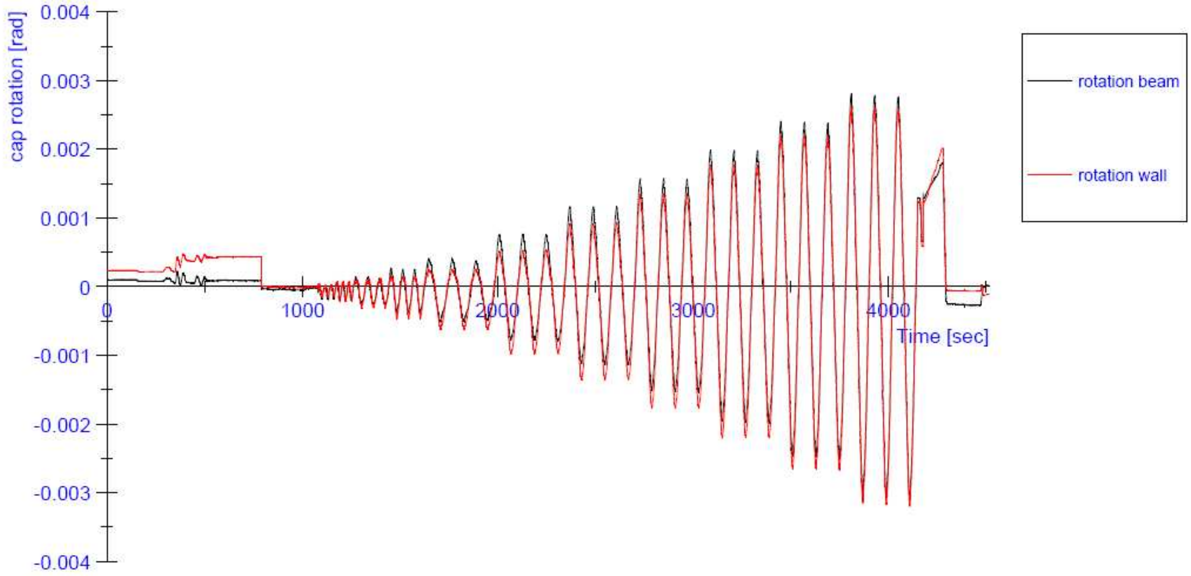

Figure 65: Progress of the in-plane rotation at the top of the wall during the test on specimen CS04

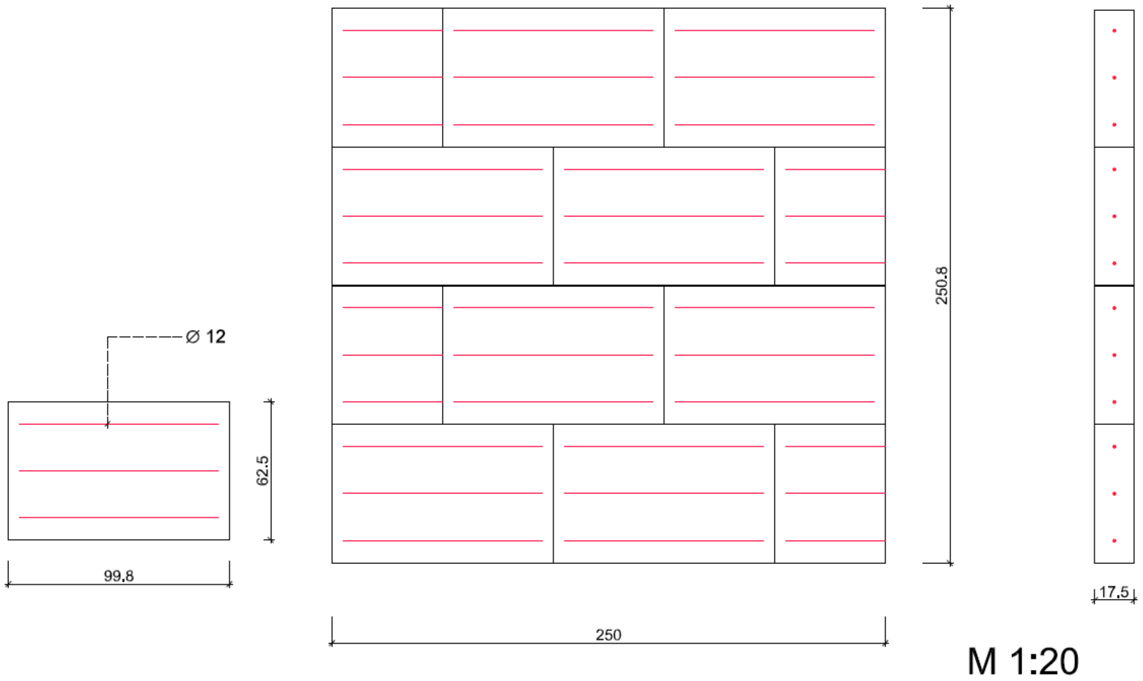

Figure 66: Dimension of the test specimen CS05

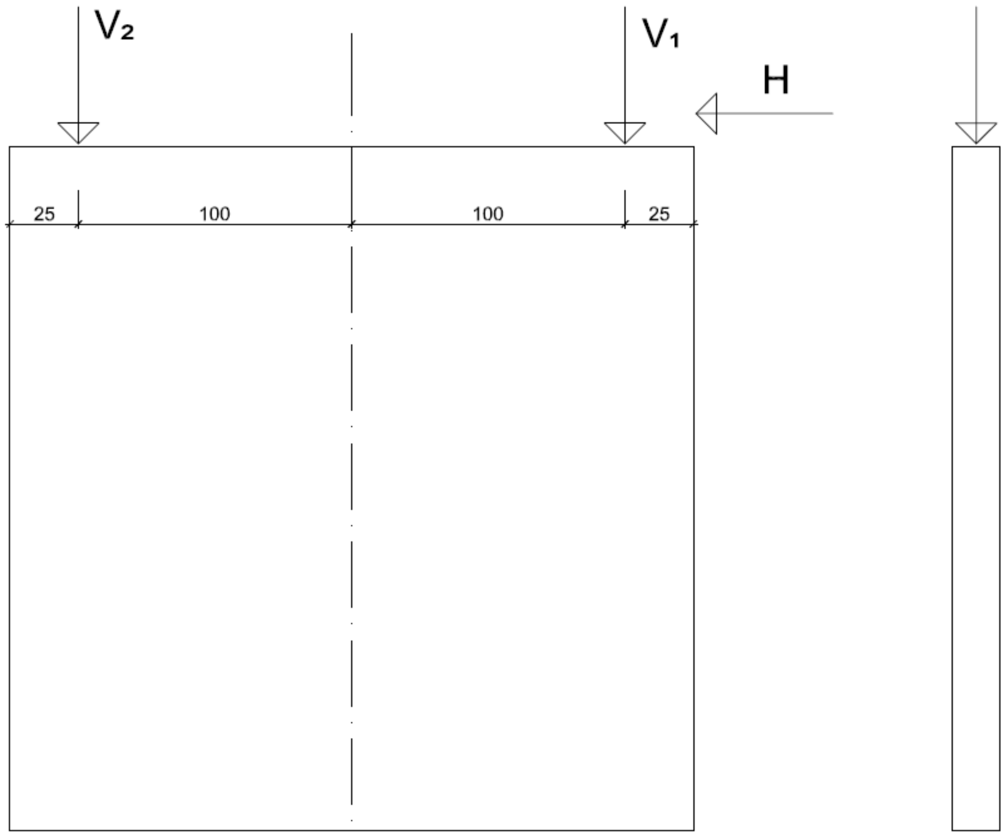

Figure 67: Position of the hydraulic actuators at test specimen CS05

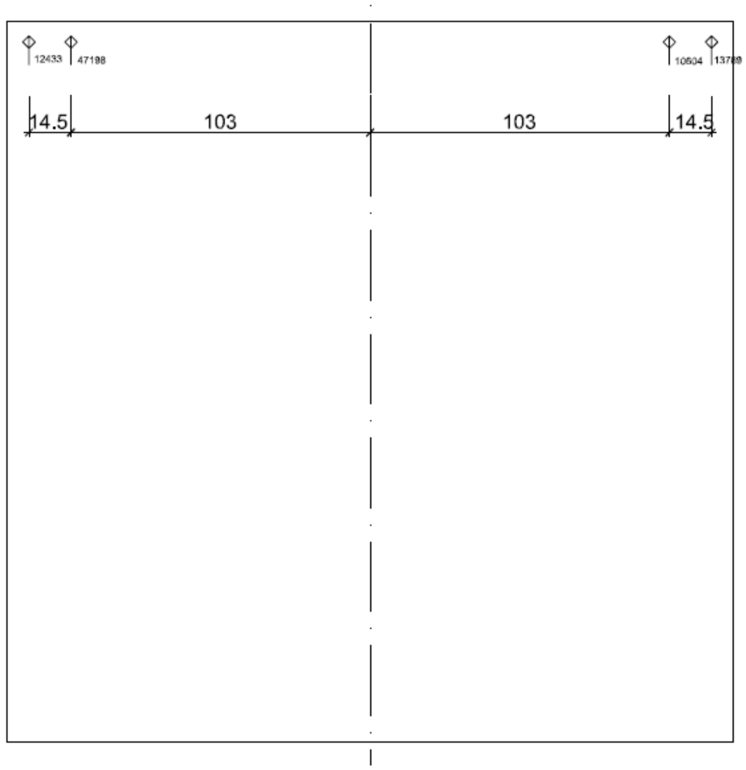

Figure 68: Position of the LVDTs at test specimen CS05

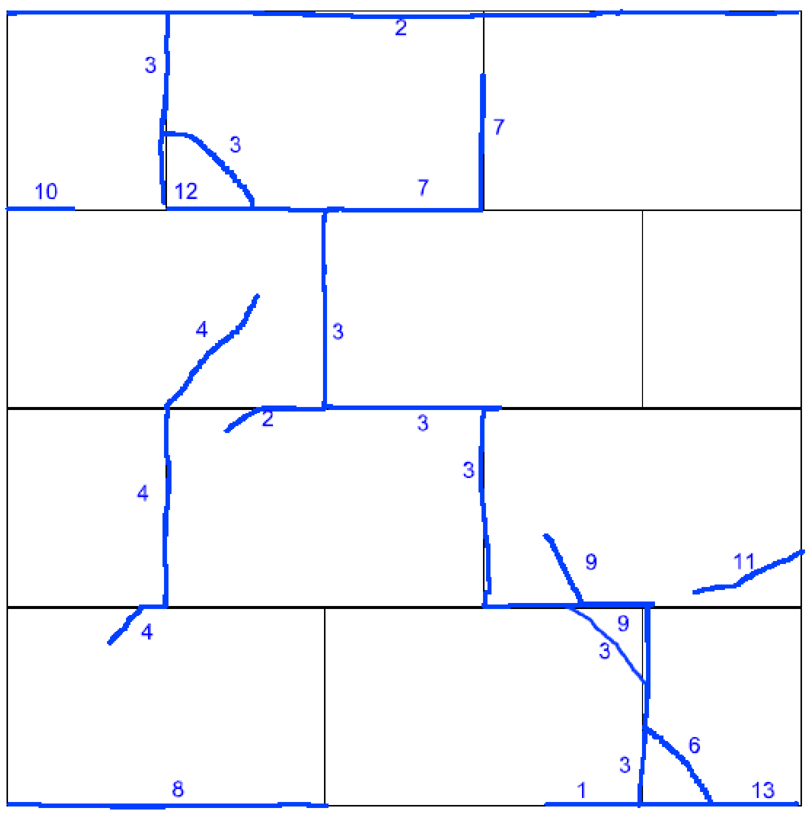

Figure 69: Crack pattern of the test specimen CS05

First crack: Final cracks:

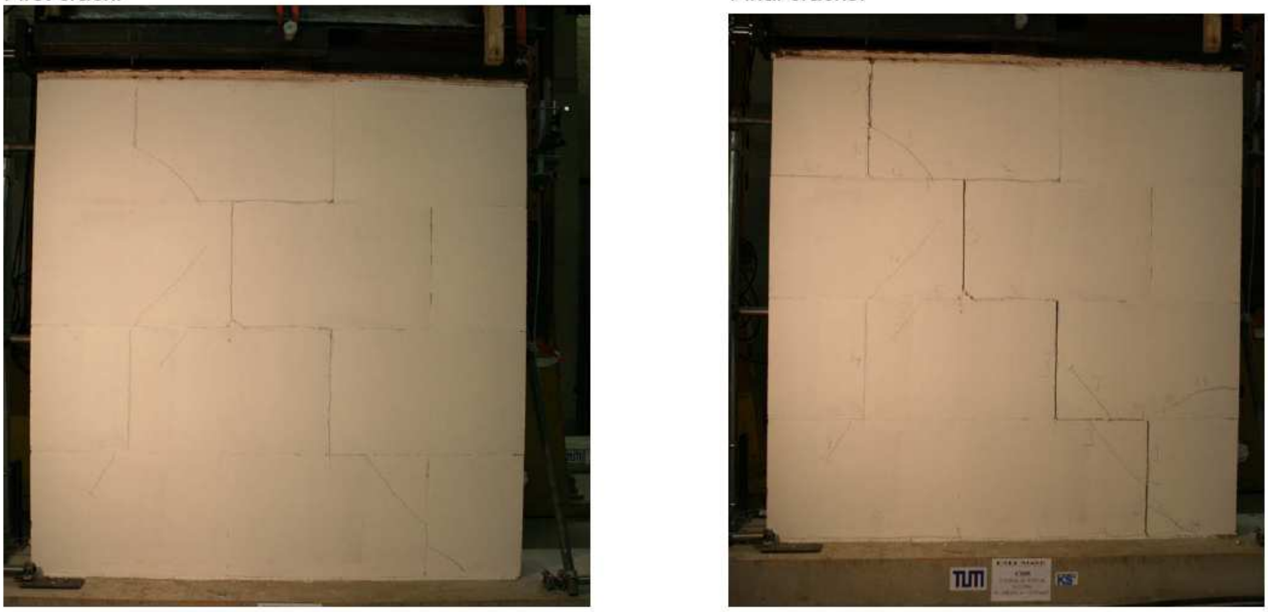

Figure 70: Crack pattern of the test specimen CS05

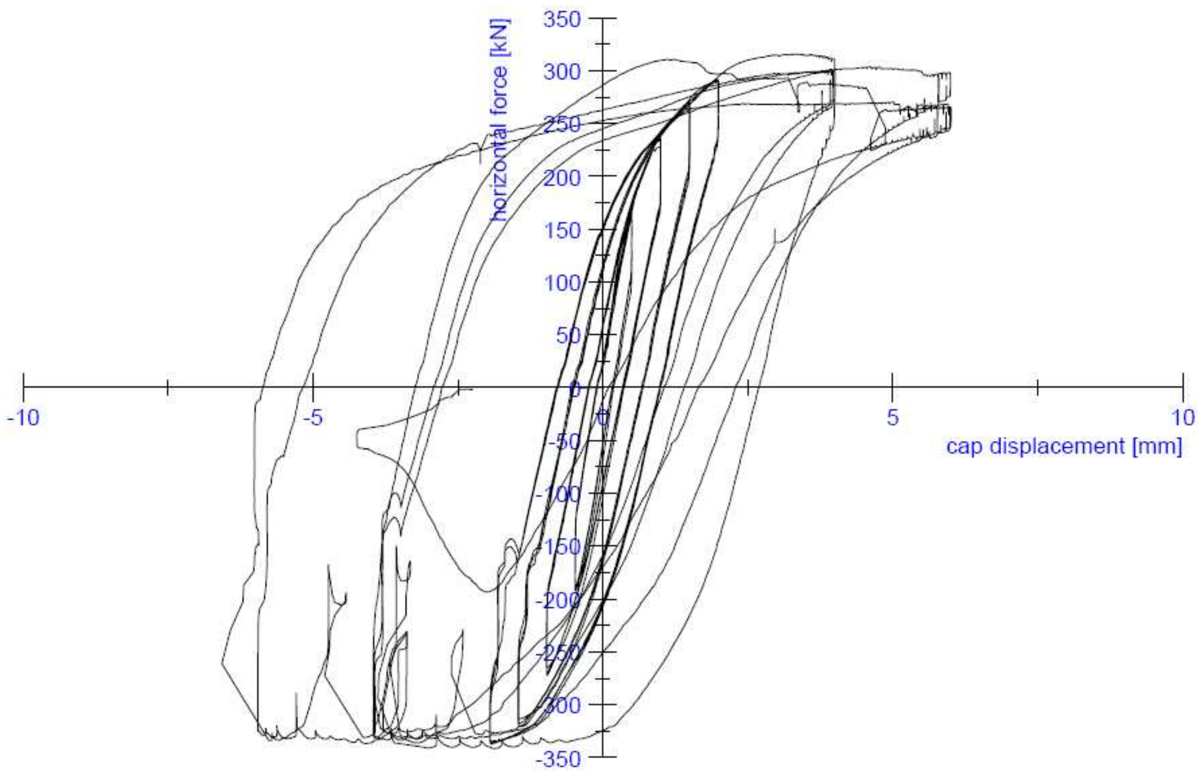

Figure 71: Load-displacement curve (hysteresis) of the test on specimen CS05

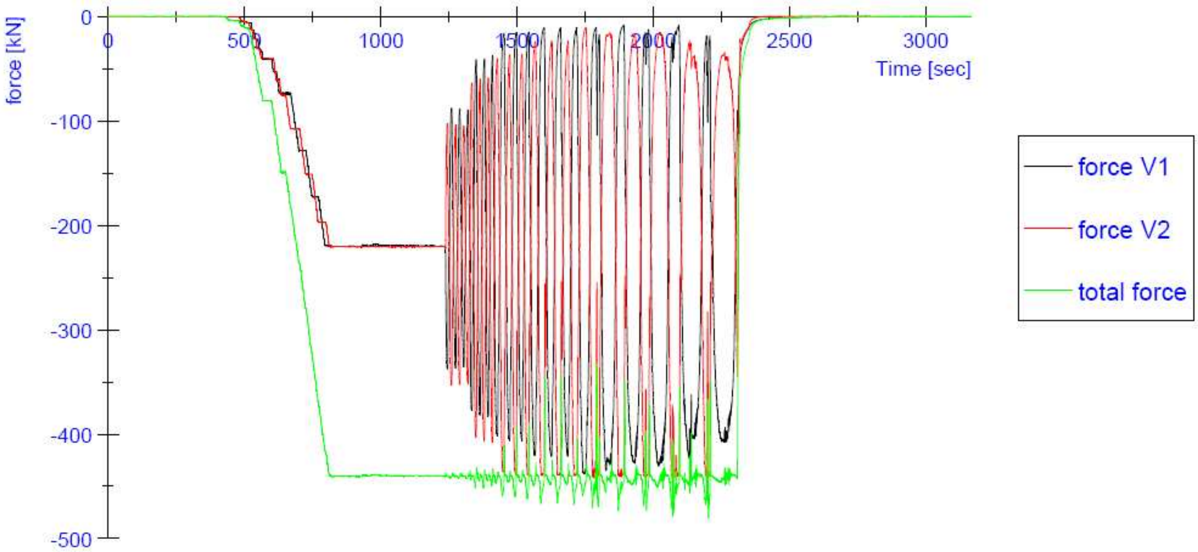

Figure 72: Progress of the vertical forces V1 and V2 during the test on specimen CS05

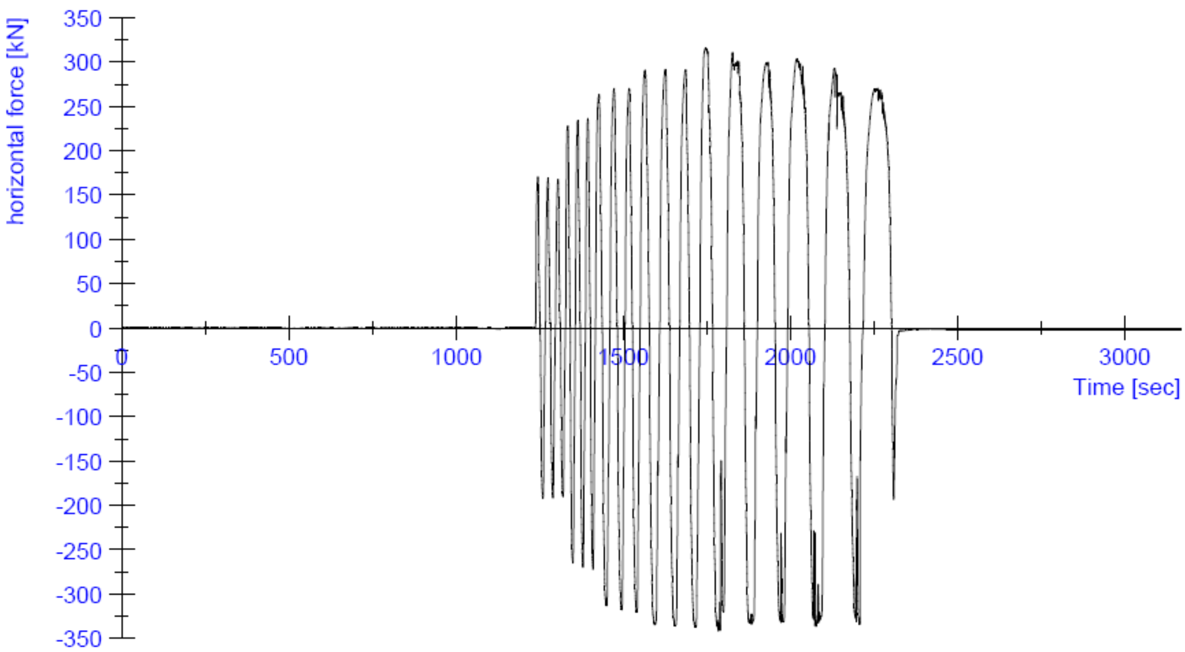

Figure 73: Progress of the horizontal force H during the test on specimen CS05

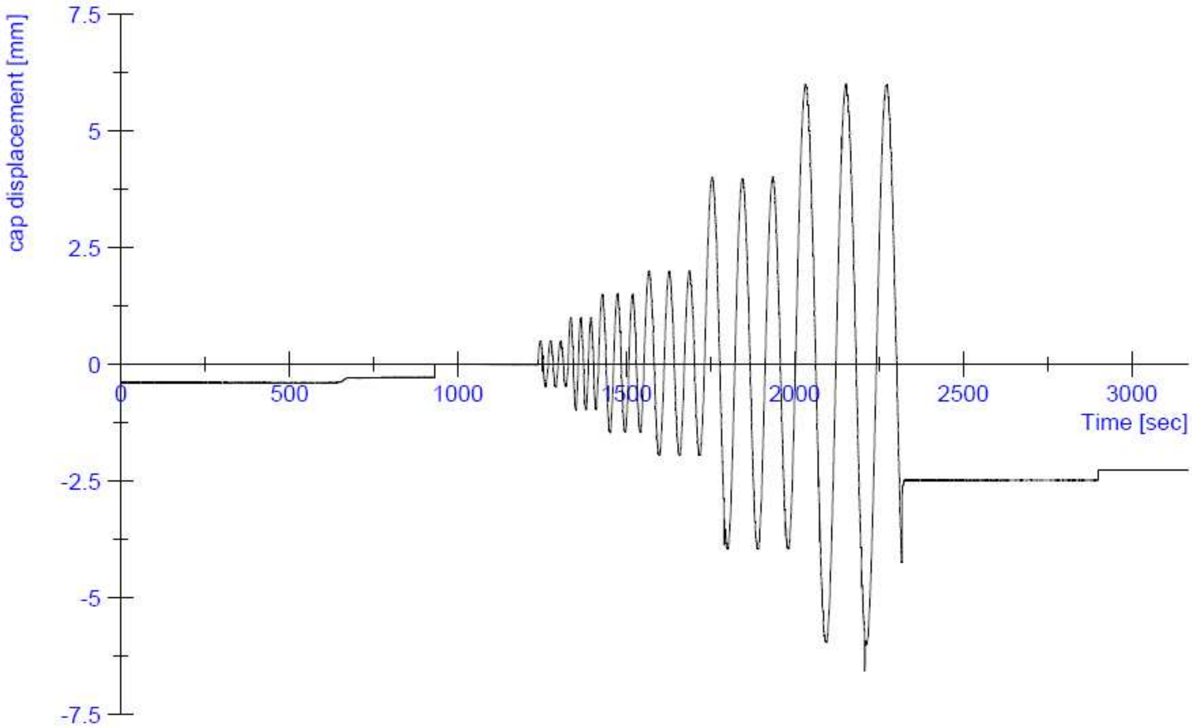

Figure 74: Progress of the horizontal displacement during the test on specimen CS05

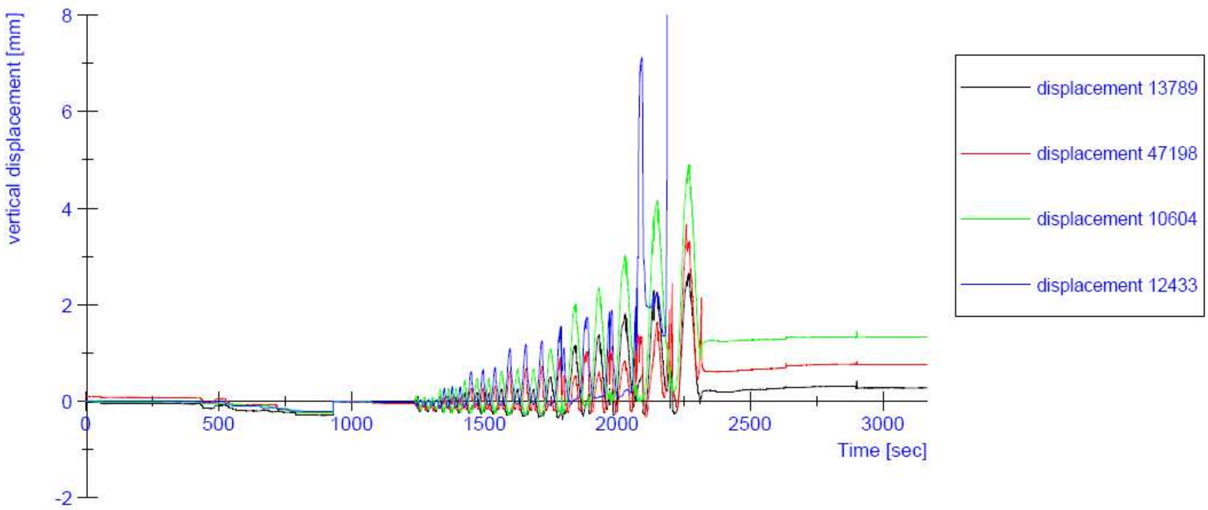

Figure 75: Progress of the vertical displacements during the test on specimen CS05

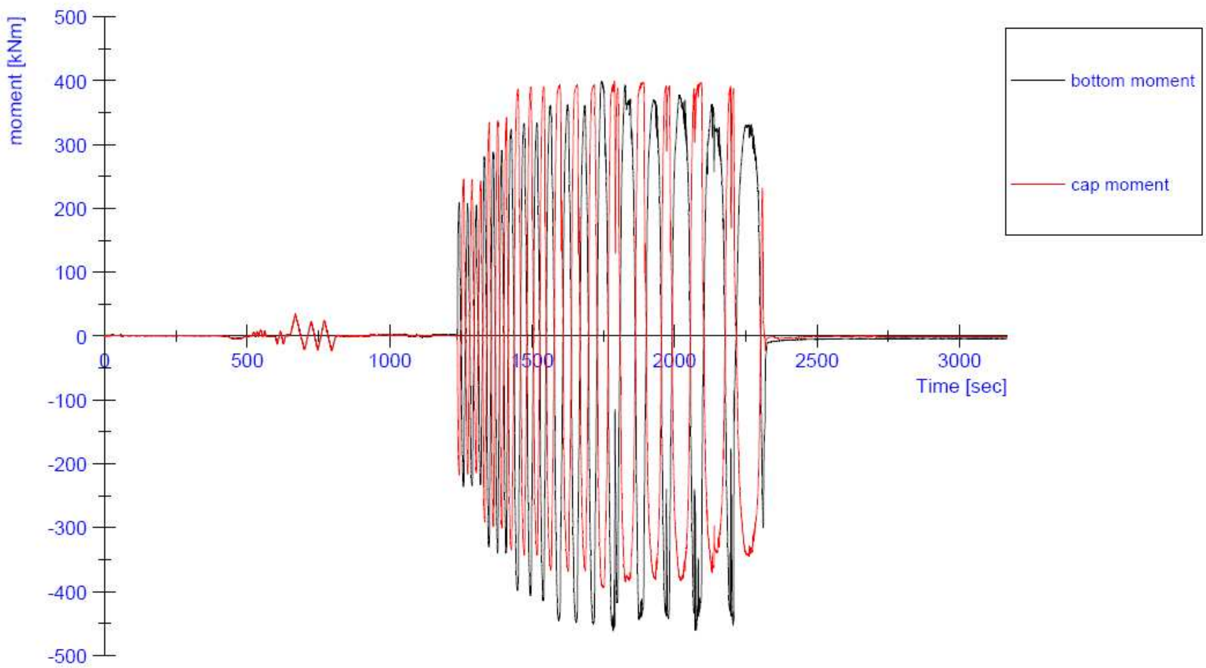

Figure 76: Progress of the in-plane bending moments at the top and at the bottom of the wall during the test on specimen CS05

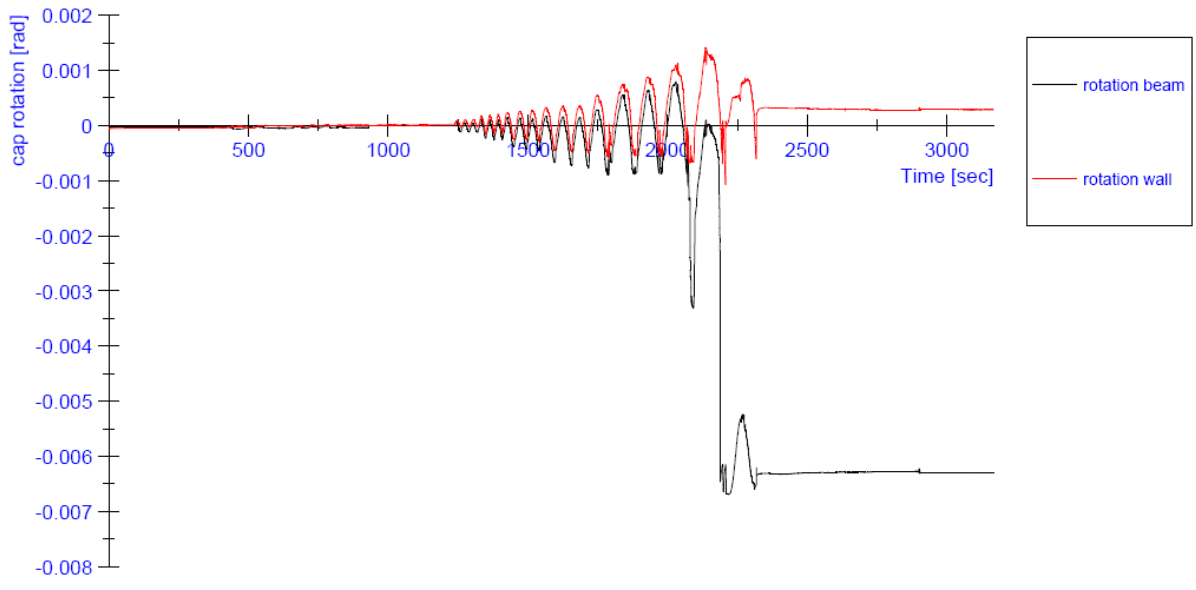

Figure 77: Progress of the in-plane rotation at the top of the wall during the test on specimen CS05

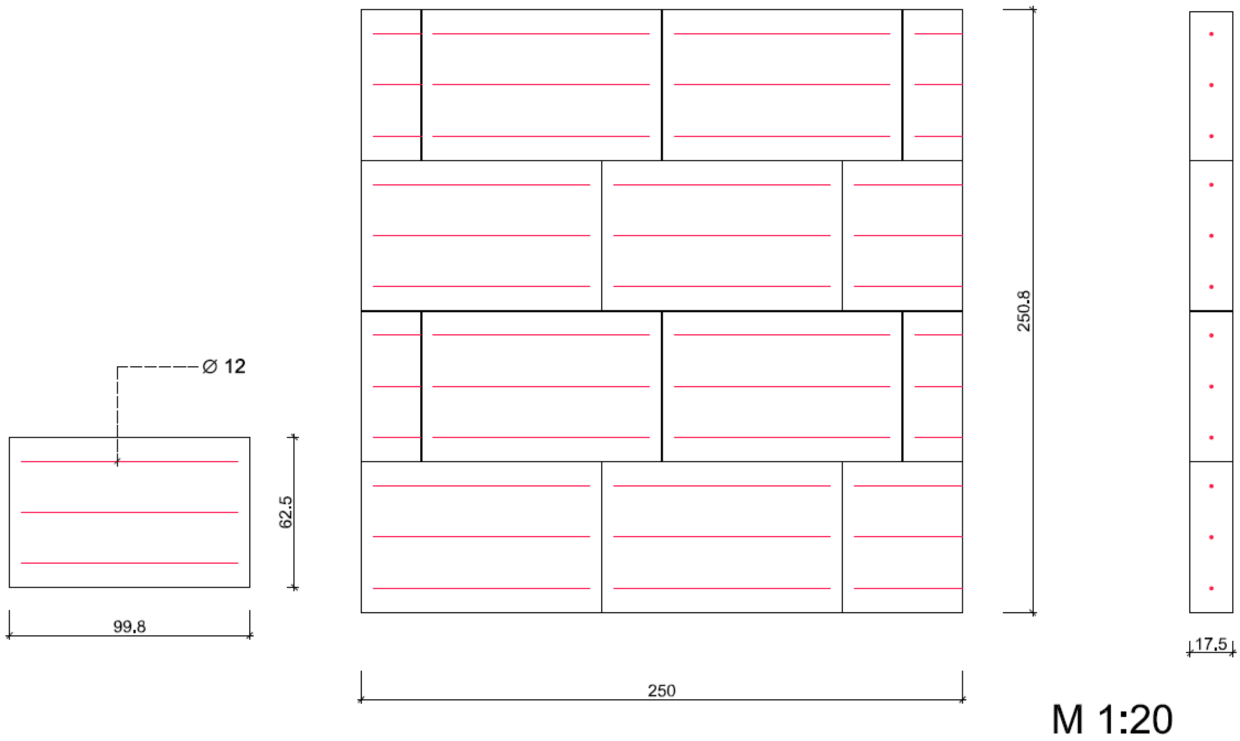

Figure 78: Dimension of the test specimen CS06 with the internal reinforcement

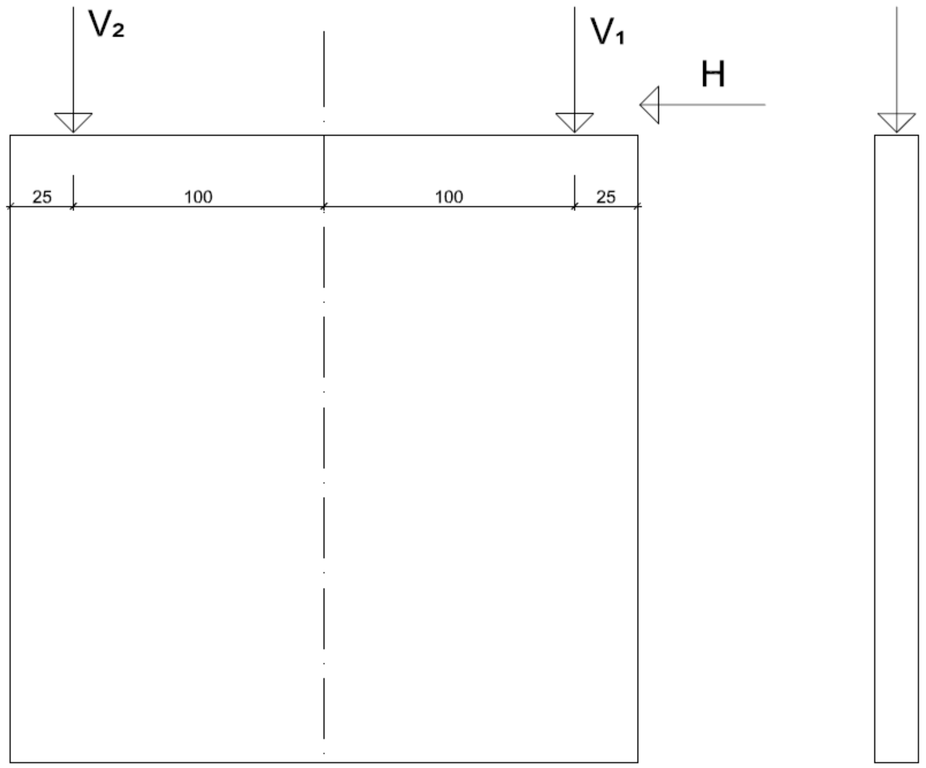

Figure 79: Position of the hydraulic actuators at test specimen CS06

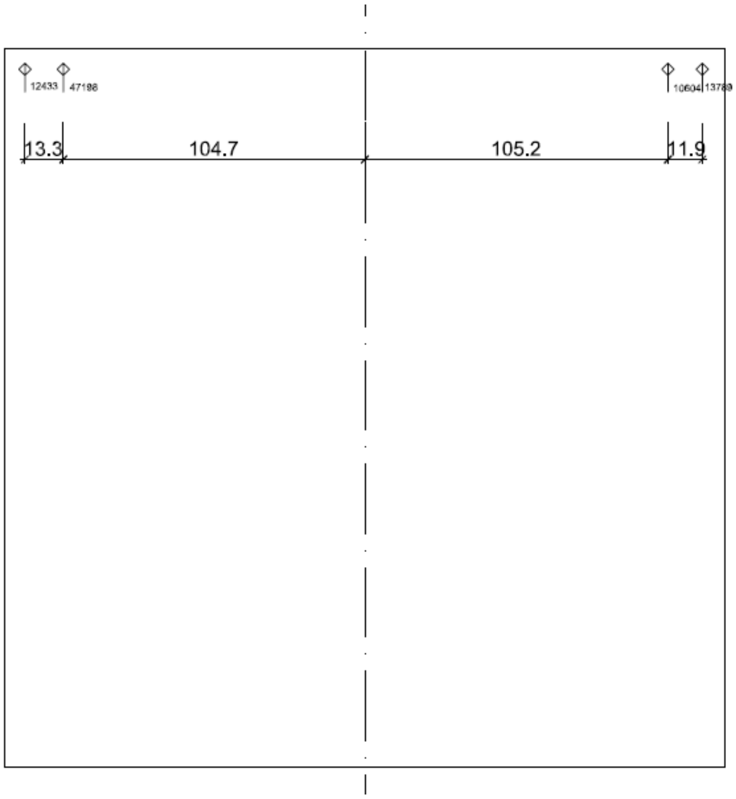

Figure 80: Position of the LVDTs at test specimen CS06

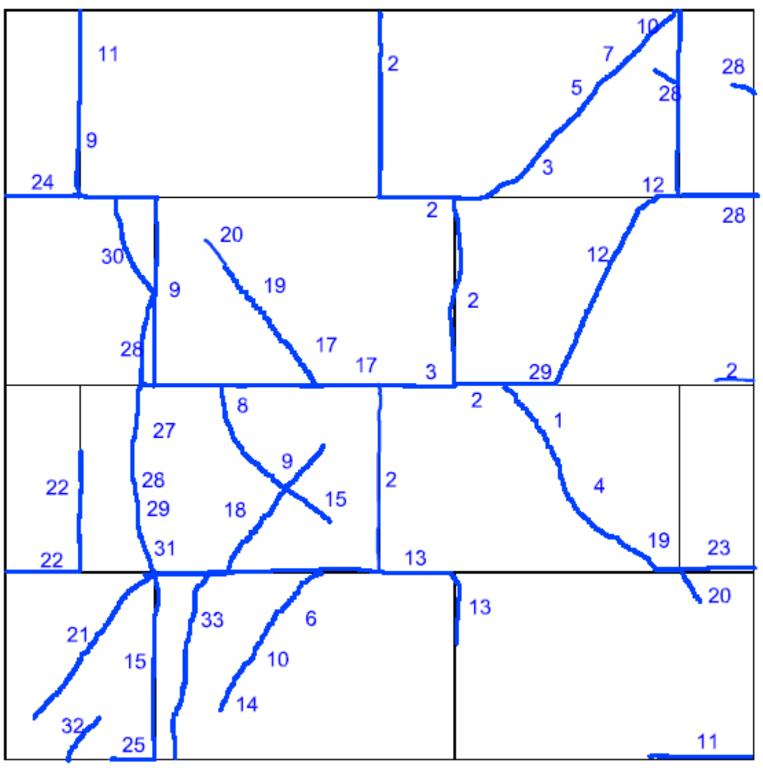

Figure 81: Crack pattern of the test specimen CS06

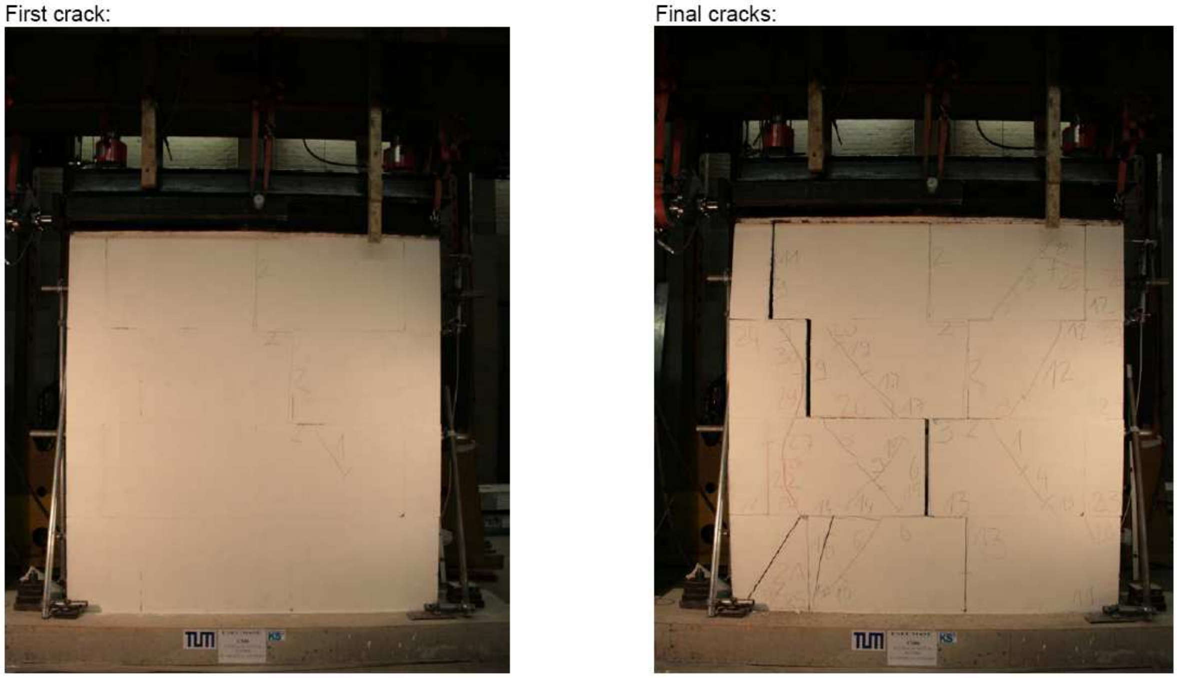

Figure 82: Crack pattern of the test specimen CS06

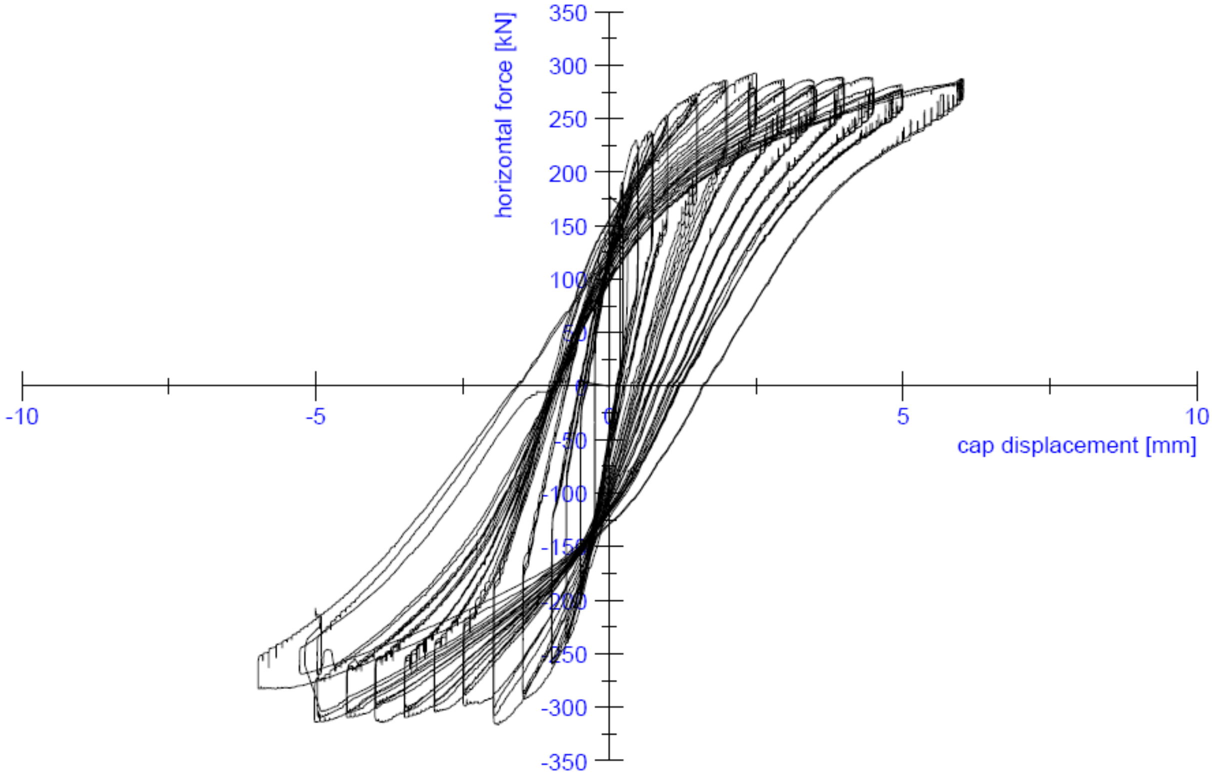

Figure 83: Load-displacement curve (hysteresis) of the test on specimen CS06

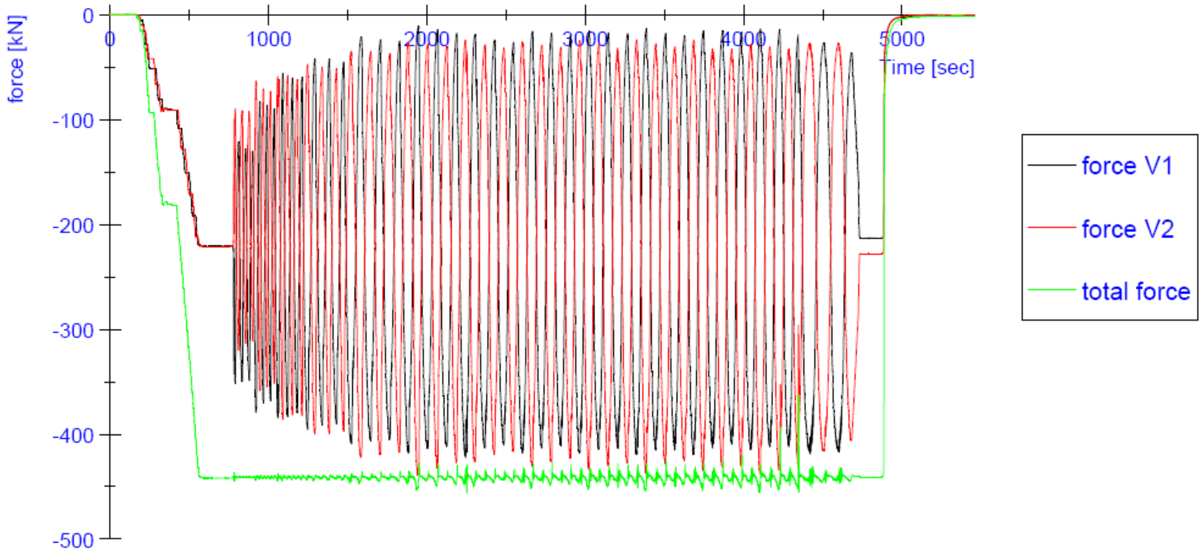

Figure 84: Progress of the vertical forces V1 and V2 during the test on specimen CS06

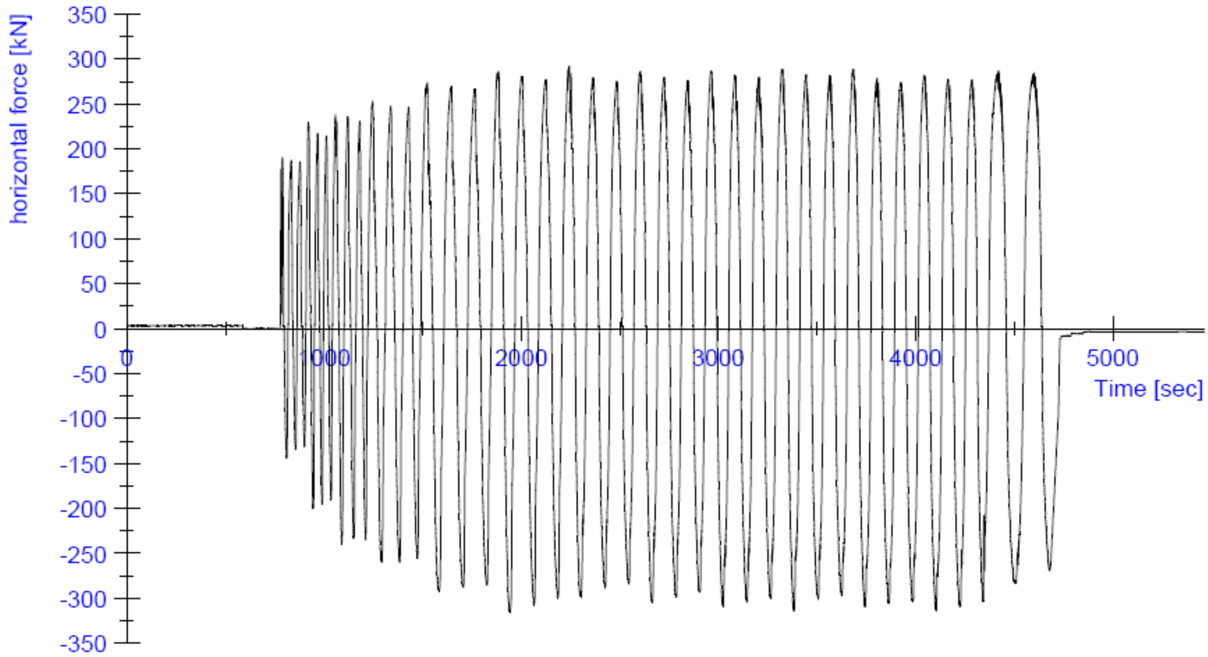

Figure 85: Progress of the horizontal force H during the test on specimen CS06

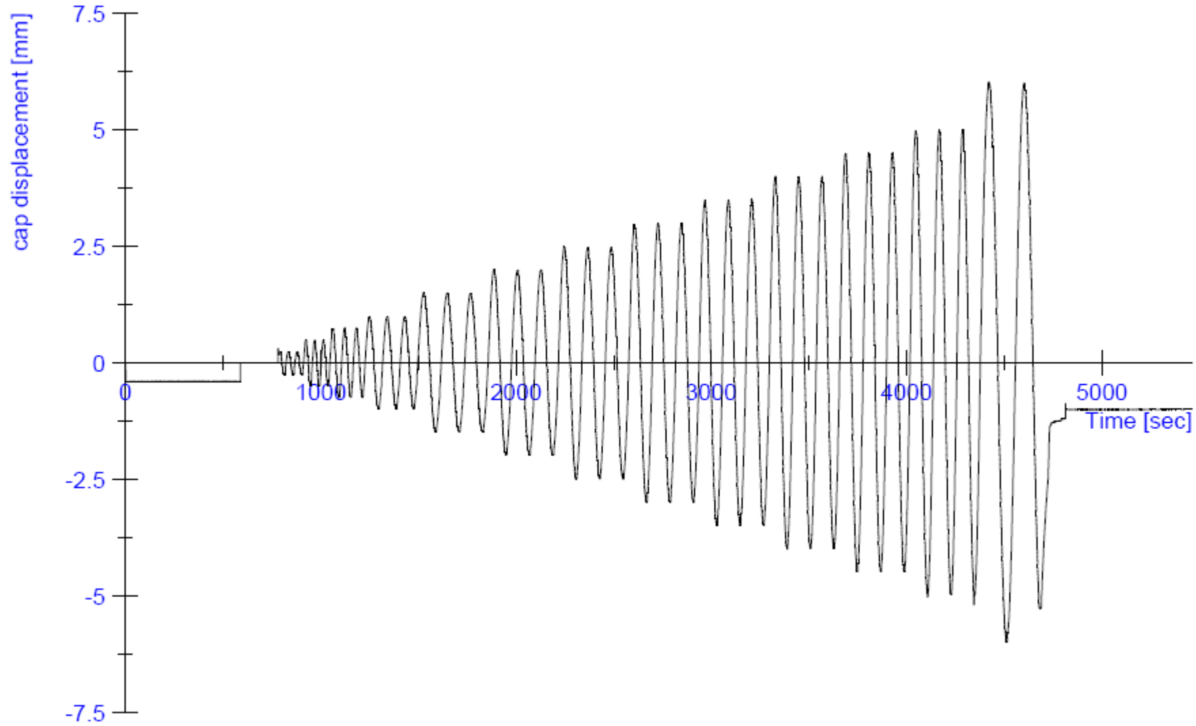

Figure 86: Progress of the horizontal displacement during the test on specimen CS06

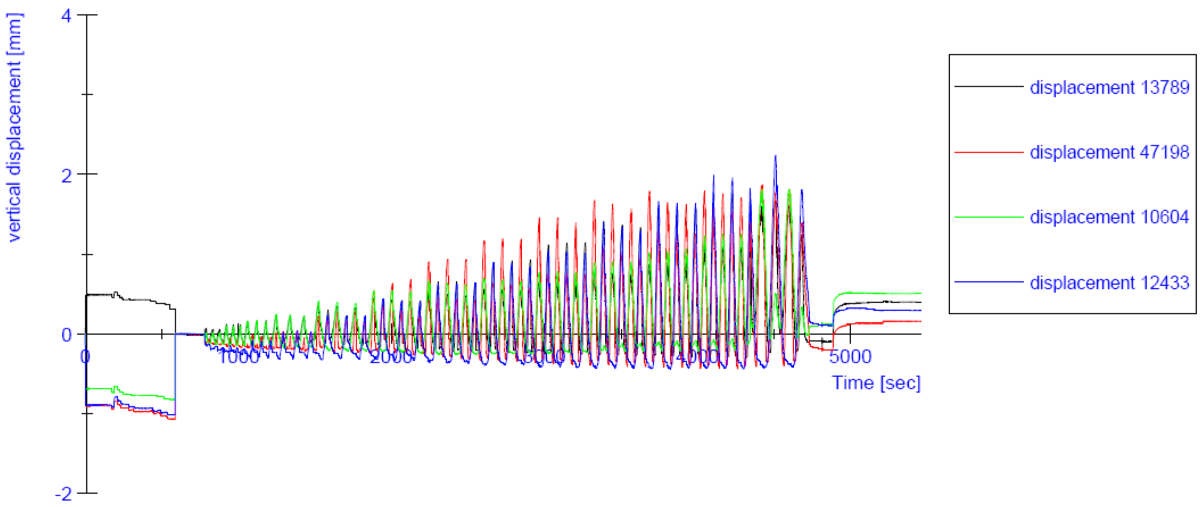

Figure 87: Progress of the vertical displacements during the test on specimen CS06

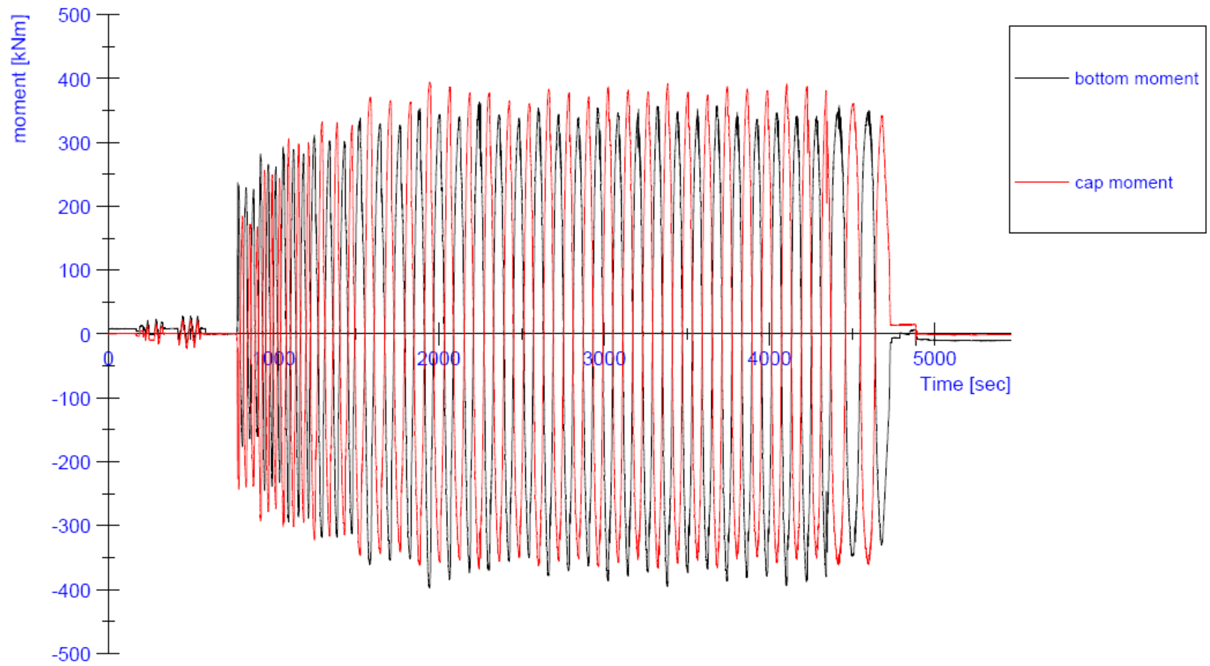

Figure 88: Progress of the in-plane bending moments at the top and at the bottom of the wall during the test on specimen CS06

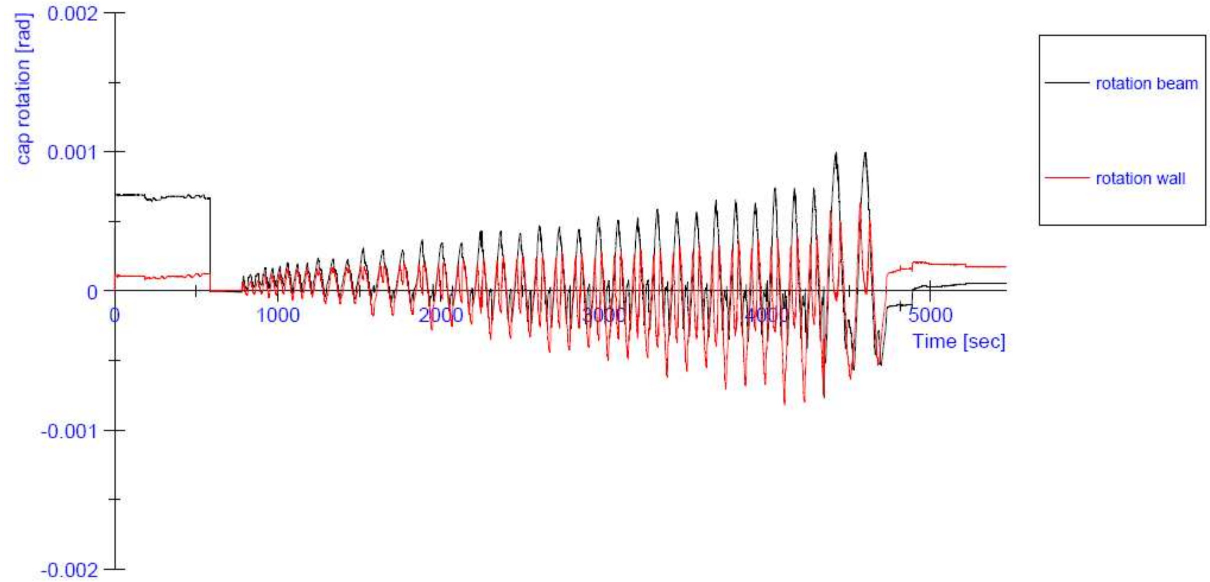

Figure 89: Progress of the in-plane rotation at the top of the wall during the test on specimen CS06

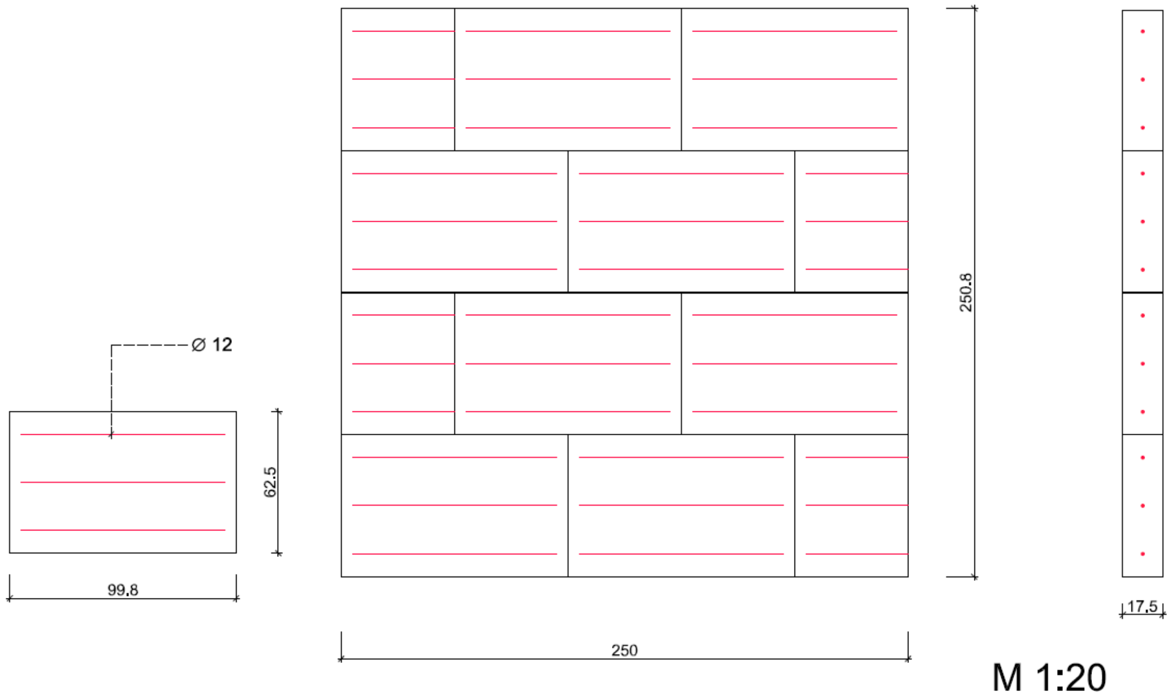

Figure 90: Dimension of the test specimen CS07 with the internal reinforcement

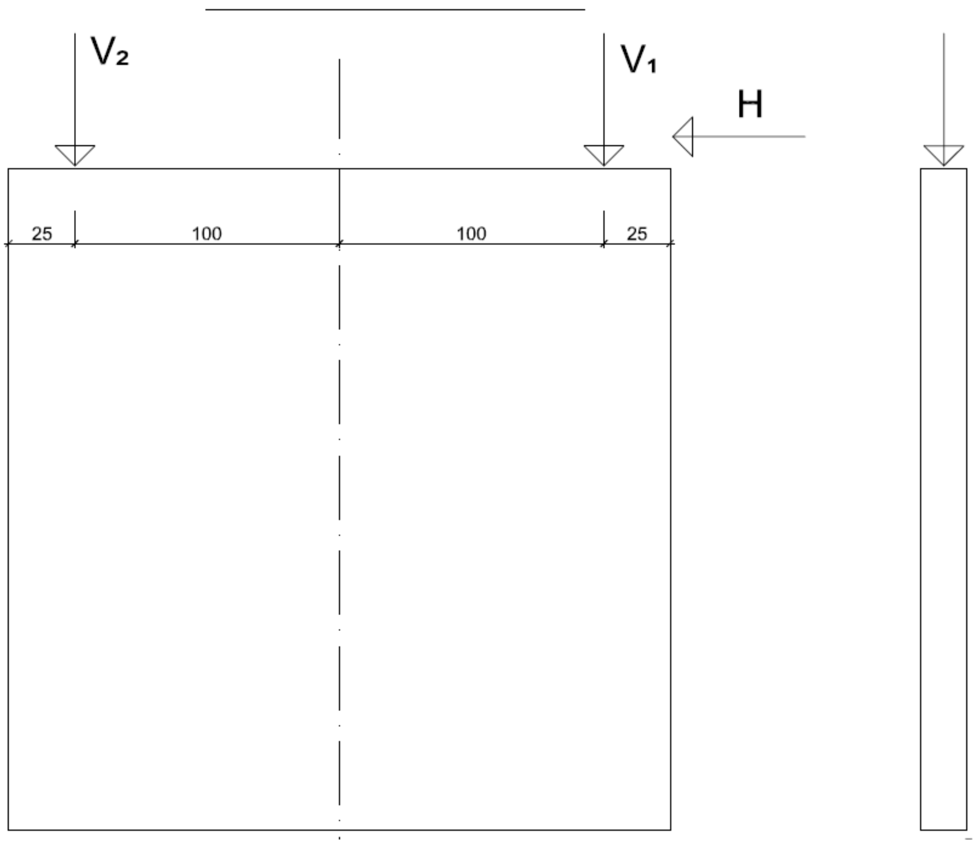

Figure 91: Position of the hydraulic actuators at test specimen CS07

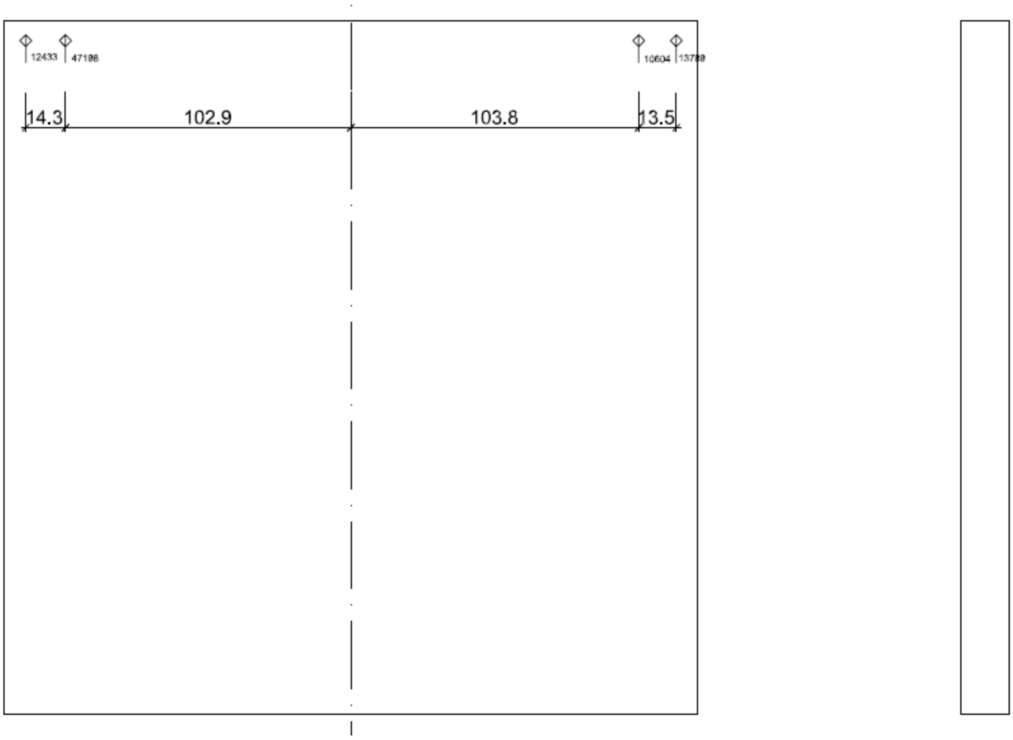

Figure 92: Position of the LVDTs at test specimen CS07

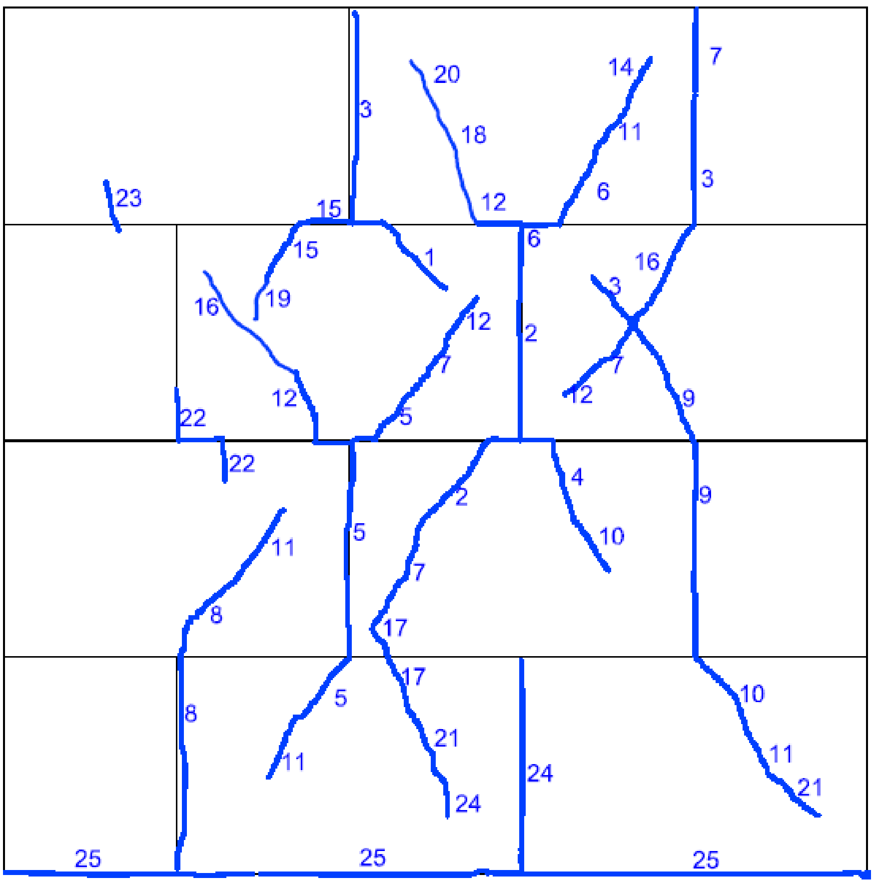

Figure 93: Crack pattern of the test specimen CS07

First crack:

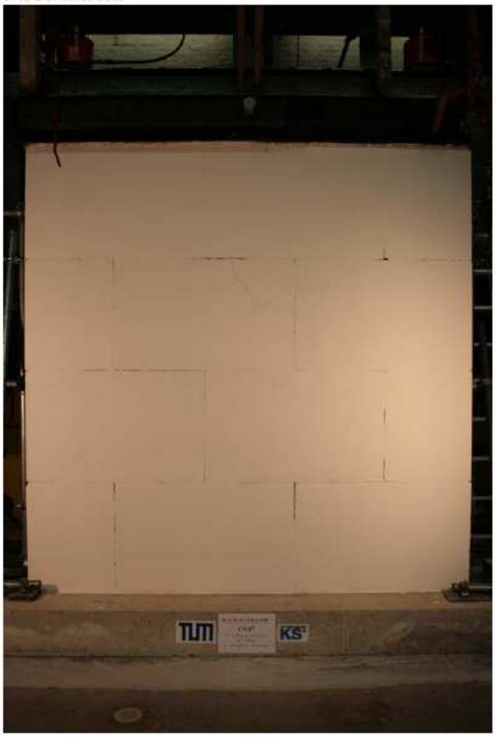

Final cracks:

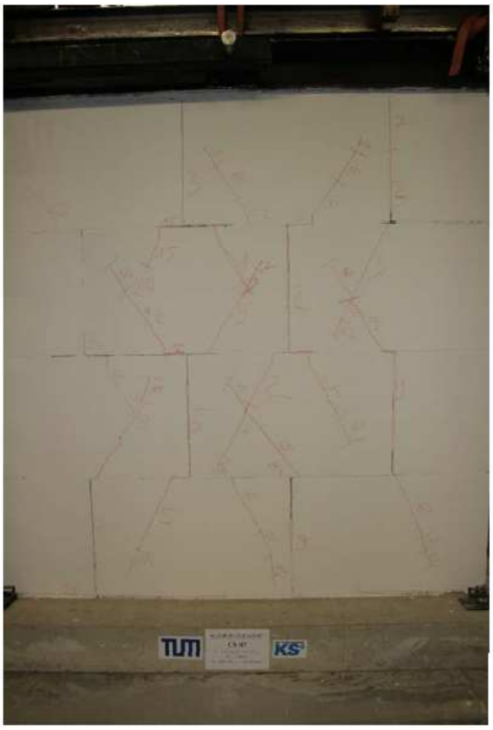

Figure 94: Crack pattern of the test specimen CS07

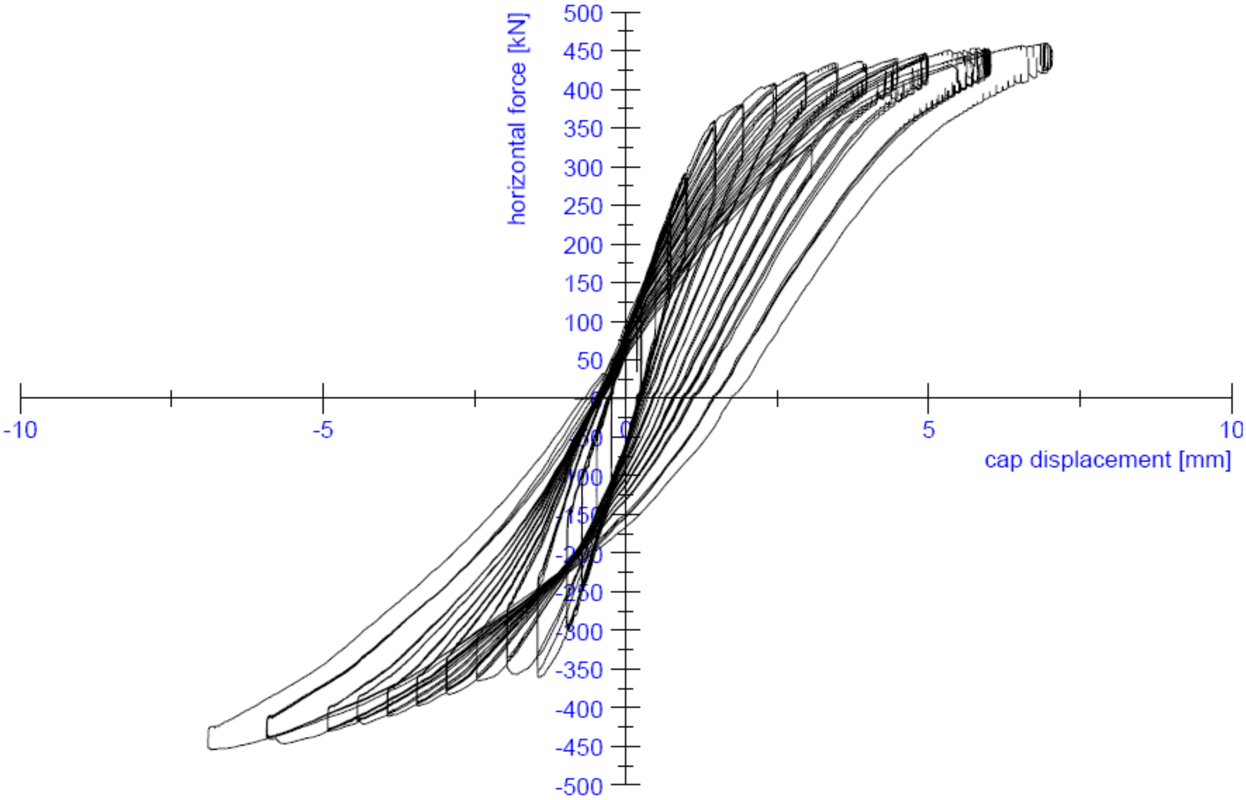

Figure 95: Load-displacement curve (hysteresis) of the test on specimen CS07

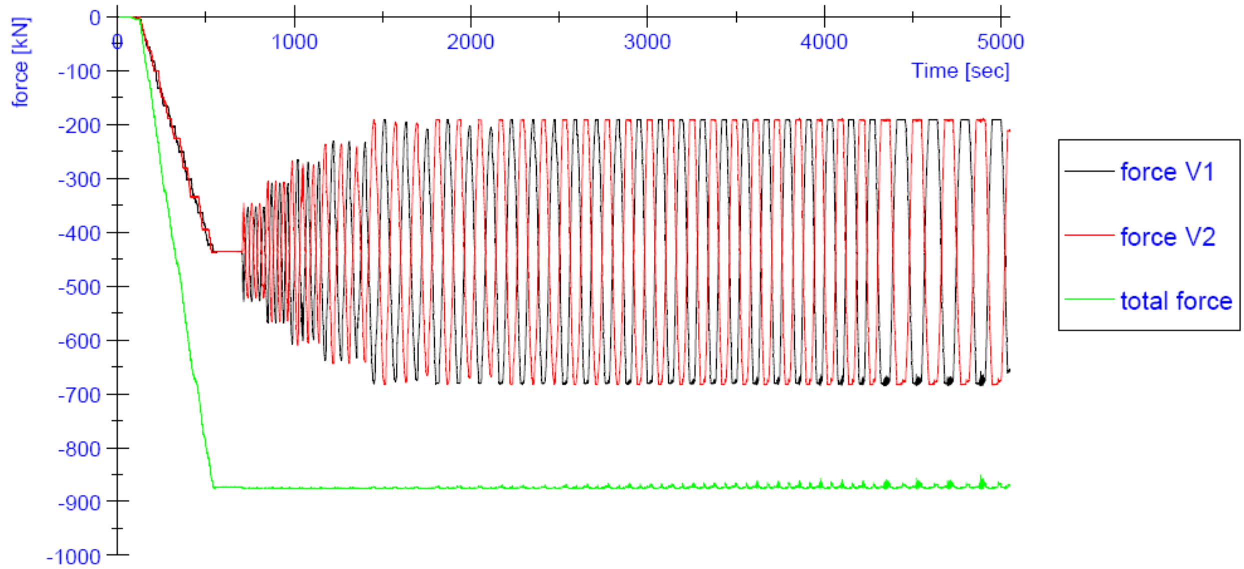

Figure 96: Progress of the vertical forces V1 and V2 during the test on specimen CS07

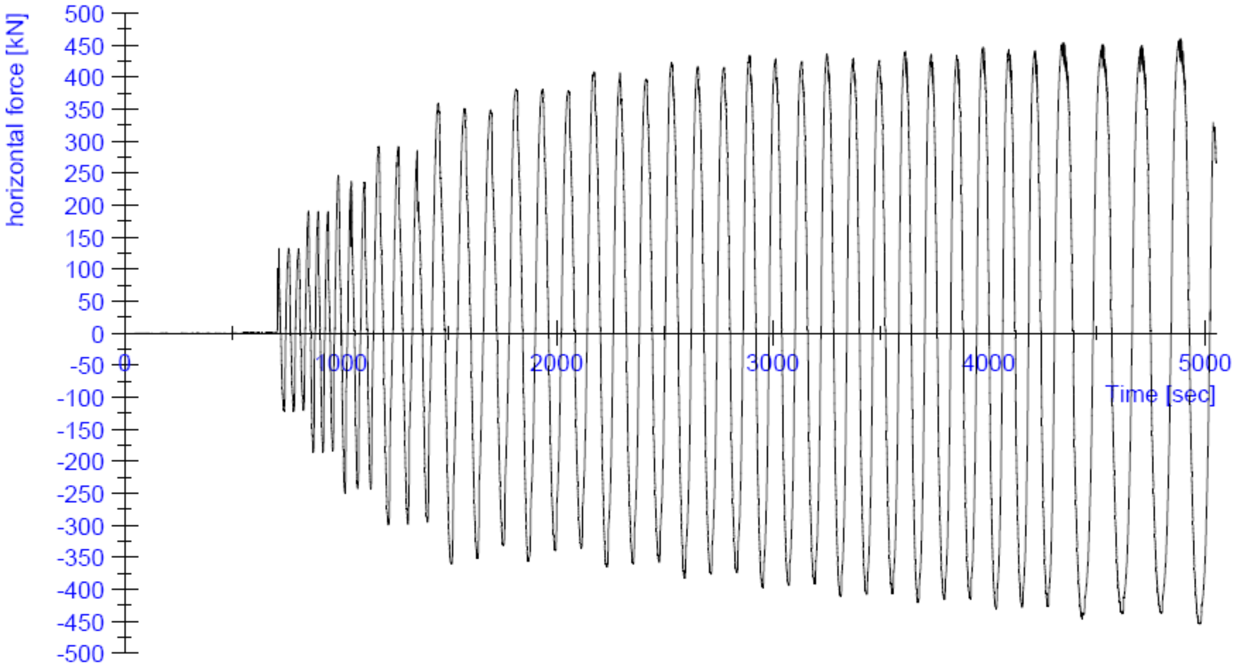

Figure 97: Progress of the horizontal force H during the test on specimen CS07

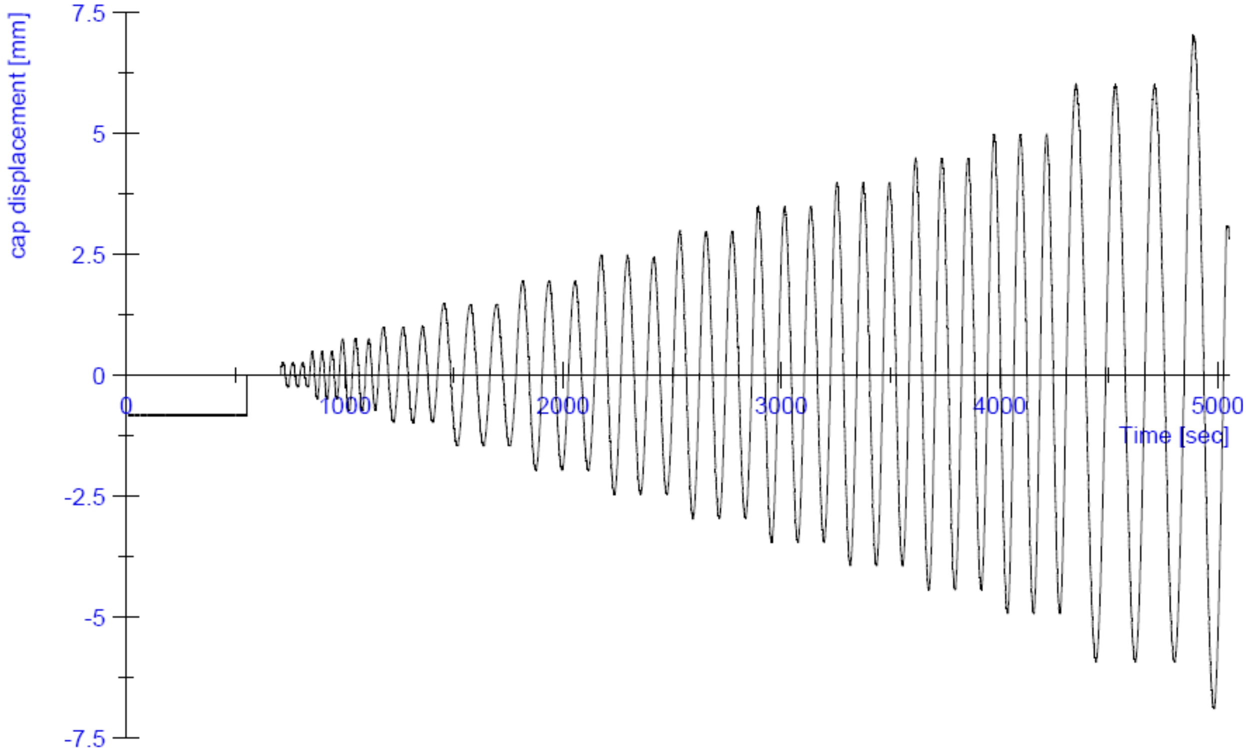

Figure 98: Progress of the horizontal displacement during the test on specimen CS07

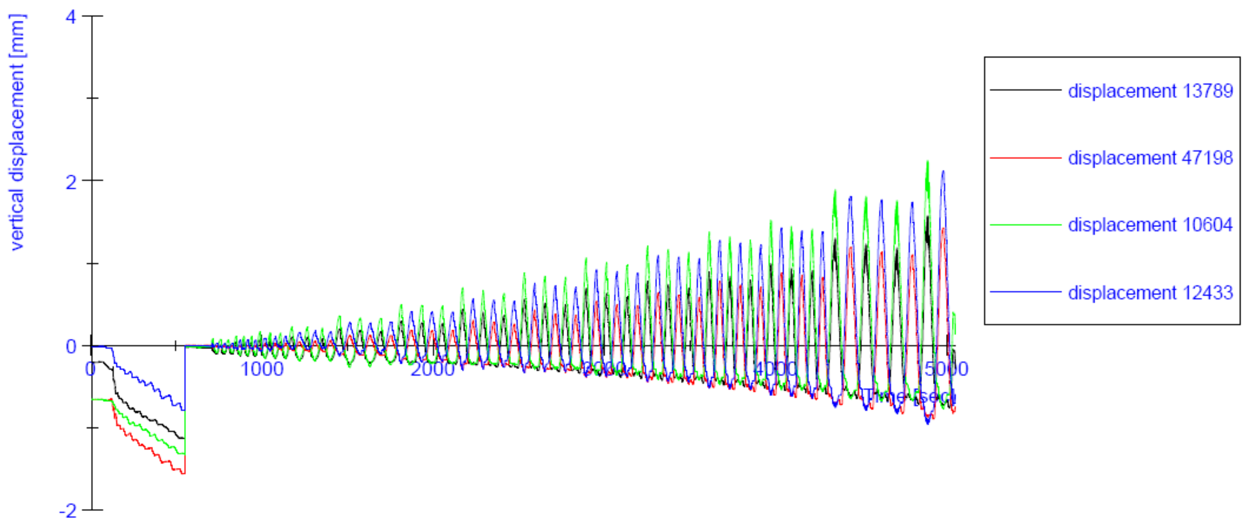

Figure 99: Progress of the vertical displacements during the test on specimen CS07

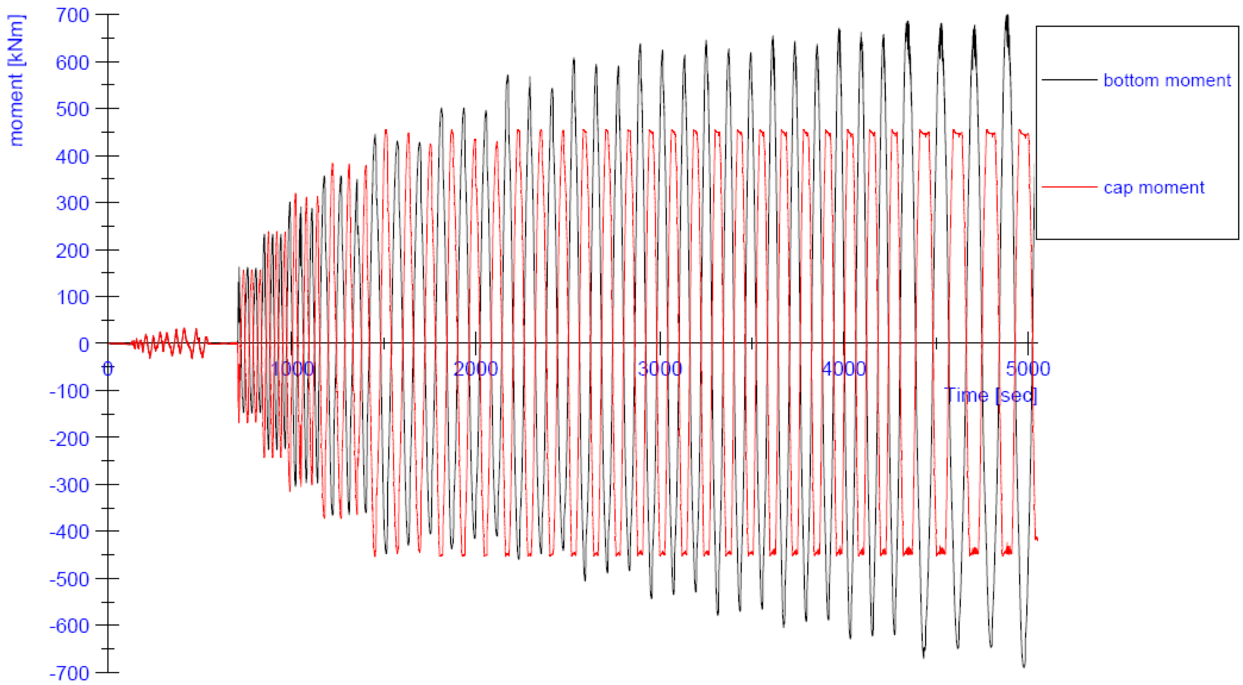

Figure 100: Progress of the in-plane bending moments at the top and at the bottom of the wall during the test on specimen CS07

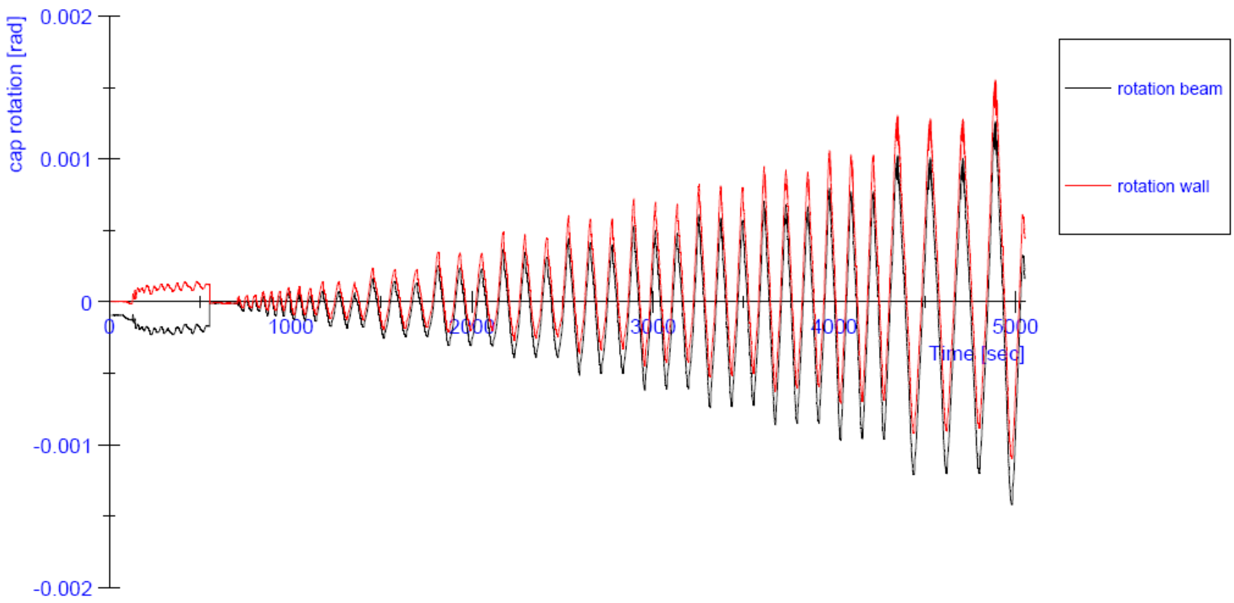

Figure 101: Progress of the in-plane rotation at the top of the wall during the test on specimen CS07

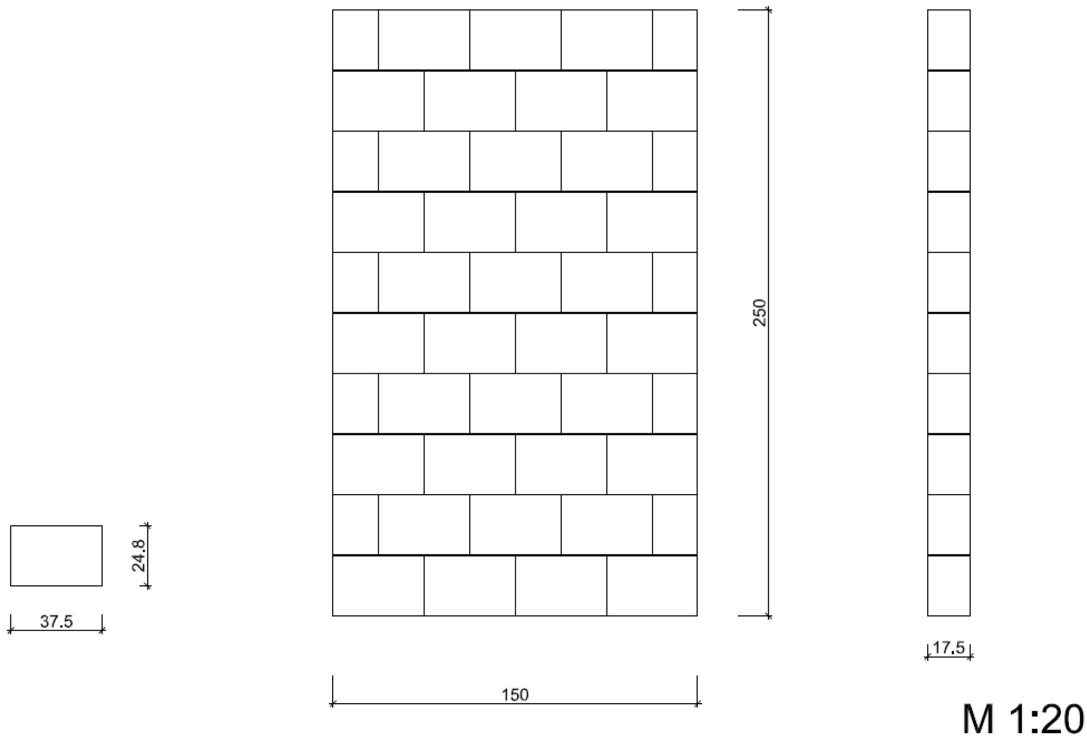

Figure 102: Dimension of the test specimen Clay01

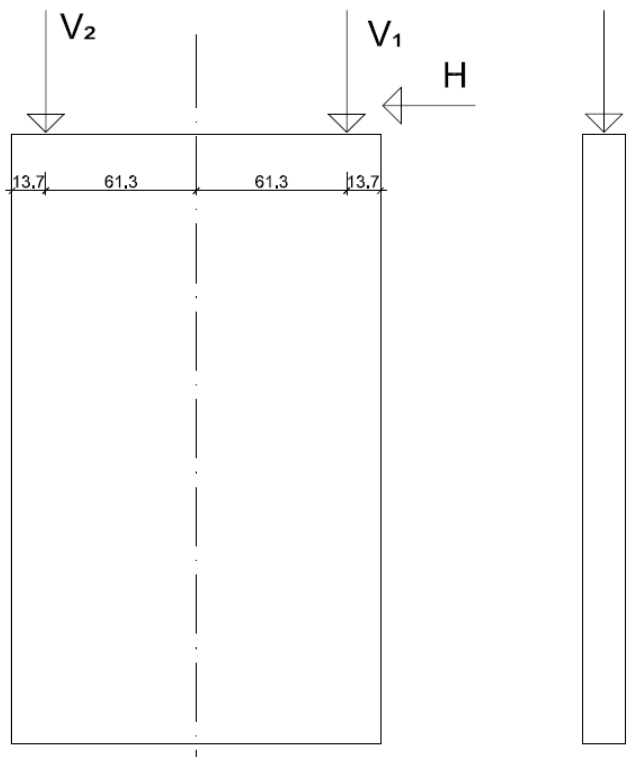

Figure 103: Position of the hydraulic actuators at test specimen Clay01

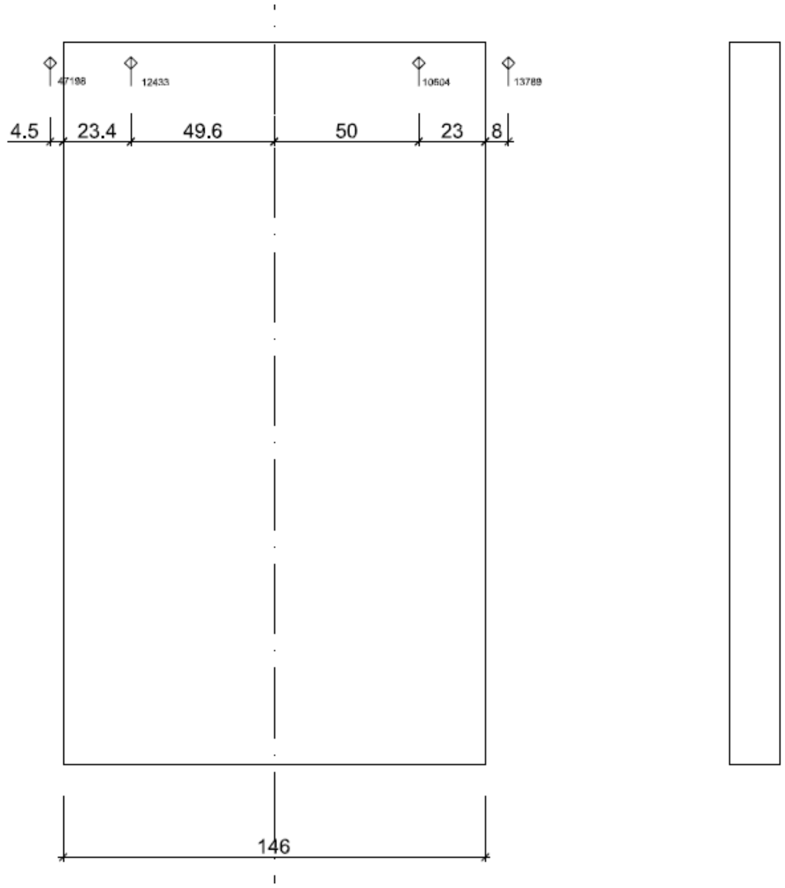

Figure 104: Position of the LVDTs at test specimen Clay01

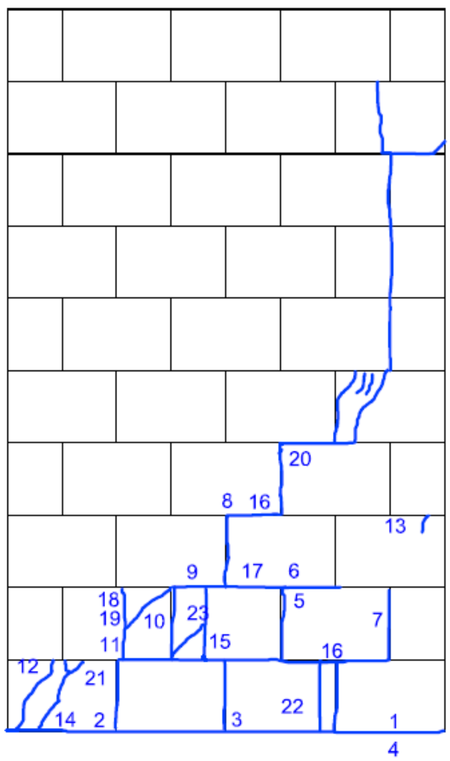

Figure 105: Crack pattern of the test specimen Clay01

First crack: Final cracks:

Figure 106: Crack pattern of the test specimen Clay01

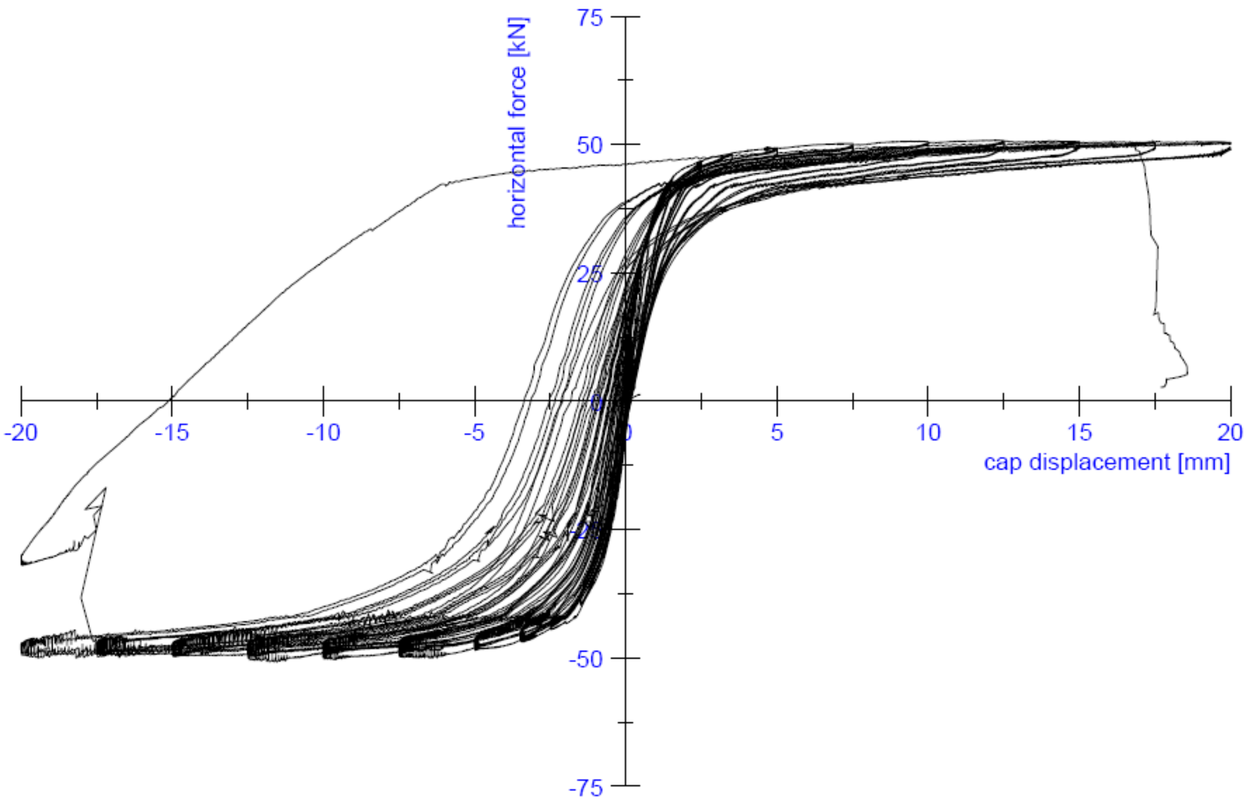

Figure 107: Load-displacement curve (hysteresis) of the test on specimen Clay01

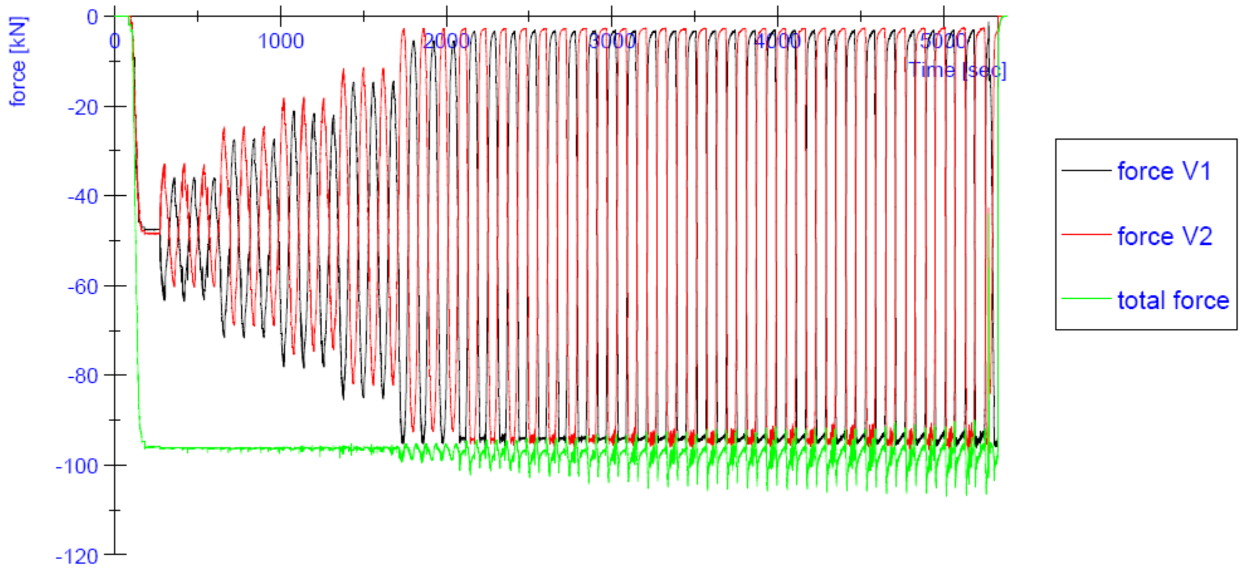

Figure 108: Progress of the vertical forces V1 and V2 during the test on specimen Clay01

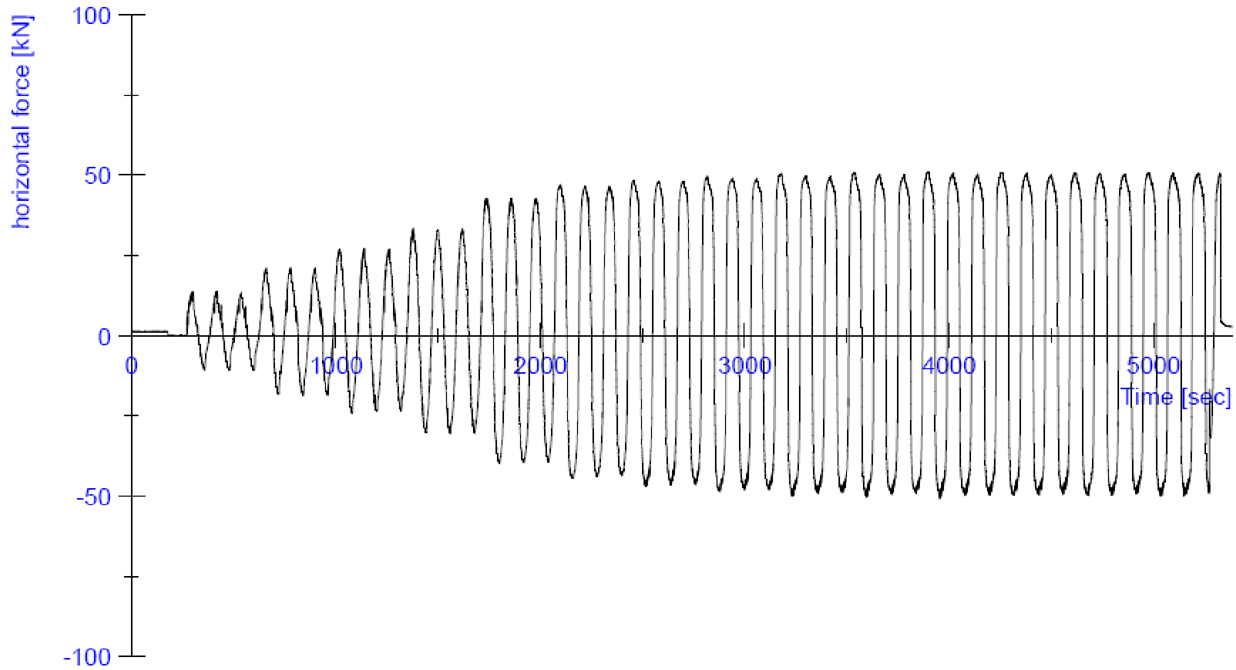

Figure 109: Progress of the horizontal force H during the test on specimen Clay01

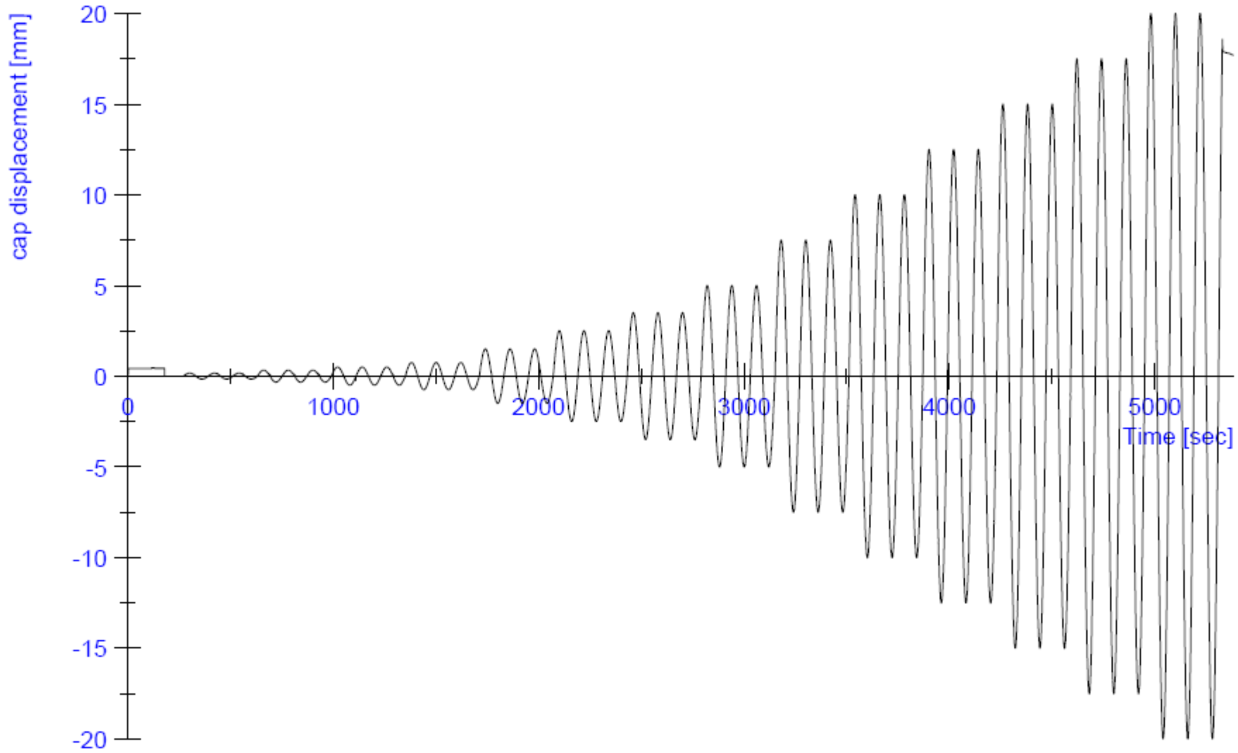

Figure 110: Progress of the horizontal displacement during the test on specimen Clay01

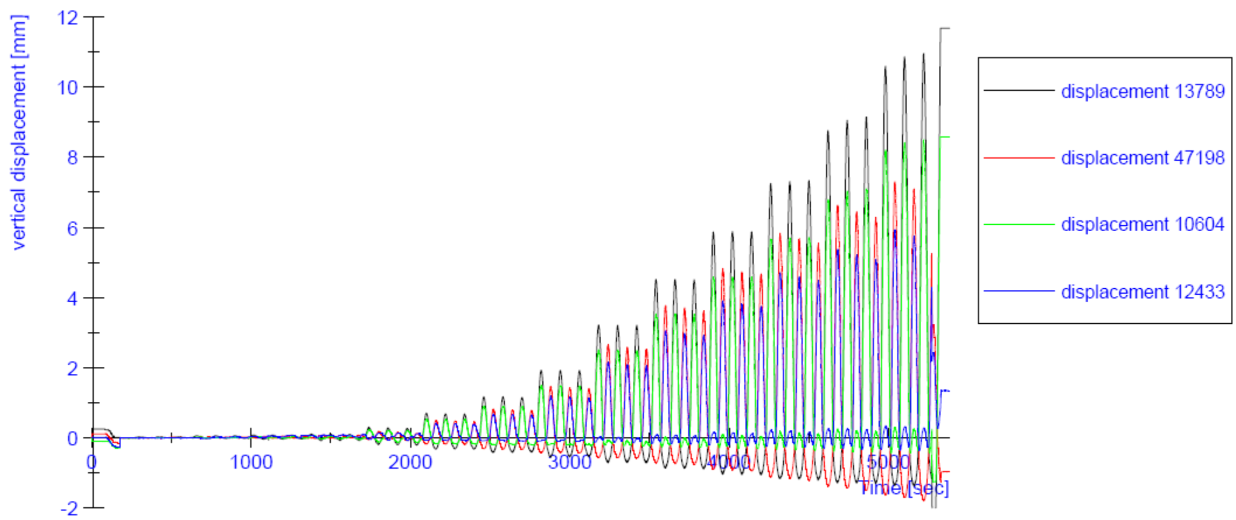

Figure 111: Progress of the vertical displacements during the test on specimen Clay01

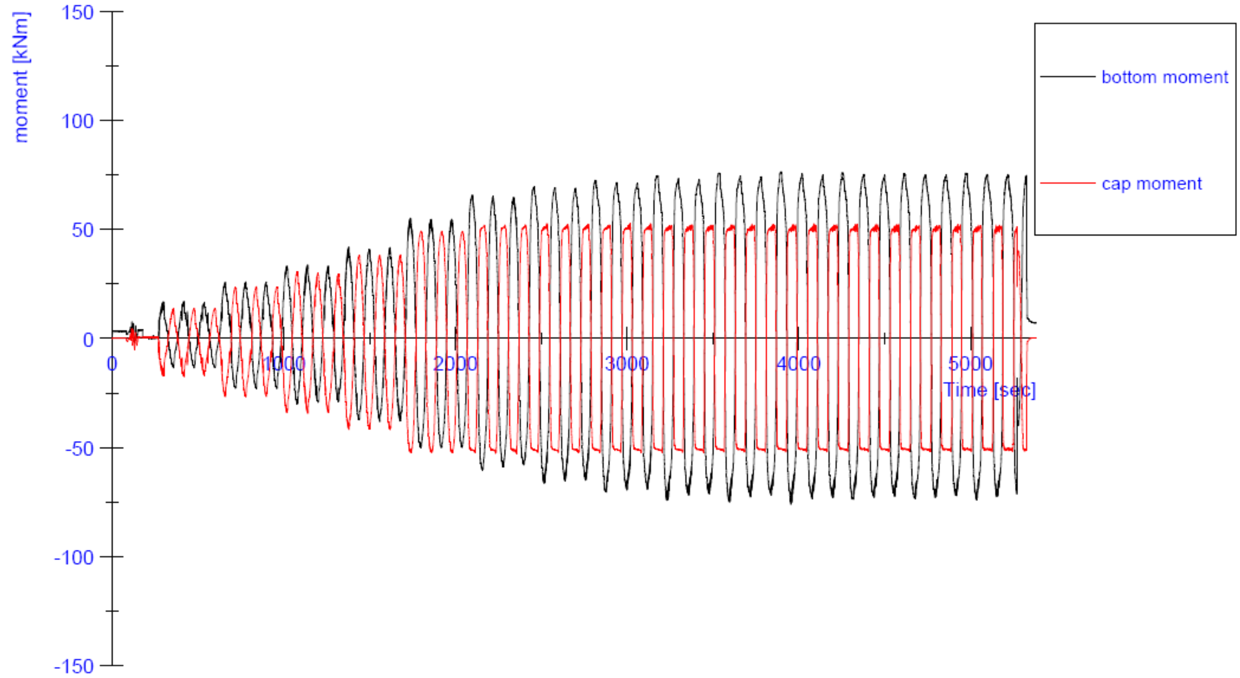

Figure 112: Progress of the in-plane bending moments at the top and at the bottom of the wall during the test on specimen Clay01

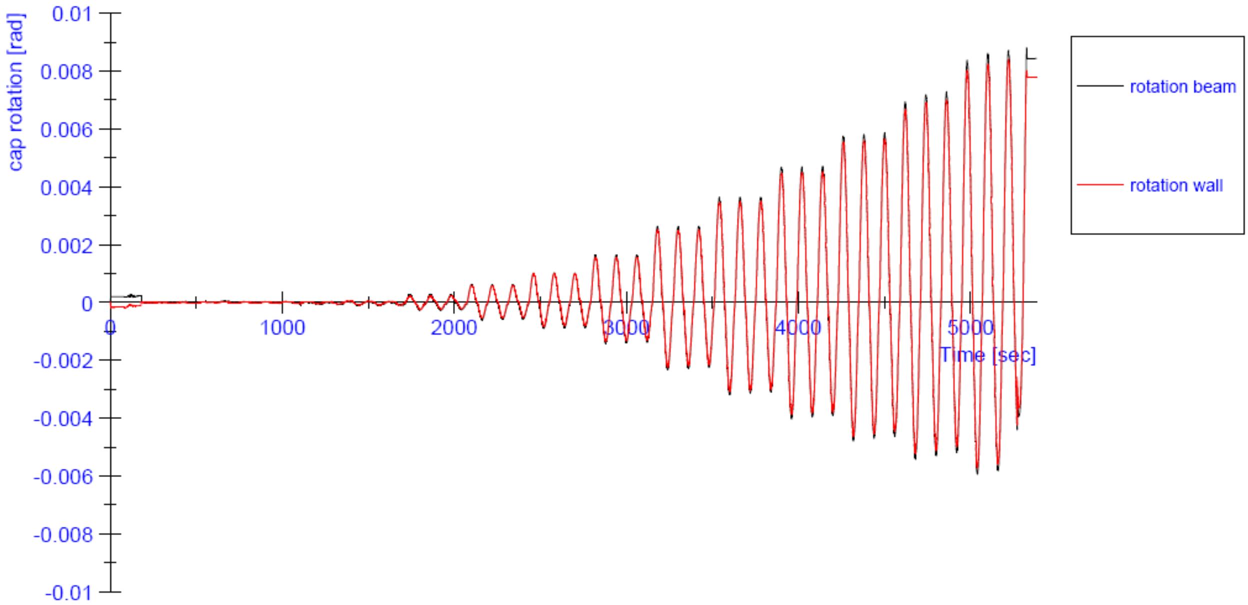

Figure 113: Progress of the in-plane rotation at the top of the wall during the test on specimen Clay01